Biosorption of Anionic Metal Species

Hui Niu

Department of Chemical Engineering
McGill University, Montreal, Canada

A thesis submitted to the Faculty of Graduate Studies and Research
in partial fulfillment of the requirements
of the degree of Doctor of Philosophy

National Library
of Canada

Acquisitions and
Bibliographic Services

395 Wellington Street
Ottawa ON K1A 0N4
Canada

Bibliothèque nationale
du Canada

Acquisisitons et
services bibliographiques

395, rue Wellington
Ottawa ON K1A 0N4
Canada

Your file Votre référence
ISBN: 0-612-85728-X
Our file Notre référence
ISBN: 0-612-85728-X

ABSTRACT

Certain types of dead, inactive biomass can very effectively immobilize and concentrate heavy metals. In this work, a (bio-)sorption process has been studied using the biomass of waste crab shells which is particularly suited for extracting anionic metal species such as gold-cyanide, chromate and vanadate. These metal species are much difficult to remove from solutions.

The current work demonstrated the crab-shell biosorbent potential. Acid Washed *Ucides cordatus* Shells (AWUS) removed more metal than other excellent biosorbents such as *Bacillus* (bacterium), *Penicillium* (fungus) or *Sargassum* (alga), with metal uptakes up to 0.79 mmol V/g dry AWCS, 0.54 mmol Cr/g, and 0.17 mmol Au/g. The bound metals could easily be eluted from the biosorbent (AWUS) by a simple alkali wash. Repeating 3 adsorption-desorption cycles without performance deterioration indicated the reusability of the biosorbent.

The mechanism of anion biosorption was confirmed to be adsorption by electrostatic attraction. FTIR analyses indicated amide groups as the key sites for metal anion binding. They are particularly effective at low pH when they become fully protonated. The anionic metal speciation in the solution also played important role affecting the anion uptakes.

Biosorption study in the V-Cr binary system established that the presence of vanadate greatly depressed the Cr uptakes, however, vanadate uptake was not interfered by chromate.

The developed one-site anionic metal species adsorption equilibrium model, considering the non-ideality in the liquid phase and the interference of Cl^-, agreed reasonably well with the anion adsorption by AWUS as a function of solution pH and ionic strength. *Multi*-metal equilibrium adsorption models extended from the Langmuir model effectively described the metal interference behaviour.

RÉSUMÉ

Certains types de biomasse morte peuvent immobiliser et accumuler très efficacement des métaux lourds. Nous avons étudié un processus de biosorption à l'aide d'une biomasse résiduelle de coquilles de crabe particulièrement efficace comme agent d'extraction d'espèces métalliques anioniques comme le cyanure d'or, le chromate et le vanadate, substances difficiles à éliminer des solutions.

Nos travaux ont démontré le grand potentiel de biosorption des coquilles de crabe. La coquille d'*Ucides cordatus* lavée à l'acide (CULA) a éliminé une plus grande quantité d'espèces métalliques anioniques que d'autres biosorbants efficaces comme la bactérie *Bacillus*, le champignon *Penicillium* et l'algue *Sargassum*. Nous avons obtenu avec cette matière des degrés de biomobilisation atteignant 0.79 mmol V/g de CULA sèche, 0.54 mmol Cr/g et 0.17 mmol Au/g. Les métaux liés étaient faciles à éluer de la CULA au moyen d'un simple lavage aux alcalis. Aucune baisse de rendement n'a été notée après trois cycles d'adsorption-désorption, ce qui indique le potentiel de réutilisation de ce biosorbant.

Nous avons confirmé que le mécanisme de biosorption des anions intervenait surtout dans l'adsorption par attraction électrostatique. À l'aide d'analyses IRTF, nous avons établi que les groupes amides sont les principaux sites de fixation des anions métalliques. Ces groupes sont particulièrement efficaces lorsque le pH est bas et qu'ils sont entièrement protonés. La spéciation en solution des métaux anioniques a également une profonde incidence sur la biomobilisation des anions.

Une étude de biosorption menée à l'aide du système binaire V-Cr nous a permis d'établir que la biomobilisation du Cr était sensiblement réduite par la présence de vanadate, tandis que la présence de chromate n'avait aucun effet sur la biomobilisation du vanadate.

Compte tenu de la non-idéalité de la phase liquide et de l'interférence du Cl^-, le modèle d'équilibre d'adsorption anionique métallique à un site que nous avons élaboré concorde avec l'adsorption des anions par la CULA en fonction du pH et de la force ionique. Des modèles d'équilibre d'adsorption *multi*-métallique déduits à partir du modèle de Langmuir cadrent avec le comportement d'interférence des métaux.

PUBLICATIONS

List of Publications

Results of Section 3.1 have been published as refereed papers:

1) Niu, H. and Volesky, B. 1999. Characteristics of gold biosorption from cyanide solution. *J. Chem. Technol. Biotechnol.* 74(8), 778-784.

Results of Section 3.2 have been published as a refereed paper:

1) Niu, H. and Volesky, B. 2001. Biosorption of anionic metal complexes. *Biohydrometallurgy: Fundamentals, Technology and Sustainable Development. Part B - Biosorption and Bioremediation*. V. S. T. Ciminelli and J. O. Garcia, Eds. Elsevier Science B.V.: Amsterdam, **B:** 189-197.

Results of Section 3.6 have been published as refereed papers:

1) Niu, H. and Volesky, B. 2001. Gold adsorption from cyanide solution by chitinous materials. *J. Chem. Technol. Biotechnol.* 76(3), 291-297.

2) Niu, H. and Volesky, B. 2000. Gold-cyanide biosorption with L-cysteine. *J. Chem. Technol. Biotechnol.* 75(6), 436-442.

CONTRIBUTIONS OF CO-AUTHORS

Professor B. Volesky, the supervisor of this dissertation, co-authored all resulting publications. Except for Prof. Volesky's invaluable supervision in the biosorption research area and correction of the manuscripts, I proposed the research objectives, established the methodologies, conducted the experiments and eventually wrote drafts of manuscripts describing the results obtained.

ACKNOWLEDGEMENTS

I would like first to thank my husband, Mr. Huabing Yang. Without his tremendous support and encouragement, I would not be here to pursue my Ph.D. studies. Especially, during the past year when I was affected with an acute spinal problem, his considerable caring and warm encouragement allowed me to overcome all suffering and gave me strength to continue.

I also thank my parents, sisters and brothers, both biological and in-law, for their great support and concern for the completion of this work.

Most importantly, I would like to thank Dr. Volesky for his invaluable supervision and insight during the many aspects of this work. His input, particularly regarding the written and oral presentations of the research results, was very helpful and instructive. In addition, I am very grateful to Dr. Volesky and Chemical Engineering Department at McGill for providing me with financial support, which made it all possible.

A special gratitude is given to Dr. Honqing Liu for his advice and perception on the modeling work. I also greatly appreciated the many discussions with the bioenvironmental research group members, particularly Dr. Y. S. Yun, Dr. J. Yang, Dr. M. M. Figueira, Mr. Tom Davis and Ms. V. G. N. S. Diniz for their constructive opinions. I am also very grateful to all McGill faculty members and undergraduates who had supported and assisted my Ph.D. work.

Finally, but not least, I very much appreciated the help I received from Mr. Ed Siliauskas, who not only helped me solve problems but also found the time to explain and discuss. Special thanks are given to Mr. Michael Harrigan for his tremendous help on the corrections of the written English in this dissertation. My thanks go also to all the members in Chemical Engineering Department for making the work environment pleasant, friendly, and productive.

SYMBOLS AND ABBREVIATIONS

a	parameter adjustable in Dybel-Huckel equation
A	constant in Dybel-Huckel equation
b	parameter adjustable in Dybel-Huckel equation.
B	constant in Dybel-Huckel equation
BNH	fictitious free weak-base group on AWUS
$BNH_2^+ Cl^-$	adsorbed Cl^-
$BNH_2^+ H_xM_pL_q^{Z-} H^+_{z-1}$	adsorbed anionic metal species
$B^{(Cr)}$	chromium binding site
$B^{(Cr)}$-Cr	adsorbed Cr
$B^{(Cr)}$-V	adsorbed V on Cr binding site
$B_T{}^{(Cr)}$	total chromium binding capacity of AWUS (mmol/g)
B_T	total anionic metal binding capacity of AWUS (mmol/g)
$B_{T,2}$	total anionic metal binding capacity of the second site on AWUS (mmol/g)
$B^{(V)}$	vanadium binding site
$B^{(V)}$-Cr	adsorbed Cr on V binding site
$B^{(V)}$-V	adsorbed V
$B_T{}^{(V)}$	total vanadium binding capacity of AWUS (mmol/g)
C	sorbate C in the liquid phase
CD	adsorbed species C by site D on the solid phase
Chitosan-$NH_{i+1}^+ Cl^-$	loaded Cl^- on chitosan
Chitosan-NH_i	amino group on chitosan
Cr_T	total chromium in the solution
D	free site D on the solid phase
ΔG	free energy for the adsorption reaction (kJ/mol)
ΔH^0	enthalpy change (adsorption heat) (kJ/mol)
$H_xM_pL_q^{Z-}$	anionic metal species in the solution
i	species i in the liquid phase

I	ionic strength (M)
i_s	species i in the solid phase
${}^{ad}K_M$	equilibrium constant of $H_xM_pL_q^{Z-}$ biosorption lumping activity coefficients of the species on the solid phase $(mol/L)^{-(Z+1)}$
$\log {}^{ad}K_M$	log of ${}^{ad}K_M$
$\log {}^{ad}K_{M,2}$	log of ${}^{ad}K_M$ (in $(mol/L)^{-(Z+1)}$) for the second site
${}^{ad}K_M^{int}$	intrinsic equilibrium constant of $H_xM_pL_q^{Z-}$ biosorption $(mol/L)^{-(Z+1)}$
K_{app}	apparent adsorption equilibrium constant $(mol/L)^{-1}$
${}^{ad}K_{Cl}$	Cl^- equilibrium binding constant $(mol/L)^{-2}$
$\log {}^{ad}K_{Cl}$	log of ${}^{ad}K_{Cl}$
$\log {}^{ad}K_{Cl,2}$	log of ${}^{ad}K_{Cl}$ (in $(mol/L)^{-2}$) for the second site
$K_{Cr,i}$	chromium protolysis constant in molar scale
K_{Cr}	Langmuir constant representing the affinity of chromate for its binding sites on AWUS (L/mmol)
K_{Cr}^{V}	Langmuir constant representing the affinity of chromate for vanadate binding sites on AWUS (L/mmol)
K_{HCl}	HCl adsorption constant (L/mol)
K_{int}	intrinsic adsorption equilibrium constant (L/mol)
K_V	Langmuir constant representing the affinity of vanadate for its binding sites on AWUS (L/mmol)
K_V^{Cr}	Langmuir constant representing the affinity of vanadate for chromate binding sites on AWUS (L/mmol)
Kw	water dissociation constant $(mol/L)^2$
pKa	the logarithm of the conjugate acid dissociation constant
m	constant, equals to -0.1 in Davis equation
$M(CN)_m^{n-}$	metal cyanide complex
p	the number of metal per anionic metal species
q	the number of oxygen per anionic metal species

q_{cal}	uptake calculated by model (mmol/g)
q^{Cr}	uptake of chromium in all forms (mmol/g)
q_{exp}	uptake obtained experimentally (mmol/g)
Q_{HCl}	total binding capacity for HCl (mol/g)
Q_T	total binding capacity of HCl on chitosan (mol/L)
q^{HCl}	HCl uptake (mol/g)
q_i^M	metal initially loaded on the biosorbent (mmol/g)
q^M	equilibrium metal uptake (mmol/g)
q^V	vanadaium uptake (mmol/g)
R	gas constant
R_M	metal removal (%)
$RNH_3^+ OH^-$	ionized hydroxide of resin
ΔS^0	entropy change (kJ/mol*K)
T	absolute temperature (K)
v:	working volume of the adsorption sample (L)
w:	the dry net biosorbent weight representing the weight of the sorbent without counting the mass of loaded metals(g).
X	the number of proton per anionic metal species
Z	the charge of anionic metal species
Z_-	the anion valence of the electrolyte
Z_+	the cation valence of the electrolyte
Z_i	charge of ion i.
$\gamma_\pm$	the mean electrolyte activity coefficient
γ_i	activity coefficient of ion species i in the solution
$\gamma_{i,s}$	activity coefficient of ion species i_s on the solid phase
μ_i	chemical potential of species i in the bulk solution (kJ/mol)
$\mu_{i,s}$	chemical potential of surface species i_s (kJ/mol)
$\mu_{i,s}^0$	standard chemical potential of species i on the solid phase (kJ/mol)
μ_i^0	standard state chemical potential of species i in the solution (kJ/mol)

$\sum_i ([H_xM_pL_q^{z-}])_i$	sum of the equilibrium metal concentration in the solution (mM)
[ ]	equilibrium concentration of the species, (mmol/g) for surface species and (mM) for liquid species
$[\ ]_0$	initial concentration of species, default units same as that of [ ]
{ }	activity of the species, default units same as concentration

Abbreviation:

AWUS	Acid Washed *Ucides* Shells
Err	objective error function
RUS	Raw *Ucides* Shells

TABLE OF CONTENTS

LIST OF FIGURES

CHAPTER 3

LIST OF TABLES

CHAPTER 1

INTRODUCTION AND LITERATURE REVIEW

1.1 Sources of Heavy Metal Anions

While a large portion of current research has been oriented towards the removal of heavy metal cations, the importance of anions became a growing concern in the fields of mining, metallurgical and surface finishing industries.

1.1.1 Mining and Metallurgical Industries

In the mining processes, metals are usually extracted from the ores through a leaching process. The objective of the leaching process is to extract metals by forming metal complexes soluble in the solution and the important amounts of the formed metal complexes are very often in anionic forms. The most powerful process to extract gold from ores is the cyanide leaching process (Marsden and House, 1993a). With the oxidant, gold could be effectively extracted from ores by forming gold-cyanide complex ($Au(CN)_2^-$) dissolving in the cyanide solution, according to the following reactions (Marsden and House, 1993b).

$$2Au + O_2 + 4CN^- + 2H_2O = 2Au(CN)_2^- + H_2O_2 + 2OH^- \quad (1.1)$$

$$2Au + 4CN^- + H_2O_2 = 2Au(CN)_2^- + 2OH^- \quad (1.2)$$

$Au(CN)_2^-$ is then concentrated by adsorption - desorption technology followed by electro-winning recovery (Marsden and House, 1993c).

The predominant occurrence of gold as a native metal is often alloyed with selenium, arsenic, silver, and so on (Marsden and House, 1993d). In addition, heavy metals such as iron, copper and zinc also coexist in the gold ores. During the gold leaching process, these metals could also dissolve in the solution by forming anionic metal complexes such as SeO_4^{2-}, AsO_4^{3-} and $M(CN)_m^{n-}$ (M: Ag, Fe, Cu, or Zn) (Marsden and House, 1993b) . All these metal anions have to be separated appropriately. The mining industry constitutes one of the major sources of anionic metal complexes production.

In the extractive metallurgical industry, vanadium has been estimated to comprise about 136ppm (i.e.0.0136%) of the earth's crust rocks. It is the fifth most abundant transition metal after Fe, Ti, Mn and Zn (Greenwood and Earnshaw, 1985a). Vanadium bearing phosphate rock deposits, such as in the regions of Idaho, Montana, Wyoming and Utah, contain 0.15 to 0.35% V and small amounts of Cr, Ni and Mo as well as 24 to 32% P_2O_5 (Rostoker, 1975). The usual extraction process for vanadium is to first obtain the ferrophosphorous derivatives from the electric-furnace smelting of a charge of phosphate rock, silica, coke and iron ore. The mix is roasted at 750 – 800°C converting the vanadium, chromium and phosphorus to the water-soluble compound sodium metavanadate ($NaVO_3$), sodium chromate (Na_2CrO_4) and trisodium phosphate (Na_3PO_4). The soluble salts are extracted by leaching with water and these anionic metal species are separated so as to produce technical grade vanadium compounds. The metallurgical industry constitutes another major source of metal anions.

1.1.2 Surface Finishing Industries

Metal finishing industries include electroplating, anodizing, chromating and electroless plating operation. The objective of all these processes is to enhance the physical appearance, strength, and/or corrosion resistance of surfaces of various objects. The liquid effluents generated by these processes are the spent plating baths and the

process rinse water. According to a survey of Canadian surface finishing industries performance (EPS, 1987a), 275 companies discharged in total 1,364 m^3 of wastewater per year. Within the pollutants, Cr reaches a significant average amount of 50ppm, whereby Cr could be either in Cr (VI) or Cr (III) forms. The primary toxic effect of chromium is its ability to cause genetic damage (Jaworski, 1985). This arises from the ability of its ions to cross the cell boundaries. Hexavalent chromium such as CrO_4^{2-} can cross the cell and the nuclear membranes much more easily than trivalent chromium. Once inside a cell, Cr (VI) ion will tend to be reduced to Cr^{3+}. The presence of Cr^{3+} can affect DNA synthesis and the structure of chromosomes. Thus the hexavalent Cr ion is considered to be a more toxic form (Jaworski, 1985). The standard limit for Cr in the surface finishing effluents is 1 mg/L (EPS, 1987b). Surface finishing effluent constitutes another major source of anion treatment in waste management.

1.2 Properties of Anionic Metal Species

Anionic metal species demonstrate different solution chemistry according to their charge state and characteristics of their complexes. Some anions are very stable, existing as completely dissociated anions. Some are prone to hydrolyze by protonation or deprotonation, and others even demonstrate complicated speciation behavior. Even though some metals are initially in anionic forms such as $Au(CN)_2^-$, CrO_4^{2-} and VO_4^{3-}, they could exist as different kinds of species dissolving in the aqueous solution depending on the solution conditions. A good knowledge of the solution chemistry of the anionic metal species is necessary in understanding the metal removal mechanism.

In order to explain the solution chemistry of metal anions, $Au(CN)_2^-$, CrO_4^{2-} and VO_4^{3-} were selected as examples because of their application background representing the mono-valent, divalent or multi-valent heavy metal anions, respectively.

$Au(CN)_2^-$: Gold-cyanide complex is very stable, the dissociation constant of Au from the cyanide complex is $10^{-38.9}$ (Marsden and House, 1993e). Under conventional conditions (room temperature), it does not dissociate readily (Eaton et al., 1995a). Even at 85°C, it has to be with the catalyst to make Au dissociate from the complex (Eaton et al., 1995a). $Au(CN)_2^-$ could exist as a stable mono-valent anion in the aqueous solution (Marsden and House, 1993b). The form of $HAu(CN)_2$ was found only under very acidic conditions such as 0.5 – 1 N H_2SO_4 (Sillen and Mortell, 1964c). In the gold leaching process, gold is concentrated by steam activated carbon containing strong or weak-bases.

Gold-cyanide could be reducible in the presence of a strong reducer such as Zn, which is used to precipitate Au from a cyanide complex to have elemental Au (Marsden and House, 1993c).

CrO_4^{2-}: Chromate is a typical divalent heavy metal anion. It is prone to protolysis in aqueous solution (Sillen and Mortell, 1964a; Baes and Mesmer, 1976c; Greenwood and Earnshaw, 1985c; Cabatingan et al., 2001).

Chromate exists in different ionic forms and as neutral acid as well in aqueous solution. The distribution of species is dependent on the total chromate concentration and the pH of the solution. The following equations represent the equilibria governing that distribution in aqueous solution at 25°C:

$$H_2CrO_4 = HCrO_4^- + H^+ \qquad (1.2.1)$$

$$Kcr,1 = \frac{\{HCrO_4^-\}\{H^+\}}{\{H_2CrO_4\}} = 10^{0.26} \quad \text{(mol/L)} \qquad (1.2.2)$$

$$HCrO_4^- = CrO_4^{2-} + H^+ \qquad (1.2.3)$$

$$Kcr,2 = \frac{\{CrO_4^{2-}\}\{H^+\}}{\{HCrO_4^-\}} = 10^{-5.9} \quad \text{(mol/L)} \qquad (1.2.4)$$

$$2HCrO_4^- = Cr_2O_7^{2-} + H_2O \qquad (1.2.5)$$

$$Kcr,3 = \frac{\{Cr_2O_7^{2-}\}}{\{HCrO_4^-\}^2} = 10^{2.2} \qquad (mol/L)^{-1} \qquad (1.2.6)$$

$$HCr_2O_7^- = Cr_2O_7^{2-} + H^+ \qquad (1.2.7)$$

$$Kcr,4 = \frac{\{Cr_2O_7^{2-}\}\{H^+\}}{\{HCr_2O_7^-\}} = 10^{0.85} \qquad (mol/L) \qquad (1.2.8)$$

Kcr,i is the corresponding protolysis constant. { } represents the activity of the species.

Since the equilibrium constant for the first order dissociation constant of $H_2Cr_2O_7$ is too large, the equilibrium of this protolysis reaction is not considered (Greenwood and Earnshaw, 1985c).

Chromate is reducible. With reducers such as sulphur dioxide, sodium bisulfite, sodium metabisulfite and ferrous sulfate (EPS, 1977; Greenwood and Earnshaw, 1985d), Cr(VI) could be rapidly reduced to Cr(III) at low pH. This characteristic forms the fundamentals for Cr(VI) removal by precipitation. Only when Cr(VI) is reduced to Cr(III), the precipitation of Cr could be conducted through forming $Cr(OH)_3$.

VO_4^{3-}: Vanadate (V), representing multi-valent metal anion, appears in more complicated forms than the above metals when it is in aqueous solution (Sillen and Mortell, 1964a; Pope and Dale, 1968; Kepert, 1973; Baes and Mesmer, 1976b; Greenwood and Earnshaw, 1985e; Gupta and Krishnamurthy, 1992e; Larson, 1995). At pH13, colorless vanadium (V) is orthovanadate VO_4^{3-}. As pH decreases, other forms of anionic species of V(V) such as $VO_3(OH)^{2-}$, $V_2O_7^{4-}$, $V_4O_{12}^{4-}$, $V_3O_9^{3-}$, $VO_2(OH)_2^-$, $V_{10}O_{27}(OH)^{5-}$, and $V_{10}O_{26}(OH)_2^{4-}$ occur . At the lower pH range of 1-4, there are even cationic VO_2^+ and neutral V_2O_5 and $VO(OH)_3$ produced. The distribution of species of V(V) presenting in the solution depends on solution pH and vanadium concentration at specific temperatures. The species distribution relationship and equilibrium constants were well documented (Sillen and Mortell, 1964a; Larson, 1995).

V (V) could be reduced to V (IV), V (III) and V, however, in the presence of air, V(V) is the most stable oxidized state of vanadium in aqueous solution (Gupta and Krishnamurthy, 1992e).

According to the characteristics of the heavy metal anions, the following conventional methods have been developed to remove metal anions.

1.3 Conventional Treatment for Removal of Heavy Metal Anions

1.3.1 Activated Carbon

The activated carbon process has been conventionally used to extract heavy metals from solution. The raw materials for activated carbon are coal, peat, leather, almond shell, coconut shell and many other carbon containing materials. The activated carbon could be divided into three categories depending on the ways to be activated, i.e. L-carbon, H-carbon and steam carbon (Mattson and Mark Jr., 1971). H-carbon and Steam carbon activated at a temperature higher than 750°C or by steam, mainly containing strong or weak-base functional groups, are used for anion adsorption, while L-carbon activated at lower than 400°C generates acidic groups for cation adsorption.

The activated carbon process has been used for the removal of anions such as gold-cyanide, chromate, and vanadate (Gupta and Krishnamurthy, 1992a; Marsden and House, 1993f; Ouki and Neufeld, 1997). However, usually an abundance of other inorganic or organic materials also dissolved in the solution often occurs causing sorbent fouling. Generation of activated carbon usually takes place under harsh acidic conditions that make the carbon fragile. In an example of gold extraction, in each adsorption-desorption cycle, the carbon could lose 40 % of its original weight (Marsden and House, 1993g).

1.3.2 Ion Exchange

Ion exchange has also been applied to anionic metal species recovery. Anion exchanger could be either strong-base resin or weak-base resin. While anion adsorption by strong-base resin is usually pH independent, that by weak-base resin is very much pH dependent. As the binding on strong-base resin is usually strong, the elution of the resin needs to be with other anions having higher affinity. However, adsorption on weak-base resin is weaker and the elution is very easy, simple by hydrolysis with sodium hydroxide, as is done in gold-cyanide adsorption by weak-base resin (Gupta and Krishnamurthy, 1992b; Marsden and House, 1993h). Weak-base resins are usually characterized by primary, secondary, and tertiary amine. The continuous removal of heavy metals by ion exchange takes place in fixed-bed columns that are packed with resins. The selectivity of ion exchange resins is high, however, the resins are prone to fouling by organic substances also (Harland, 1994). Ion exchange resins are expensive. Therefore, in order to keep the operating cost sufficiently low, the ion exchange processes are usually applied only to effluents that are otherwise "clean" and contain a medium or low level of heavy metals.

1.3.3 Solvent Extraction

Solvent extraction involves the interchange of ions between an aqueous solution and a liquid organic solvent. The whole solvent extraction process essentially consists of three steps: (1) extraction, (2) scrubbing, and (3) stripping (Gupta and Krishnamurthy, 1992d). The extraction refers to the initial transfer step in which the main solute, often together with some of the impurities is transferred from the aqueous feed to solvent. Scrubbing is the process of selectively removing the co-extracted solutes (impurities) from the loaded solvent by treatment with a new immiscible (aqueous) liquid phase. Stripping is the process of recovering main solute(s) from the loaded solvent or extract

back into aqueous phase. Solvent extraction process has been applied for the separation of anionic metal complexes such as gold-cyanide and vanadate (Gupta and Krishnamurthy, 1992d; Marsden and House, 1993i). Liquid extractants offer some potential advantages over activated carbon and ion exchange resin; namely rapid extraction kinetics and high metal loading. However, unlike carbon materials, liquid extractants' potential use is likely to be restricted to treatment of clarified solutions. Also, liquid extractants have some solubility in water that results in solvent losses to the aqueous phase.

1.3.4 Precipitation

The removal of heavy metals by precipitation is based on the low solubility of heavy metal compounds. The treatment consists of two stages. In the first stage, insoluble solid metal compounds are formed. Then the solids are removed from water by sedimentation in a settling tank. While cationic metals could be usually precipitated with hydroxides, anionic metal complexes have to undergo more complicated high cost procedures such as reduction or organic complexation (Heininger and Meloan, 1992; Marsden and House, 1993c).

In the case of $Au(CN)_2^-$, gold could be precipitated with zinc from hot, higher grade gold-cyanide bearing solution produced by carbon purification process (Marsden and House, 1993c). This process has been applied widely for gold recovery process.

Cr(VI) could be also removed by precipitation. Under this method, Cr (VI) has to be first reduced to Cr(III) and precipitate according to (EPS, 1977):

$$3SO_2 + 2H_2CrO_4 = Cr_2(SO_4)_3 \downarrow + 2H_2O \qquad (1.3.1)$$

$$4H_2CrO_4 + 3Na_2S_2O_5 + 3H_2SO_4 = 3Na_2SO_4 + 2Cr_2(SO_4)_3 \downarrow + 7H_2O \qquad (1.3.2)$$

Vanadium could be precipitated by co-precipitation technology with ferric or ferrous salts (Gupta and Krishnamurthy, 1992c; Nurdogan and Meyer, 1995), or organic complexants (Heininger and Meloan, 1992).

The efficiency of the treatment hinges on the rates of formation and of settling of the insoluble metals. The fact that those rates are usually very low with low metal content leads to an increase in the consumption of precipitation agents and to the design of large mixing and settling tanks. Therefore, the removal of heavy metal by precipitation from diluted effluents is not economical. Furthermore, the treatment generates toxic sludge, which has to be dewatered, stabilized and disposed of.

In summary, the disadvantages of the above conventional methods arise an incentive to develop an alternative technology for effective metal anion removal.

1.4 Biosorption

1.4.1 Description of Biosorption Technology

Biosorption is a process, which utilizes inexpensive non-living biomaterials to sequester heavy metals. Biosorbents are prepared from the naturally abundant and/or waste biomass of algae, moss, fungi, bacteria or parts of plants and animals, that is inactivated and usually pretreated by washing with acid or base before final drying (Volesky, 1990a). While simple cutting or grinding of the dry biomass may yield stable biosorbent particles (Fourest and Roux, 1994), some types of biomass have to be either immobilized in a synthetic polymer matrix (Jeffers and Corwin, 1993) or grafted on an inorganic support material such as silica in order to yield particles with the required mechanical properties (Mahan and Holcombe, 1992). The biosorption process can operate in cycles consisting of loading, regeneration, and rinsing (Jeffers et al., 1991). The operation commences by combining the sorbent material with metal-bearing

effluents. Heavy metals are then taken up from the liquid by the biosorbent. When the metal sorption capacity of the biosorbent is exhausted, the biosorbent may be regenerated with solutions of acids or hydroxides. The regeneration produces small volumes of heavy metal concentrates suitable for conventional metal recovery processes (Brierley et al., 1986; Aldor et al., 1995).

As compared to conventional methods for removing toxic metals from industrial effluents, such as activated carbon sorption, ion exchange, solvent extraction or precipitation, the biosorption process offers: 1) low operating cost; 2) minimization of the volume of chemical sludge to be disposed of; and 3) high efficiency in detoxification of very diluted effluents. These advantages have served as the primary incentives for developing full-scale biosorption processes for heavy metal removal.

1.4.2 Achievements over the Past Decade

Pioneering research in the field of biosorption has led to the identification of a number of effective biosorbents. The operation factors such as pH and ionic strength during the biosorption processes have been studied, in some cases revealing their relevance to the biosorption behavior. Even though the biosorption mechanism has not been clarified thoroughly, several kinds of possible mechanisms involved in metal biosorption have been revealed. The following parts summarize the main achievements in the study of biosorption field.

1.4.2.1 Biomass Types

Although many biological materials bind heavy metals, only those with sufficiently high metal binding capacity and selectivity for heavy metals are suitable for

use in full-scale biosorption processes. The first major challenge for the biosorption field was to select the most promising types of biomass from an extremely large pool of readily available and inexpensive biomaterials. While this task has not been completed, a good number of biomass types such as *Bacillus subtilis, Penicillium chrysogenum* and *Sargassum sp.* have been tested for cationic metal binding capabilities under various conditions (Holan et al., 1993; Niu et al., 1993; Schiewer, 1996a; Ghafourian and Latifi, 2001).

The research of anion biosorption gained momentum relatively recently. Kuyucak tested the removal of gold chloride ($AuCl_4^-$) by brown alga *Ascophyllum nodosum* (Kuyucak, 1987) indicating that Au(III), some of it reduced to Au(I) as well as elemental gold, could constitute up to 40% of the alga's dry weight.

Studies of hexavalent Cr(VI) binding by peat moss (Sharma and Forster, 1993), corncob (Bosinco et al., 1996), and *Sargassum natans* (Kratochvil et al., 1998) revealed that, while some Cr(VI) was sorbing onto the biomass, a portion of the initial Cr(VI) was reduced to Cr(III) over the course of equilibration and a part of Cr was bound as Cr(III).

The binding of molybdate (MoO_4^{2-}) by chitosan or chitin has recently been studied (Milot et al., 1997; Guibal et al., 1999). In order to avoid the dissolution of biosorbent beads under acidic conditions, the chitosan was partially cross-linked with glutaraldelyde. Dambies et al. (1999) studied arsenic sorption on molybdate-impregnated chitosan gel beads. It was found that the sorption capacity of raw chitosan for As(V) was increased by impregnation with molybdate. While the extraction of chitin or chitosan is costly, natural biomaterials containing them do have a potential for anion adsorption.

1.4.2.2 Characteristics of Biosorption

The particular amount of metal bound depends not only on the given biosorbent but also on the type of the metal ion, its concentration as well as other physico-chemical

factors such as the solution temperature, pH, ionic strength and ion interference by other metals present.

Temperature Effect

It was noted that the temperature could influence the sorption process. Kuyucak and Volesky (Kuyucak and Volesky, 1989a) observed that the binding of Co by the brown alga *Ascophyllum nodosum* increased by 50-70% when the temperature was raised from 4 to 23°C. With further temperature increase to 40°C the binding increased only slightly, whereas temperatures of 60°C or more caused a change in the texture of the sorbent and a loss in the sorption capacity.

The effect of temperature on biosorption depends on the adsorption heat (enthalpy change). The intrinsic adsorption equilibrium constant K_{int} could be described thermodynamically as follows (Stumm and Morgan, 1996b):

$$K_{int} = \exp\left(\frac{-\Delta H^0 + T\Delta S^0}{RT}\right) \tag{1.4.1}$$

$$= \exp\left(\frac{-\Delta H^0}{RT}\right)\exp\left(\frac{-\Delta S^0}{R}\right) \tag{1.4.2}$$

where ΔH^0 is the enthalpy change (adsorption heat), ΔS^0 is the entropy change, R is gas constant and T is the temperature. For physical adsorption, adsorption heat $\Delta H^0 < 0$, adsorption reaction is exothermic and preferred at lower temperatures. For chemisorption, $\Delta H^0 > 0$, adsorption reaction is endothermic and favored at higher temperatures. This corresponds to the observation of Hang and Smidsord (Haug and Smidsrod, 1970) for alkaline earth metal binding to alginate where the reaction was exothermic. For the binding of Cu, however, the reaction exhibited a positive enthalpy change (i.e. was endothermic), since the equilibrium constant rose with temperature.

A natural biomass usually contains more than one type of sites for metal binding. The effect of temperature on each kind of site can thus contribute to the overall metal uptake. This was confirmed in Cu adsorption by potassium-saturated microbial biomass (Weppen and Hornburg, 1995). For most metals, the heat of reaction was constant, independent of the degree of site occupation. For Cu, however, the heat of reaction decreased with increasing degree of site occupation from 27 to 14 kJ/mol, indicating the involvement of different binding sites or the formation of different types of Cu complexes with the biomass. For other heavy metals, the heat of adsorption reaction was between ~7-11 kJ/mol, for light metals between ~2.1-6 kJ/mol (Weppen and Hornburg, 1995).

In conclusion, for practical applications of biosorption a reasonably narrow temperature range can be expected (Schiewer, 1996c). In this range, the effect of temperature is small as compared to other influencing factors (Tsezos and Deutschmann, 1990).

Influence of pH

Of great importance in both cation and anion biosorption is the pH value of the solution. However, the optimum pH for anion biosorption is opposite to that of cation biosorption. While cation biosorption is favored at increased pH > 4.5 (Schiewer and Volesky, 1995; Kratochvil, 1997), anion adsorption is preferred in a lower pH range of 1.5-4 (Giles and Hassan, 1958; Giles et al., 1958; Kuyucak and Volesky, 1989a; Roberts, 1992a). This was determined based on the characteristics of the biomass as well as considering the speciation of metals in the solution.

There are three ways how the pH can influence metal biosorption (Schiewer, 1996b).

First, the state of the active sites could be changed by the solution pH. When the metal binding groups are weakly acidic or basic, the availability of free sites is dependent on the pH. In the case of dye with $-SO_3^-$ adsorption by chitin, only when chitin amide groups were protonated with a positive charge, the dye could be effectively bound through its anionic sulfate group onto the positively charged chitin amide groups (Giles and Hassan, 1958; Giles et al., 1958). Chromate adsorption by chitosan was enhanced by lowering pH to 5.7 and was relatively independent of pH from pH 2.5 to pH 5.7 (Roberts, 1992f). The logarithm of the conjugation acid dissociation constants (p*Ka*) could be one of the key parameters in determination of the optimum pH for charging the sites. It was determined that p*Ka* of chitin is lower than 3.5 and that of chitosan is 6.5 (Domard, 1987; Roberts, 1992a). For chitinous materials, if the anion binding is through electrostatic attraction, when the solution pH is increased, the bound anions could be eluted from the sorbents.

Second, the speciation of the metal in solution is pH dependent, whereas metals in aqueous solutions occur as hydrolyzed ions when pH is low, especially metal anions of high charge and a small size (Stumm and Morgan, 1970a; Baes and Mesmer, 1976a; Morel, 1983). The speciation of metal anions was shown (in Section 1.2 in this thesis) using chromate and vanadate as examples. Biosorption behavior of those anionic metal species systems is expected to be affected by the anionic speciation.

Third, extreme pH values, as they are employed for regeneration (desorption) of the sorbent, may damage the structure of the biosorbent material. Distortion of cells was observed under the microscope, accompanied by significant biomass weight loss and decrease in the sorption capacity (Kuyucak and Volesky, 1989b).

Ionic Strength Effect

The influence of ionic strength on biosorption had not been established until Schiewer and Volesky (Schiewer, 1996a) systematically studied the effect of ionic

strength on the biosorption of cations such as Zn, Cd, Cu and Na. The increased ionic strength suppressed biosorption as a result of the increased electrostatic charge. It was also established that the effect of ionic strength on adsorption is relevant to the way that the metal is bound. Electrostatic attraction based adsorption, such as that of Na, is severely affected by increased ionic strength (Hayes and Leckie, 1987).

Presence of Other Anions

Other sorbable ions in the solution may compete with the metals of interest for sorption sites. The binding of the primary metal ion is then decreased.

For cation biosorption, it was concluded that the light metals (Schiewer, 1996a) bind less strongly than the heavy metal ions. The overall affinity sequence follows that established in the metal adsorption by the ion exchange resin.

For anion biosorption, no studies systematically addressed the interference of other anions on the adsorption of anions of interest. However, the study of anion exchange established that the selectivity of anion exchanger could be enhanced by the counter ion of higher valence, with the smaller (solvated) equivalent volume and greater polarizability, and interacting more strongly with the fixed ionic groups on the matrix and participating least in complex formation with the co-ion. The established affinity is as follows (Helfferich, 1995): $SO_4^{2-} > I^- > NO_3^- > CrO_4^{2-} > Br^- > SCN^- > Cl^- > F^-$. Among the three strong acids, SO_4^{2-}, NO_3^- and Cl^-, Cl^- has the lowest affinity for the resin. Therefore, it would be appropriate to use strong electrolyte Cl^- salts as background electrolyte for ionic strength control.

1.4.2.3 Mechanism of Biosorption

The metal binding in biosorption has been attributed to a number of different sequestration mechanisms such as adsorption, ion exchange and micro-precipitation (Volesky, 1990b). It is a recognized fact that a combination of several mechanisms, each functioning independently, can contribute to the overall metal uptake. In the studies of biosorption conducted so far, very little attention has been paid to the examination of a well-defined metal uptake (by a specific mechanism) as opposed to the overall uptake where several types of sequestration may be taking place simultaneously. Systematic understanding of the metal uptake mechanisms and their relationships may greatly clarify the otherwise confusing broad definition of biosorption in the literature.

In the context of this work, the term adsorption refers to binding of a solute to free sites that are previously not occupied by other ions. If the sites are initially occupied by other ions and if this second ion is released upon the binding of the first ion, then the term ion exchange is used.

Adsorption and ion exchange can be the results of three kinds of binding forces. One is a chemical force, another is physical force, and the third is the combination of both. Chemical forces extend over a very short distance (0.1-0.2 nm) (Myers, 1991). This type of bond is rather strong, ranging from 20 – 900 kJ/mol (Stumm and Morgan, 1970b; Myers, 1991; Smith, 1981). Covalent bonds are formed by merging electron clouds such that a non-ionic molecule is formed. These bonds are directional (characteristic bond angles and lengths) and localized (Myers, 1991).

Physical forces can be subdivided into electrostatic and London-van der Waals forces (Myers, 1991). The energy of physi-sorption is reported as 2-20 kJ/mol and 20-40 kJ/mol by Smith (Smith, 1981) and Pagenkopf (Pagenkopf, 1978), respectively. In the resulting bonds, the electrons stay in their original systems. Electrostatic (or coulombic) forces between ions or between ions and dipoles extend over a long range and are the strongest among the physical bonds (Myers, 1991) with energies >> 40 kJ/mol (Stumm

and Morgan, 1970b). The interaction is repulsive for ion charges of the same sign and attractive for unlike charges. The magnitude of the force is proportional to the charge of each ion and inversely proportional to the square of the distance between the ions.

London-van der Waals forces can be divided into three categories: dipole-dipole interaction (creating orientational energy), dipole-induced dipole interaction and the London dispersion force (Myers, 1991). The first two are closely related to coulombic forces while the last one is of a quantum-mechanical nature and acts over a long range of up to ~10 nm (Myers, 1991). The energy of the dispersion force (8-40 kJ/mol) is larger than the one of orientational or induced dipole (or: polarization (Westall, 1987) energy (<8 kJ/mol) (Stumm and Morgan, 1970b). An example of a typically strong (almost ionic) dipole interaction is hydrogen bonding. It occurs between molecules in which H is bound to a very electronegative atom such as N or O (Russell, 1980).

It was confirmed that the metal cation biosorption by *Sargassum* involved ion exchange (Schiewer, 1996a). In the case of heavy metals, the binding force is chemical–sorption through the formation of covalent bonds (Figueira et al., 1999). However, in the case of most alkaline metal cations, the binding is by electrostatic forces.

The mechanism of anion biosorption has only been studied relatively recently. Kratochvil (1997) had proposed a mechanism of chromate adsorption by *Sargassum*, whereby anionic chromate was bound through acid adsorption:

$$\text{Biomass} + H^+ + HCrO_4^- = \text{Biomass-}H_2CrO_4 \qquad (1.4.3)$$

some of the chromate was reduced by *Sargassum* to Cr(III) that was then bound onto the acidic groups on *Sargassum*.

In $AuCl_4^-$ adsorption by *Sargassum*, Au(III) was reduced to Au(I) and elemental gold. Biosorption mechanism involved the redox, ion exchange as well as micro-precipitation (Kuyucak and Volesky, 1989c).

Giles et al. described (Giles and Hassan, 1958; Giles et al., 1958) dye with $-SO_3^-$ adsorption by chitin as follows:

$$\text{chitin-NH} + H^+ + \text{Dye}-SO_3^- = \text{chitin} - NH_2^+ - {}^-SO_3\text{-dye} \quad (1.4.4)$$

They attributed the dye adsorption by chitin amide to the electrostatic attraction.

However, the anion adsorption mechanism is determined not only by the functional groups on the sorbents but also by the characteristics of anionic metal solutes.

In conclusion, the study of anionic metal species biosorption is just at the initial stage. The major challenges for this field are to select the most promising types of biomaterial, determine the characteristics of the metal binding and eventually elucidate the mechanism of anionic metal species biosorption.

1.5 Properties of Crab Shells

Chitin-containing biomaterials have been recognized as effective biosorbents for metal removal (Muzzarelli, 1977; Muzzarelli et al., 1981; Dambies et al., 1999; Guibal et al., 1999). Chitin is a natural polysaccharide consisting of (1, 4) 2-acetamide-2-deoxy-D-glucose units, some of which are deacetylated (chitosan) (Roberts, 1992c). The ability of chitin/chitosan to form complexes with metal ions, particularly transition and post-transition metal ions, is well documented (Muzzarelli, 1973b; Muzzarelli, 1977; Roberts, 1992m). The study of the uptake of dyes by chitin (Roberts, 1992d) showed the potential of chitin for anion adsorption. Chitin can be obtained from fungi, insect, lobster, shrimp and krill, but the most important commercial sources are the exoskeletons of crabs obtained as waste from seafood industrial processing (Roberts, 1992e). It is estimated that millions of tons of crab shell waste material are disposed of by the seafood industry annually (Roberts, 1992n).

1.5.1 Composition of Crab Shells

Chitin of crab shells makes up to 58-85% of their organic fraction (Roberts, 1992g). In addition, crab shells contain sclerotins (an insoluble protein that serves to stiffen the chitin of the cuticle of arthropods) 10-32% of the dry shell weight. The main inorganic material is $CaCO_3$. Other metal contents may vary dependent on the location of occurrence. In crab shells, chitin is closely associated with proteins, inorganic material, pigments and lipids (Roberts, 1992h).

Extracting each major shell component, followed by an appropriate chemical analysis, can determine the composition of specific crab shells. The inorganic content can be determined from the amount of shell ash (AOAC, 1984). The metal elements can be measured by dissolving the ash and analyzing the metal concentration with ICP-AES. The minerals can also be removed directly from the shells, which is called demineralization (Roberts, 1992h). Usually it is conducted by a variety of acids including HCl, HNO_3, H_2SO_4, CH_3COOH and HCOOH. The most widely used acid for this purpose is HCl. Roberts (Roberts, 1992h) summarized the conditions for a number of processes. The concentration of HCl used may vary from 0.2 to 2 M. The extraction is carried out at room temperature for 2-48 hrs.

Crab shell protein could be extracted by a wide range of agents including NaOH, Na_2CO_3, $NaHCO_3$, KOH, K_2CO_3, $Ca(OH)_2$, $NaHSO_3$, $CaHSO_3$, Na_3PO_4 and Na_2S, but NaOH is preferred in the literature (Roberts, 1992h). Protein extraction could be conducted at either room temperature or 65-100°C for 1-72 hrs (Bemiller and Whistler, 1962; Roberts, 1992h). Protein could be analyzed by either Kjeldahl Nitrogen (AOAC, 1990) or Biuret reaction (Roberts, 1993).

Pigment could be measured by extracting it with ethanol or acetone and its content could be obtained by weight difference (Roberts, 1992h).

Chitin is determined gravimetrically after removing protein, minerals, pigments and moisture (Ferrer et al., 1996).

1.5.2 Main Biomolecules in Crab Shells

Chitin

Chitin is one of the most abundant organic materials in crab shells. It is a natural polysaccharide consisting of (1, 4) 2-acetamide-2-deoxy-D-glucose units, some of which are deacetylated (chitosan) (Roberts, 1992i). The structure of chitin is:

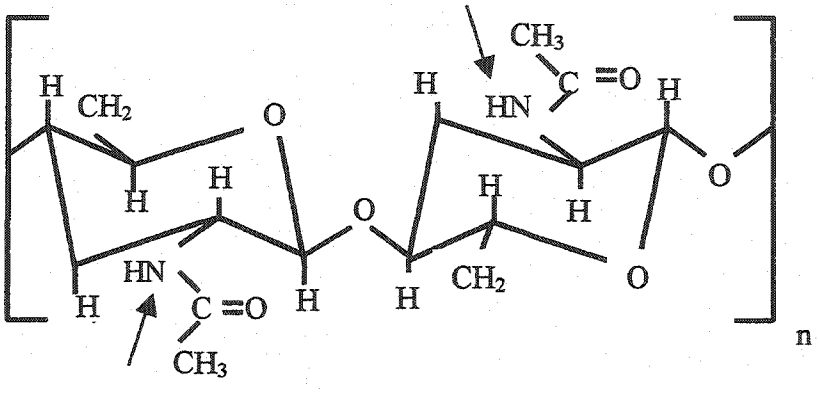

And that of chitosan is

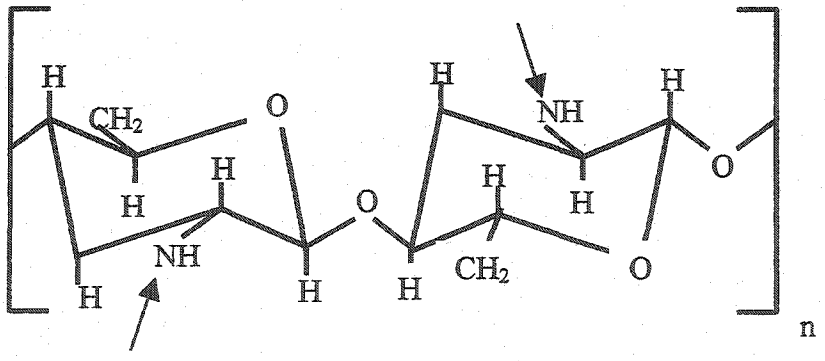

While the names "chitin" and "chitosan" are widely used in the literature, neither term represents a unique chemical structure. The terms chitin and chitosan describe a continuum polymorphic form of copolymers of N-acetyl–D–glucosamine and D-glucosamine residues, the two being distinguished by insolubility or solubility in dilute aqueous acid solutions (Roberts, 1992i). The N-acetylation degree, i.e. the percentage of acetylated amine, could be determined by titration, overall N/C ratio in chitin, or NMR spectroscopy (Roberts, 1992p).

There are three categories of chitin (Roberts, 1992j): α –, β – and γ-chitin. In α-chitin, the chains are anti-parallel, in β -chitin, they are parallel, and in γ -chitin, two chains come "up" to each chain "down". The most abundant form is α-chitin found where extreme hardness is required, as in arthropod cuticle, and is frequently associated with sclerotised protein (chitin proteoglycan), or inorganic materials or both. The strength of chitin is determined by the N-acetylation degree, i.e. the percentage of acetylated amine group (called amide). Natural chitin usually exhibits high N-acetylation degree (Roberts, 1992j). The acetyl group can be dissociated under strongly basic conditions aided by heating. As N-acetylation degree is increased, the solubility of chitin is increased in acidic solutions.

Similar to conventional amine family, the N atom of the chitin amide group or chitosan amine group is able to donate and share the lone electron pair with the empty orbit of other cations, featuring thus with weak-base characteristics. The conjugated acid dissociation constant p*Ka* of chitosan is 6.5 (Domard, 1987), and that of chitin is <3.5 (Roberts, 1992a).

Therefore, only when the solution pH is lower than the corresponding p*Ka*, the amine/ amide sites could be effectively protonated with a positive charge, and an anion could thus be bound.

Protein

Crab shell protein is usually sclerotised and cross-linked with chitin to strengthen the shells (Roberts, 1992h). In protein, the α-carboxyl group of one amino acid is joined to the α-amino group of another acid by a peptide bond (also called amide bond) (Stryer, 1988). The acid-base constants of some major sites of proteins at 25°C were summarized by Buffle (Buffle, 1988b). The study results of protein from five different sources of crab shells showed the main residual amino acids to be aspartic acid, glycine and serine. However, there doesn't appear to be an universal chitin proteoglycan (Roberts, 1992k).

Chitin-Protein Complex

As stated above, chitin from animal sources usually occurs in association with protein functioning as a lower modulus matrix surrounding the chitin. In crab shells, the complex of chitin proteoglycan is more important than any of the separated form. It was concluded that the true chitin proteoglycan has covalent bonds between the chitin and protein. Another conclusion suggested that protein link with chitin is most probably through the protein amide linking with the C-1, N-glycosidic or C-2,N-acylglucosaminyl structure (Roberts, 1992l).

Despite the convincing evidence of chitin-protein covalent bonds, other evidence indicates that not all the chitin chains are linked to protein molecules. Electron-microscopy studies (Roberts, 1992l) have shown two morphological types of the complex, one in which cylindrical chitin fibrils are imbedded in a protein matrix in an approximately hexagonal packing arrangement, and the other in which the chitin is arranged in layers interspersed with layers of protein. It was concluded that protein chains are only bound to chitin chains at the chitin/protein interface.

This chitin-protein complex is very stable and could not be easily destroyed by mild acid/base treatment. It is the complex structure that prevents crab shell effectively

penetrable and swelling in aqueous solutions (Roberts, 1992o) as it also provides a strong supporting structure naturally grafted with functional groups.

Chitin and chitosan show a promising potential for metal removal. However, the processes to extract these molecules in purified forms are relatively costly. Furthermore, chitosan is soluble in acidic solutions and therefore it needs to be cross-linked to strengthen its structure when it is to be used in adsorption processes. As a result, there arises an incentive to examine the possibility of using crab shells as a natural biosorbent material that may only require a simple and cheap pretreatment by acid washing.

1.6 Adsorption Equilibrium Modeling

In order to quantitatively describe an adsorption phenomenon, a mathematical model is required. Generally, the basic adsorption reaction could be described as follows:

$$C + D = CD \tag{1.6.1}$$

C represents the species C in the liquid phase, D represents the free site D on the solid phase. CD represents the adsorbed species C by site D.

Applying the chemical potential (Stumm and Morgan, 1996c) to each component i in the bulk solution, the corresponding chemical potential μ_i,

$$\mu_i = \mu_i^0 + RT \ln \{i\} \tag{1.6.2}$$

$$= \mu_i^0 + RT \ln [i]\, \gamma_i \tag{1.6.3}$$

$$= \mu_i^0 + RT \ln [i] + RT \ln \gamma_i \tag{1.6.4}$$

where μ_i^0 is the standard chemical potential of species i, { }and [ ] represent the concentration and the activity, respectively. γ_i is the activity coefficient of species i, defined so that it equals 1 at the reference state.

Then the chemical potential of surface species i_s, $\mu_{i,s}$ could be defined similarly as above,

$$\mu_{i,s} = \mu_{i,s}^{0} + RT \ln \{i_s\} \quad (1.6.5)$$

$$= \mu_{i,s}^{0} + RT \ln [i_s] + RT \ln \gamma_{i,s} \quad (1.6.6)$$

where $\mu_{i,s}^{0}$ is the standard chemical potential of species i on the sorbent, $\{i_s\}$is the activity of species i_s, $[i_s]$ and $\gamma_{i,s}$ are the corresponding concentration and activity coefficient of i. Again $\gamma_{i,s}$ tends to 1 at the reference state condition.

At equilibrium, the free energy for the adsorption equation, ΔG,

$$\Delta G = 0, \ \ i.e. \ \Delta\mu_i = 0, \quad (1.6.7)$$

Therefore, for an adsorption equilibrium

$$\mu_{CD,s} - \mu_C - \mu_{D,s} = 0, \quad (1.6.8)$$

Substituting the chemical potentials in the above equation by the corresponding expressions defined as above,

$$\mu_{CD,s}^{0} - \mu_C^{0} - \mu_{D,s}^{0} + RT \ln \frac{[CD_s]}{[C][D_s]} \frac{\gamma_{CD,s}}{\gamma_C \gamma_{D,s}} = 0 \quad (1.6.9)$$

Since:

$$\mu_{CD,s}^{0} - \mu_C^{0} - \mu_{D,s}^{0} = -RT \ln K_{int} \quad (1.6.10)$$

where K_{int} is the intrinsic adsorption equilibrium constant. Combining the above two equations:

$$K_{int} = \frac{[CD_s]}{[C][D_s]} \frac{\gamma_{CD,s}}{\gamma_C \gamma_{D,s}} \quad (1.6.11)$$

In the actual conditions of adsorption, γ_i and $\gamma_{i,s}$ usually differ from 1, which means that both liquid phase and solid phase are non-ideal. However, under some specific conditions when one phase differs from the ideal state far more seriously than the other, it is usual to lump the species activity coefficients of other phases to the

equilibrium constant to reduce the complexity and focus on the key problem affecting the equilibrium. This extra thermodynamic treatment can simplify the mathematical calculations involved in both the area of engineering application and thermodynamic theory. However, if all phases differ from the ideal state seriously, the non-ideality of each phase has to be considered in the modeling.

According to the consideration of non-ideality in either liquid or solid phase in the adsorption system, the established adsorption models could be divided into the following categories.

1.6.1 Models without Considering Non-Ideality

Under this category, the activity coefficients of all species are lumped into the adsorption equilibrium constant that is therefore apparent. The typical model in this category is the Langmuir isotherm (Langmuir, 1918). Langmuir isotherm was initially developed based on considering sorption as a chemical phenomenon. It was assumed that the forces extended by chemically unsaturated surface atoms do not extend further than the diameter of one sorbed molecule. Therefore the sorption considered can only be of a monolayer character. In addition, it was assumed that the adsorbed species do not interact with one another, neither do the species in the liquid phase. The bulk solution and sorbent phases are treated as ideal. Combined with the mass balance of active sites, the following isotherm relationship was developed:

$$q = \frac{Q_T K_{app} C_C}{1 + K_{app} C_C} \tag{1.6.12}$$

where q is the uptake of sorbate C, Q_T is the total binding capacity, C_C is the equilibrium concentration of C in the solution, K_{app} is the apparent equilibrium constant.

Because of its simplicity and user-friendliness, Langmuir equation has become a widely used empirical model for quantitative description of the sorption behaviors where the binding mechanism is not known.

Most mathematical biosorption models used in the literature adopt a simple Langmuir isotherm (Crist et al., 1988; Crist et al., 1992; Ruiz et al., 2001). The equilibrium constants were determined as a function of the equilibrium concentration of the species of interest without reference to the important factors such as pH, ionic strength, and interference of ions. As a result, the equilibrium constants are dependent on the solution conditions seriously limiting the prediction capability of these models over more extended sorption conditions.

Recently, Schiewer and Volesky (Schiewer and Volesky, 1995) proposed a model for the sorption of metal cations such as Cu, Cd and Zn by *Sargassum*. While this model is based on the Langmuir approach, it is capable of describing not only the binding of the species of interest but also the protolysis reactions of sites and the binding of other interference ions considered. In short, the effect of pH on the state of active sites and ion competition have been incorporated in the model enabling thus the description of the isotherm trends at different pH and the interference from other ions. However, as the non-ideality of the liquid phase was neglected in the model, the modeling results still deviated from the experimental data.

In the anion adsorption field, Yoshida (Yoshida and Kishimoto, 1995) developed a model for hydrochloric acid (HCl) adsorption on chitosan sorbent based on acid-base neutralization approach. In order to incorporate the pH effect on adsorption, he employed an empirical polynomial relationship between the equilibrium constant and pH. Takatsuji et al. (Takatsuji and Yoshida, 1998) studied the equilibrium of organic acid adsorption on a chitosan-based resin. The anionic glutamic acid adsorption was treated as an homogenous acid base reaction. The crucial improvement of this model is to consider the effect of pH on glutamic acid speciation in the solution. However, the assumption of the ideality in the system limited the model prediction under extended

conditions. At this time, the establishment of a reliable anion biosorption equilibrium model still remains an outstanding challenge.

1.6.2 Models Considering Non-Ideality in the Liquid Phase Only

In this category of models, while the species activity coefficients in the solid phase are lumped into the equilibrium constant, the non-ideality in the liquid phase is to be considered. Liquid solutions occurring frequently in chemical and biological processes, usually contain ionic species, especially aqueous solutions of acid, base and salt (Sandler, 1989). In such aqueous solutions, charged particles interact with coulombic forces at a small separation range and, because of the formation of ion clouds around each ion, damped coulombic forces at larger separation distances. These forces are much longer-range than those involved in the interactions of neutral molecules, so that solute ions in the solution interact at very low concentrations. Consequently, electrolyte solutions are very non-ideal in the sense that the activity coefficient is significantly different from unity at very low electrolyte concentrations. Also the greater the charge on the ions, the stronger their interaction and the more non-ideal the solution.

To get the theoretical expression of the activity coefficient, P. Debye and E. Huckel (Robinson and Stokes, 1959) used a statistical mechanistic model incorporating the effect of the long-range coulombic forces as well as the short-range interactions between ions, representing the crudest possible model by taking the ions to be non-deformable spheres of equal radii. In any actual solution, there will also be the short-range interactions between ions and solvent molecules to consider, as well as other types of short-range interaction between ions, which cannot be adequately represented by the rigid-spheres model. The original Debye-Huckel model was extended, in a highly empirical fashion, by adding a term linear in the concentration (Robinson and Stokes, 1959). Davis (Davis, 1938) had further modified the equation by assigning the empirical values to the model constants. As a result, Davis' form is useful as a guide to the

behavior of the activity coefficient of an electrolyte when no experimental measurements are available. Davis equation can be applied for electrolyte solutions at ionic strength less than 0.5 M (Robinson and Stokes, 1959).

In order to obtain the equation valid at a medium ionic strength, Bromley (Bromley, 1973) further improved the extended Debye-Huckel model by incorporating the effect of ionic strength on the short-range forces in a binary interaction. This model could be used to calculate the activity coefficient at the ionic strength up to 6 M. However, when ionic strength was higher than 6 M, the Bromley equation could give a significant error.

There are few solution models valid for moderate and high concentrations of electrolytes. Perhaps the most successful is the model of Pitzer (Pitzer, 1979). However, it contains a very large number of parameters, especially for the binary systems.

In the biosorption field, Yang and Volesky (Yang, 2000) used Davis equation to calculate the activity coefficients of solution species in the system of cationic uranium adsorption by *Sargassum*. The model could successfully describe the cationic U uptake at 0.1 M ionic strength.

Unfortunately, a model considering the non-ideality in the liquid phase for anion biosorption has not been proposed as yet.

1.6.3 Models Considering the Non-Ideality in the Solid Phase

Under this category, the non-ideality of the adsorbed phase is considered whereby that in the liquid phase is either considered or not. According to the consideration of the physical property of the sorbent – penetrability, the adsorption models can be divided into the following sub-categories.

Surface Complex Model

The surface complex model was initially derived for adsorption on impenetrable oxides. It was originally based on the Electrical Double Layer (EDL) theory proposed by Gouy and Chapman and later extended by Grahame (Grahame, 1947). Eventually, the early model development efforts led to new ways of describing the surface charge development and to sorption models that embody the central features of the EDL theory but emphasize the chemical reaction of sorbing ions with functional groups: the surface complexation approach. In the surface complexation model, all non-ideal behaviors of the surface species are attributed to the effect of a mean charge potential and are correlated with the surface charge by Gouy-Chapman equation (Dzombak and Morel, 1990). The activity coefficients of liquid species are usually calculated by Davis equation.

This model family includes the Constant Capacitance Model (Stumm et al., 1980), the Generalized Two Layer Model (Davis et al., 1978; Dzombak and Morel, 1990; Hayes et al., 1991) and the Triple Layer Model (Hayes and Leckie, 1988). In the previous two models, the adsorption of background electrolytes was neglected. However, in the actual process, when the concentration of background electrolyte reaches 0.1M, the complexation of electrolytes on the surface is very significant (Davis et al., 1978). Therefore, in Triple Layer Model the adsorption of both heavy metal ions and background electrolytes is considered by placing them on different planes, respectively, inside the electrical double layer. So far the family of these models has been used to effectively describe the adsorption behavior of inorganic oxides. However, there are a large number of parameters in the model resulting in a random regression for the parameters (Hayes and Leckie, 1988).

Donnan Model

The major advantage of Donnan based adsorption model includes an estimate of the water uptake (swelling) using osmotic coefficients. Therefore, this model is

particularly applicable to penetrable sorbents. An application of this approach for differently charged polymers has been pioneered by Marinsky and coworkers (Marinsky, 1987) who established the use of Donnan model for interpreting protein equilibrium in organic polyelectrolyte such that humic and fulvic substance (Marinsky et al., 1982a; Marinsky et al., 1982b; Ephraim et al., 1986; Ephraim and Marinsky, 1986; Marinsky and Ephraim, 1986) and alginic acid (Lin and Marinsky, 1993). The model attributes the non-ideal behavior in the adsorbed phase to the osmotic effect and electric charge corrected by Donnan term. Schiewer (Schiewer and Volesky, 1997b; Schiewer and Volesky, 1997a) developed a model based on Donnan theory examining the Cd, Zn and Cu cation biosorption by *Sargassum*. The model could describe the sorption tendency correctly. However, neglecting the non-ideality in the liquid phase in the model limited the model usability in the system at elevated ionic strength.

Wilson Model for Ion Exchange

Wilson model was originally developed representing the excess free energy of mixing non-electrolytes, or for a binary system (Wilson, 1964). Later, Smith (Smith and Woodburn, 1978) applied Wilson's theory to determine the activity coefficient of species on the strong anion exchange resin phase, and successfully described the adsorption equilibria of SO_4^{2-}—NO_3^-—Cl^-, without considering the penetrability of the sorbent. Shallcross (Shallcross et al., 1988) further applied Wilson model to the adsorption of cations such as Ca, Mg and Na on strong-base resin. The modeling results are quite satisfactory. However, Wilson model are restricted to the systems that do not form coordination complexes in the resin phase and it also requires too many model parameters which limits its wider applications.

1.7 Summary of Introduction

The removal of metal anions is a growing concern in current industrial metal recovery processes. The conventional treatment by activated carbon, ion exchange, solvent extraction and precipitation has its limitation due to the low efficiency or high operating costs. These shortcomings have created a strong incentive for developing an alternative process for heavy metal removal, especially of anionic species, that would be not only effective but also particularly economically feasible. Crab shell waste material containing abundant chitin offers a promising potential for this purpose.

While the effects of important process operation factors such as pH, ionic strength and ion interference have been well established for the cationic metal species, the anion biosorption still remains very little understood. To systematically determine the characteristics of anion binding by the biosorbent, it is necessary to elucidate the effects of these factors in anion biosorption. Temperature is considered as less relevant if the biosorption is done at ambient temperatures.

While there are some indications that the binding of heavy metal cations may involve ion exchange, adsorption or both, the mechanism of anion biosorpion is not clarified.

Most anion biosorpion has been so far modeled using the simplistic Langmuir model. For predicting the effect of pH, ionic strength and competition among other anions on binding, the use of appropriate models incorporating these factors in a simple and pragmatic way is particularly desirable in order to support engineering biosorption process design and its applications in the recovery of heavy metals. The following objectives are thus generated for the current work.

1.8 Objectives

1.8.1 Development of an effective biosorbent for anionic metal species removal

- Determine the capacity of anion binding by acid washed crab (*Ucides cordatus*) shells (AWUS) compared with selected dead biomass.
- Demonstrate the reusability of AWUS

1.8.2 Identification of anionic metal species biosorption mechanism

- Determine the solution chemistry of selected metal anions in the given biosorption system
- Characterize the main binding sites
- Establish the relevance of electrostatic attraction

1.8.3 Experimental quantification of anionic metal species binding at different...

- Metal concentrations
- pH values
- Ionic strength values
- Concentrations of other specific competition anions

1.8.4 Modeling the anionic metal species adsorption equilibrium in single metal systems

- Develop adsorption isotherm models
- Determine the anionic metal species binding constants for isotherm models
- Experimental verification of the model performance for:
  - Effect of pH on metal binding
  - Effect of ionic strength

1.8.5 Modeling the anionic metal species adsorption equilibrium in a multi-metal system

- Apply extended multi-component adsorption isotherm models
- Determine the metal binding constants for isotherm models
- Experimental verification of the model performance for:
  - Metal binding in multi-metal systems

1.8.6 Modifying the biosorbents for anionic metal complex recovery

Experimental quantification of enhanced anionic metal complex binding by

- Heat-treated crab shells
- Selected bacteria, fungi and seaweed with an organic additive

CHAPTER 2

MATERIALS AND METHODS

2.1 Biosorbent Preparation

2.1.1 Crab Shells

2.1.1.1 Raw *Ucides* Shells (RUS)

Waste crab shells of *Ucides cordatus* were obtained sundried from a food processing plant in Paraiba, Piaui, Brazil. They were crushed with grinder and sieved, giving particles with diameters ranging in sizes of 0.5 to 0.85 mm, 1 to 3.35 mm and greater than 3.35 mm.

2.1.1.2 Acid-Washed *Ucides* Shells (AWUS)

Raw *Ucides cordatus* shell particles were washed with 1 N HCl (55g/L) for 6 hrs to remove minerals and then rinsed with deionized water in a mixing tank by replacing the water with fresh deionized water from time to time until the final pH stabilized at pH ~ 4.0. The residual material was dried at 55°C to prevent scorching and represented approximately 23% of the original sized crushed shells.

2.1.1.3 Burnt *Ucides* Shells

The Raw *Ucides* Shells (RUS) as well as Acid-Washed *Ucides* Shells (AWUS) with the particle size range of 1-3.35mm were burnt in a closed furnace at 900°C for 3 minutes.

2.1.2 Microorganism and Seaweed

Waste industrial biomass samples of *Bacillus subtilis* and *Penicillium chrysogenum* were collected from Sichuan Pharmaceutical Company, Chengdu, P. R. China. *Sargassum fluitans* seaweed biomass was collected beach-dried on the Gulf Coast of Florida.

Biomass was ground into particles ranging in diameters of 0.5-0.85 mm, then washed with 0.2 N HCl for 4 hours and rinsed with distilled water to pH~4.5. Finally, the biomass was dried in the oven at 55^0C to a constant weight.

2.2 Solution Preparation

Solutions of anionic metal complexes Au, Cr, and V were prepared by respectively dissolving solid $NaAu(CN)_2$, CrO_3, and Na_3VO_4 in distilled water. Ionic strength of solutions was adjusted by adding 0.01 M or 0.1 M NaCl. 0.1 M or 0.5 M HCl and NaOH were used for pH adjustment. All reagents from Sigma-Aldrich were ACS reagent grade quality.

2.3 Equilibrium Sorption Experiments

Approximately 20 – 40 mg of dried acid-washed biomaterials were mixed with 20±0.2 mL of solution containing species of interest such as anionic metal species (Section 3.1-3.6) and/or L-cysteine (Section 3.6.2) in 150 mL Erlenmeyer flasks. The pH of the solutions before and during the sorption experiments was continuously controlled with HCl or NaOH. The solution was mixed and left to equilibrate for 24 h, confirmed as sufficient time for establishing sorption equilibrium at room temperature (It was experimentally tested that the difference of selected metal uptakes at between 6 hrs and 24 hrs was less than 5 %). Sorption samples were run in duplicates, sometimes triplicates, with a blank undergoing the same treatment, and the data presented are the average values. The standard deviation of the equilibrium solution pH values for all data points was less than 0.1. Uptake of metal was determined from the difference in metal concentrations between the initial and final solutions as follows:

$$q^M = q_i^M + ([M]_0 - [M]) * v/w \qquad (2.1)$$

q^M : equilibrium metal uptake (mmol/g).

q_i^M : metal initially loaded on the biosorbent (mmol/g). As neither of the selected acid washed biosorbents in this study initially contained the selected metals such as Au, Cr and V (Troy and Koffler, 1969; Remacle, 1990; Schiewer, 1996a), q_i^M equals to 0. However, in the experiments examing AWUS reusability, q_i^M equals the residual metal uptake after the elution.

$[M]_0$: initial metal concentration (mM)

[M]: equilibrium metal concentration (mM)

w: the dry net biosorbent weight representing the weight of the sorbent without counting the mass of loaded metals(g).

v: the working volume of the adsorption sample (L).

The metal removal R_M is calculated by the following equation:

$$R_M = \frac{[M_0] - [M]}{[M_0]} \ (\%) \qquad (2.2)$$

The uptake of L-cysteine by biomass was calculated in the same way as that for metal uptake.

The relative error of experimental metal uptakes was less than 8.5%. Among those errors, around 5% is from the metal analysis and the remainder is from other sources.

2.4 Desorption Experiments

Metal desorption from metal-loaded biosorbents was examined in systems of chromate with AWUS (Section 3.2), and gold-cyanide with biomass (Section 3.6.2), respectively.

In chromium desorption, AWUS material was first loaded with Cr from the chromate solution at pH 2.0 and 9.6 mM Cr. Around 40 mg Cr–loaded AWUS materials, bearing 0.54 mmol Cr/g, were mixed with 5 mL or 10 mL of the NaOH eluant solution for 24 hours, whereby the ratio of solid (mg) to liquid (mL) (S/L) is about 8 and 4, respectively. The percentage of Cr recovery, represented by the ratio of the amount of Cr released during desorption to the equilibrium sorption uptake, was calculated for desorption experiments.

The possibility of desorbing Au from biomass was examined by first sorbing Au onto biomass in the presence of L-cysteine at pH 2 and then desorbing Au with deionized water at pH 3, 4 or 5. The pH level was adjusted with 0.1 M NaOH. Gold-cysteine pre-loaded *Bacillus* biomass contained 20.5 μmol Au /g of dry biomass, *Penicillium* biomass contained 14.2 μmol/g, and *Sargassum* biomass 4.7 μmol/g. 0.02 g Au–cysteine-loaded biomass was mixed with 5 mL of the eluant solution for 4 hours. The percentage of Au recovery was then calculated similar to that for Cr.

2.5 Experimental Determination of AWUS Reusability

The reusability of AWUS was examined by investigating the performance of AWUS on chromate adsorption after certain numbers of adsorption-desorption cycles. First, around 40 mg AWUS was used to mix with 20 mL solution of 9.6 mM Cr at pH 2.0. Then the Cr-loaded AWUS was separated from the suspension and the Cr elution from the loaded AWUS was carried out at pH 10.6. Following Cr elution by basic solution, AWUS material was rinsed with deionized water until pH 7 and then re-used for another chromium adsorption cycle. Metal uptakes were calculated based on the net dry shell weight after each adsorption-desorption cycle.

2.6 Analysis

2.6.1 Metal Concentration

The total metal concentration in solution was determined with an atomic (emission) spectrometer (sequential inductively coupled plasma AS, Thermo Jarrell Ash, Trace Scan).

Hexavalent chromium was determined according to the standard method (Eaton et al., 1995b) by measuring absorbance of the purple complex of Cr(VI) with 1, 5-diphenylcarbohydrazide at 540 nm by UV-VIS spectrophotometer. The concentration of other forms of chromium was determined as the difference between the total concentration of chromium obtained by ICP-AES and the concentration of Cr (VI).

The relative error of metal analyses was less than 5%.

2.6.2 Chloride concentration

Cl^- was analyzed using ion chromatography (Dionex, DX100) with a column type AS12A (Dionex). The retention time for Cl^- is 4.13 minutes. The relative error of the chloride analysis is less than 5%.

2.6.3 Solution pH

pH was measured by pH/ISE meter (Orion Research, Inc., 710A).

2.6.4 *Ucides cordatus* Shell Analysis

Protein in *Ucides cordatus* shells was extracted by 10% NaOH solution for 72 hrs at room temperature (Bemiller and Whistler, 1962) and then assessed using Kjeldahl Nitrogen analysis (AOAC, 1990).

Ash was determined by a standard method (AOAC, 1984).

Minerals were analyzed by first dissolving shell ash in the 35% nitric acid solution and then measuring the elements by ICP-AES.

Pigments were extracted through ethanol or acetone, and the pigment amount was assessed based on the weight difference (Roberts, 1992h).

Moisture and volatile matter were determined by the weight difference after the shell material was dried at 101-105 °C (Furman, 1962).

N-acetylation degree of chitin, defined as the percentage of acetylated amine groups in chitin, was analyzed by the ratio of N/C on the chitin extracted from *Ucides cordatus* shells treated by deproteination, demineralization and decolouration (Roberts, 1992p).

The EA 1108 CHNS (Fisons Instruments ISO MASS) apparatus was used for the elemental analysis.

The composition of both raw *Ucides* shells (RUS) and acid washed *Ucides* shells (AWUS) was analyzed and the results are summarized in Table 2.1. ± figures represent the standard deviation of the reported values. The types of detected minerals are listed in Table 2.2. N-acetylation degree of extracted shell chitin was 78±10 (%).

Table 2. 1 Composition of *Ucides cordatus* shells dried at 55°C (%)

Ucides cordatus shells	chitin	protein	ash	Moisture and volatile matter	Pigment and others
Raw shells	20±3	17±1	59±1	2±0.2	2±0.3
Acid washed shells	**53±4**	**43±3**	0.2±0.1	1±0.1	3±0.2

Table 2. 2 Mineral contents of *Ucides cordatus* shells (%)

Ucides cordatus shells	Ca	Mg	Si	Na	Al
Raw shells	**20.05±0.14**	2.05±0.07	0.16±0.01	0.82±0.04	0.06±0.01
Acid washed shells	**0.05±0.03**	/	0.02±0.01	/	0.04±0.01

2.6.5 Analysis of Total Organic Carbon (TOC)

The TOC release of AWUS in the solution was measured using the TOC analyzer (Dohrman DC-80) by both combustion and UV-persulfate methods. Aliquots of liquid samples were first filtered through 45μm pore size chromatographic filter and subsequently acidified with H_2SO_4 prior to analysis. The TOC analyzer was calibrated using 200mg/l solution of K-phthalate prepared from a standard solution containing 1000 mg/l of this chemical. The TOC in samples whose acidified aliquots produced precipitate, was determined as follows. First the Total Carbon (TC) was determined by analyzing aliquots of these samples without pH adjustment. Second, the Total Inorganic Carbon (TIC) in these samples was determined using the TIC mode of the DC-80 analyzer. Finally, the TOC was calculated as the difference between the TC and TIC.

2.6.6 Fourier-Transform Infrared (FTIR) Analysis

FTIR analysis was conducted to investigate the metal sequestered on biomaterials and the main functional groups for metal biosorption. The metal-loaded biosorbent samples were prepared by mixing 40 mg biosorbent of 0.5-0.85mm in diameter, respectively with 20 mL of metal solutions at their optimum pH for adsorption. The biosorbents were then collected by filtration and washed with distilled water and finally freeze-dried. The blank biomaterials were prepared under the same conditions except for the absence of metals. Solid $NaAu(CN)_2$, CrO_3, and Na_3VO_4 samples were also prepared for spectra comparison. Disks of 100 mg KBr containing 1% of finely ground powder of each sample were prepared less than 24 hours before analyzing. Infrared spectra of samples were recorded on a Michelson 100 FTIR spectrophotometer.

2.6.7 Electron Microscopic and EDAX Analysis

The surface morphology and components of blank AWUS and blank burnt AWUS were examined by scanning electronic microscopy (SEM) (Philips 535) and by x-ray energy dispersive spectrometer analysis (EDAX). The crab-shell samples were mounted on a stainless steel stab using a double-stick tape, coated with a thin layer of gold, and then observed with the SEM at 15 kV.

2.6.8 Cysteine Analysis

Cysteine concentration in the solution was analyzed by a UV-visible spectrophotometer (Cary 1) at 194 nm.

CHAPTER 3

RESULTS AND DISCUSSION

3.1 Screening of Biosorbents for Adsorption of Anionic Metal Species

Chitin-containing biomaterials have been recognized as effective biosorbents for some metals (Muzzarelli, 1977; Muzzarelli et al., 1981; Dambies et al., 1999; Guibal et al., 1999). The uptake of dyes by chitin through combining $-SO_3^-$ on the dye with fully-protonated amide groups on chitin (Roberts, 1992d) demonstrated the potential of chitin for anion adsorption. Crab shell material, obtained as waste from seafood industrial processing, contains abundant chitin (Roberts, 1992e). However, the capability of crab shells for anion binding has not been systematically studied as yet.

Recent experimental results demonstrated that the biomass of *Bacillus subtilis* (bacterium), *Penicillium chrysogenum* (fungus) and *Sargassum fluitans* (brown seaweed) could extract heavy metal cations from solution (Niu et al., 1993; Fen et al., 1997; Kratochvil, 1997). While Kratochvil (Kratochvil, 1997) tested adsorption of Cr (VI) by *Sargassum,*, the uptake of anions by *Bacillus subtilis* and *Penicillium chrysogenum* has not been examined.

Extraction of the gold-cyanide anionic complex is of a widespread industrial interest as it results from the commercial gold leaching process (Marsden and House, 1993a). This complex is a stable simple mono-valent anion (Marsden and House, 1993b; Eaton et al., 1995a). $HAu(CN)_2$ was found only under very acidic conditions such as in 0.5 – 1 M H_2SO_4 (Sillen and Mortell, 1964c). The $Au(CN)_2^-$ complex has been selected as a sorbate in the present work aimed at examining the capacity of the selected waste biomaterials for anion uptake.

The objective of this section was to establish the capability of Acid Washed *Ucides* Shells (AWUS) to adsorb the $Au(CN)_2^-$ complex and to compare it with uptakes by *Bacillus*, *Penicillium* and *Sargassum*. Another aspect was the development of an effective biosorbent modified for anionic metal species.

3.1.1 Au Uptake by Selected Biomaterials

A solution containing gold-cyanide and suspended biomaterials was mixed and left to equilibrate for 24 h, confirmed as sufficient time for establishing a sorption equilibrium. Figure 3.1.1-4 summarizes Au biosorption isotherms obtained respectively with AWUS, *Bacillus*, *Penicillium*, and *Sargassum* biomass at the equilibrium pH values of 2.0 – 6.0. Results showed that AWUS removed the highest amount of anionic gold-cyanide complex through the entire range of Au equilibrium concentrations from 0 to 100 μmol/g. This concentration range was examined because it corresponds to that typical for conventional gold-cyanide leach solutions (Marsden and House, 1993a). Lower Au uptakes were demonstrated for the following sequence of biomass types at pH 2 – 3.5: AWUS (23 μmol/g), *Bacillus* (8.0 μmol/g), *Penicillium* (7.2 μmolAu/g), and *Sargassum* (only 3.2 μmolAu/g). AWUS, being the best sorbent, did not reach its isotherm plateau in the concentration range considered, while the others did.

Raw crab shells of *Ucides cordatus* used in the current study were determined to consist of (d.w. basis) around 59% minerals (mainly $CaCO_3$), 20% chitin and 17% protein. This corresponds well to the composition reported in the literature (Roberts, 1992g; Lee et al., 1997). With such a high mineral content, raw shells could not adsorb anionic gold-cyanide very effectively (data not shown here).

Simple acid wash was successful in removing the minerals from raw crab shells resulting in the AWUS material containing approximately 53% chitin (with 78% N-acetylation degree), 43% protein and only 0.2% minerals. As a result, 96% of AWUS

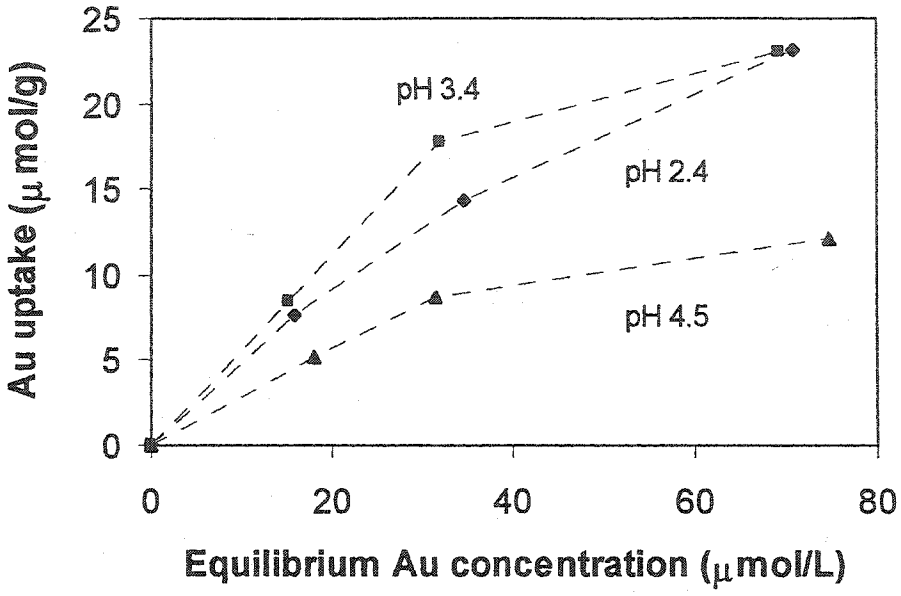

Figure 3.1. 1 Au isotherms of AWUS

AWUS particle size: 1 - 3.35mm.

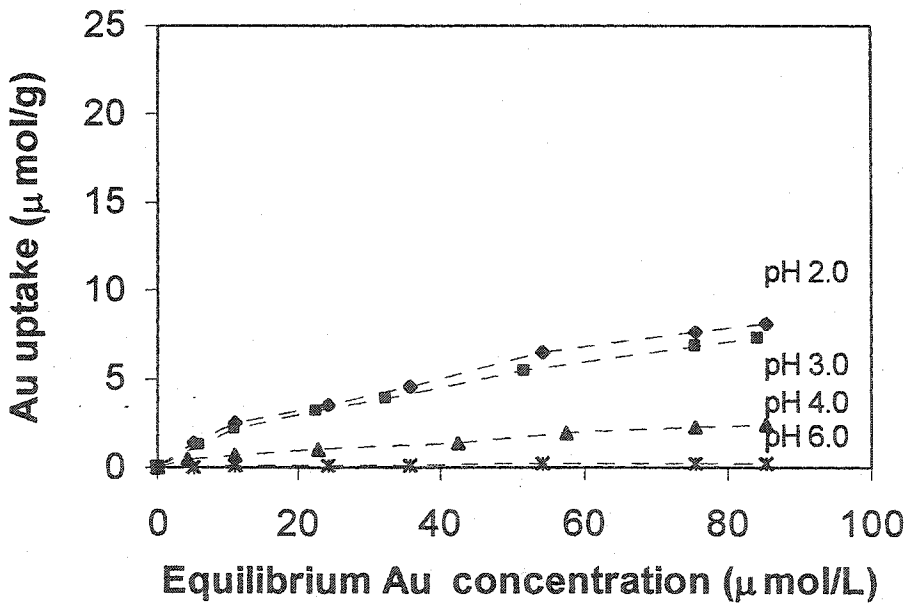

Figure 3.1. 2 Au adsorption isotherms of *B. subtilis*

Biomass particle size: 0.5-0.85 mm.

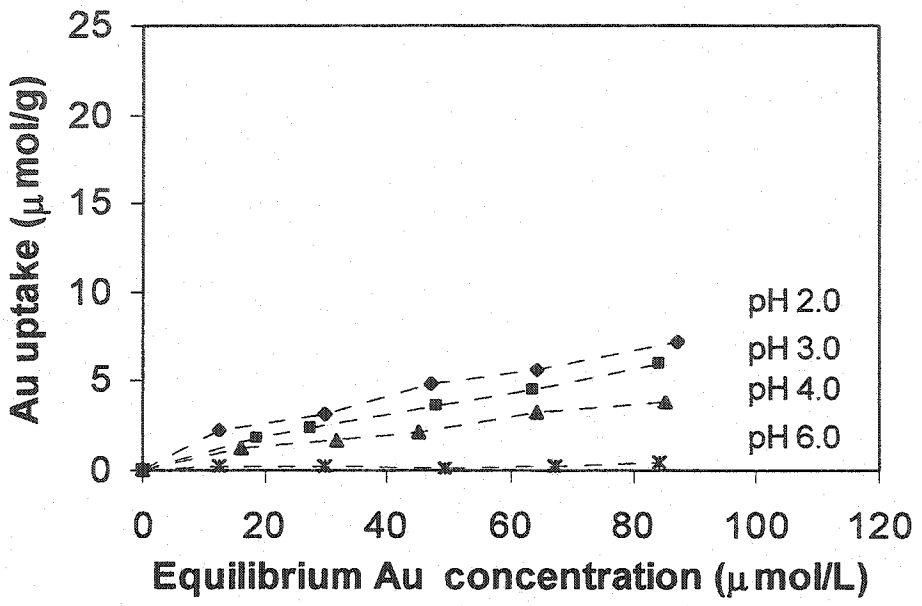

Figure 3.1. 3 Au adsorption isotherms of *P. chrysogenum*

Biomass particle size: 0.5-0.85 mm.

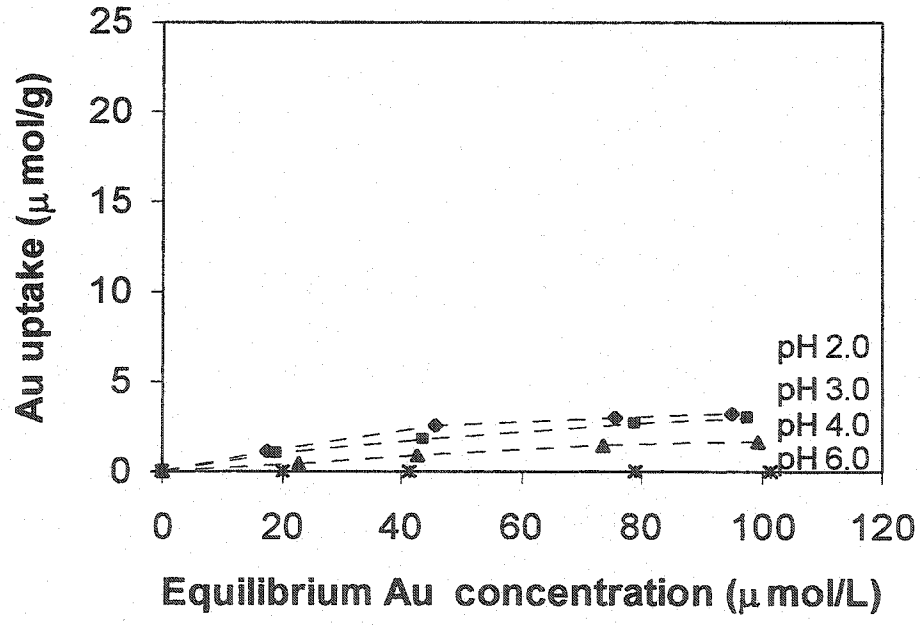

Figure 3.1. 4 Au adsorption isotherms of *S. fluitans*

Biomass particle size: 0.5-0.85 mm.

components contain amide or amine, providing abundant weak-base groups. Once these weak-base groups are fully protonated with positive charges in an appropriate environment, they are capable of binding anions.

In the case of the dead biomass, the binding capability is dependent on the types of compounds in cell walls mainly responsible for biosorption (Volesky and Holan, 1995). Cell walls of Gram-positive bacteria, e.g. *Bacillus*, contain peptidoglycan with amine, which only accounts for 40% of the cell wall material (Remacle, 1990.). Similarly, *Penicillium* cell walls contain 40% of chitin, often complexed with proteins, lipids, glucan and other substances (Troy and Koffler, 1969). The conjugate acid dissociation constant (p*K*a) of chitin amide is lower than 3.5, that of chitin amine is 6.5 (Roberts, 1992a) and of protein amine 7~10 (Buffle, 1988a). The logarithm of the proton dissociation constant of carboxyl groups in the above cell wall components is around 2.6 ~ 4.5 (Buffle, 1988b; Fen et al., 1997). As the solution pH reached 2 in the presently examined systems, negatively charged carboxyl groups and neutral weak-base amine groups on biomass became protonated, offering positive binding sites (biomass-H^+) for anionic gold-cyanide complexes which also became less repelled by the decreasing overall negative biomass charge. However, the anion-binding capacities of the available weak-base groups in the dead microbial biomass tested, compared with that of AWUS, are not promising.

In *Sargassum,* the active group is the acidic carboxyl group (Buffle, 1988a) of cell wall alginate. This group could make up to 45% of the cell wall dry weight (Fourest and Volesky, 1996). Correspondingly, the insignificant anion adsorption by *Sargassum* biomass (brown seaweed) could rather be ascribed to phenolic groups of polyphenolic compounds that are known to be present in brown seaweeds (Dodge, 1973). While the inorganic hydroxide could take up an extra proton and serve as a weak-base for anion adsorption (Hayes et al., 1990), the capacity of phenol OH in biomolecules to take up an extra proton at acidic pH is questionable. This is probably the reason why *Sargassum* biomass showed a much lower capacity for binding gold-cyanide complex.

In short, the capacity of anion biosorption is mainly dependent on the number of weak-base groups available on biomaterials that could become positively charged in an appropriate aqueous environment. Even though *Bacillus*, *Penicillium* and *Sargassum* biomass are effective for cationic metal binding (Niu et al., 1993; Fen et al., 1997; Kratochvil, 1997), they exhibited very poor performance for anionic metal species adsorption as lacking of sufficient base groups. AWUS indicated the most promising potential for anionic metal species binding.

3.1.2 Au Uptake by AWUS Particles of Different Sizes

In order to further investigate the capability of AWUS to bind anions, AWUS particles of different sizes were examined for Au uptake. Figure 3.1.5 shows the relative Au uptake by three different sizes of AWUS particles at the equilibrium Au concentration 2.34 ± 0.14 mM and pH 2.3. The largest AWUS particles with diameters greater than 3.35 mm exhibited the lowest Au uptake. As the particle diameter size decreased from 3.35mm to 1mm, Au uptake increased to 186%, almost double of that observed for the larger particles. However, for even smaller particle size of diameters between 0.5 mm and 0.85 mm, the Au uptake didn't change significantly. The results indicated that AWUS material is partially penetrable. This phenomenon was ascribed to the shell structure of α -chitin cross-linked with protein, which provides a stable matrix (Roberts, 1992o) and prevents the crab shells from effectively swelling. Its stable natural structure can be considered an advantage particularly when the crab shell material is to be used as a sorbent. However, in order for its functional group to have effective exposure, an appropriate size of shell particles has to be selected. In the current work, considering the binding site availability as well as the ease of the shell particle separation from the liquid-solid suspension, AWUS particle size of 1 to 3.35 mm was selected for extended anionic metal species binding studies reported in the following sections.

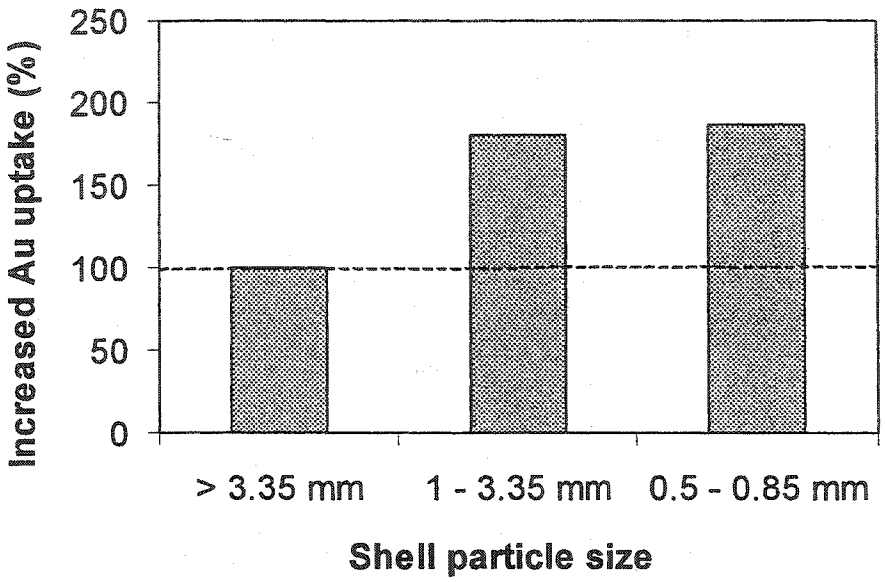

Figure 3.1. 5 Au uptake by AWUS particles of different sizes

40±1 mg AWUS, 20±0.2mL solution, equilibrium Au concentration 2.34 ± 0.14 mM, the Au uptake is 0.15 mmol/g by the largest shells particles, pH 2.3±0.1.

3.1.3 Section Summary

A promising anionic metal complex binding by Acid Washed *Ucides* Shell (AWUS) particles was established upon comparison with conventional biosorbents such as *Bacillus*, *Penicillium*, and *Sargassum* biomass. At pH 3.4 and equilibrium concentration of 75 μmol Au/L, AWUS could accumulate Au up to 23 μmol/g, while *Bacillus* biomass took up only 8.0 μmol/g, *Penicillium* biomass 7.2 μmol/g and *Sargassum* biomass merely 3.2 μmol/g.

The acid wash applied could effectively remove minerals from the *Ucides* shells. 96% of AWUS components contained weak-base amide or amine capable of binding anions in appropriate aqueous environments.

AWUS particles with diameters smaller than 3.5 mm are reasonably well penetrable and their natural structure makes them a good and stable solid sorbent with abundant and accessible functional groups for anionic metal complexes. Because of their high metal uptake and the ease of solid/liquid separation, AWUS particles in the size range of 1 to 3.35mm have been chosen for further studies in this work.

3.2 Characteristics of Anionic Metal Species Binding by AWUS

Major industrial activities such as mining and hydrometallurgical, and surface finishing industries concern the recovery of heavy metals, often in anionic complex forms such as anionic gold-cyanide ($Au(CN)_2^-$), chromate (CrO_4^{2-}), and vanadate (VO_4^{3-}) (Rostoker, 1958; Marsden and House, 1993a) conventionally recovered by activated carbon sorption, ion-exchange, solvent extraction or precipitation (Rostoker, 1958; EPS, 1987a; Marsden and House, 1993a). However, low recovery efficiencies and high costs of the above methods call for alternative high-efficiency, low-cost sorbents.

As shown in the previous section, AWUS demonstrated a promising potential for anionic metal complex ($Au(CN)_2^-$) binding. It was thus chosen for further biosorption studies of extended anionic metal species such as gold-cyanide ($Au(CN)_2^-$), chromate (CrO_4^{2-}), and vanadate (VO_4^{3-}). These anionic metal species have been selected as examples because of their application background and because they represent the mono-valent, divalent or multi-valent heavy metal anions, respectively.

The objective of this section was to determine the characteristics of anionic metal species biosorption with AWUS.

3.2.1 Effect of pH on Anionic Metal Species Uptakes

The effect of pH on the selected anionic metal species adsorption with AWUS was studied by mixing 40 mg AWUS with 0-9 mM metal solutions at pH from 1.5-4.5. All of the metal uptakes observed in this study were strongly affected by the solution pH as shown in Figure 3.2.1-3.

Au adsorption isotherms for $Au(CN)_2^-$ sorbed by AWUS at equilibrium pH of 2.4 to 4.5 are presented in Figure 3.2.1. The Au uptake increased with decreasing pH from 4.5 to 3.4. The Au uptake at pH 3.4 was 0.17 mmol/g at the Au equilibrium concentration of 2.2 mM. However, at the lower pH of 2.4 the Au uptake was lower. Furthermore, during the adsorption process the sorption system pH had an increasing tendency. This was also observed with chromate adsorption by *Sargassum* or peat moss (Sharma and Forster, 1993; Kratochvil et al., 1998) and explained to be resulting from the weak-base groups on the biomaterials picking up protons from the solution so as to bind anionic metal species. When Giles (Giles and Hassan, 1958; Giles et al., 1958) examined dye sorption by chitin at pH 1.8 - 4.7, he postulated that the weak-base functional group in chitin under these conditions was amide.

AWUS material mainly consists of chitin and proteins containing weak-base groups such as amide or amine. When the solution pH is lowered from pH 4.5 to 3.4, negatively charged protein carboxyl groups and neutral weak-base amino groups on AWUS become protonated, offering positive binding sites for anionic gold-cyanide complexes that also become less repelled by the decreasing overall negative AWUS charge. Under this condition, $Au(CN)_2^-$ could be effectively bound onto positively charged sites on AWUS. However, the lower the pH, the higher the concentration of Cl^- brought into the solution through the pH adjustment and that, in turn, could compete with the $Au(CN)_2^-$ complex for the binding sites. As a result, in the present Au concentration range (0 – 2.2 mM), pH 3.4 appears to be the best among the pH values tested with the total binding sites available for $Au(CN)_2^-$ uptake without excessive Cl^- interference.

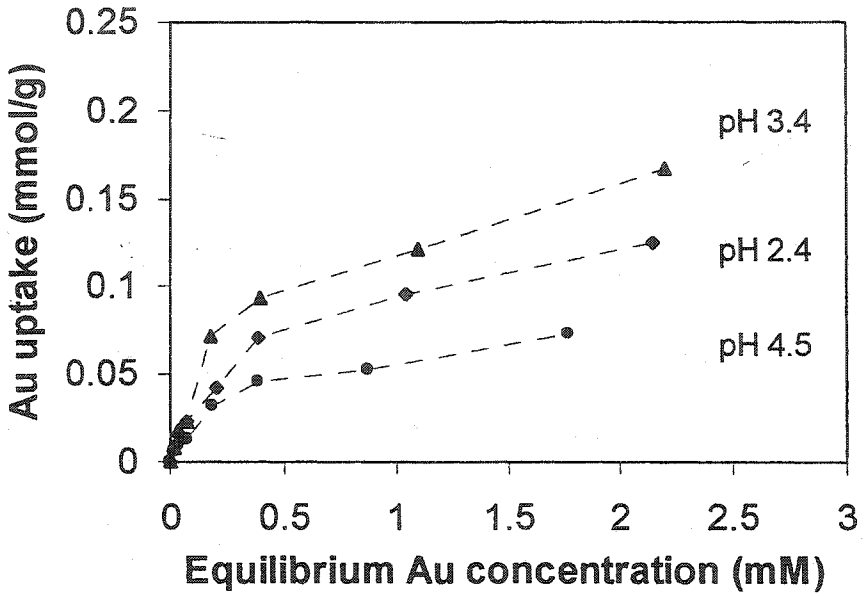

Figure 3.2. 1 Effect of pH on gold-cyanide adsorption

Cr adsorption isotherms obtained with chromate (CrO_4^{2-}) solution at pH of 2.0 to 3.6 are in Figure 3.2.2. With the pH decreasing from 3.6 to 2.0, the Cr uptake increased up to 0.54 mmol/g at the Cr equilibrium concentration of 7.7mM.

The diagram for chromate speciation in Figure 3.2.3 (Baes and Mesmer, 1976c; Greenwood and Earnshaw, 1985c) shows that the main forms of chromate in solution at pH lower than 6 are $HCrO_4^-$ and $Cr_2O_7^{2-}$. One mole of $Cr_2O_7^{2-}$ bound corresponds to 2 moles of Cr - this may be one reason to account for higher Cr uptake when compared with Au uptakes. As the divalent dichromate ($Cr_2O_7^{2-}$) ions bind onto the mono-valent positively-charged protonated amino groups on AWUS, another proton from the solution may be required to neutralize the extra-negative charge of the bound dichromate ($Cr_2O_7^{2-}$). This is probably responsible for the preferred pH for chromate uptake

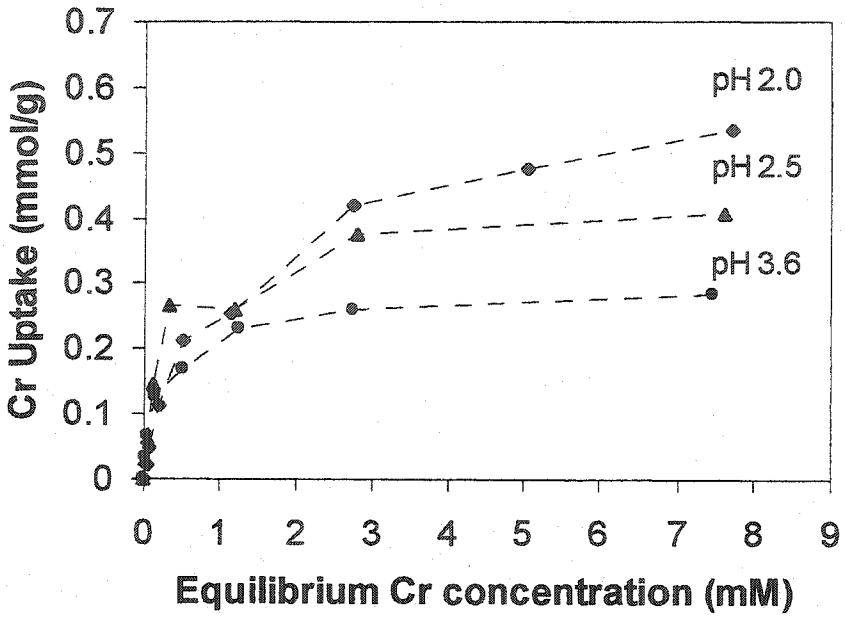

Figure 3.2. 2 Effect of pH on chromate adsorption

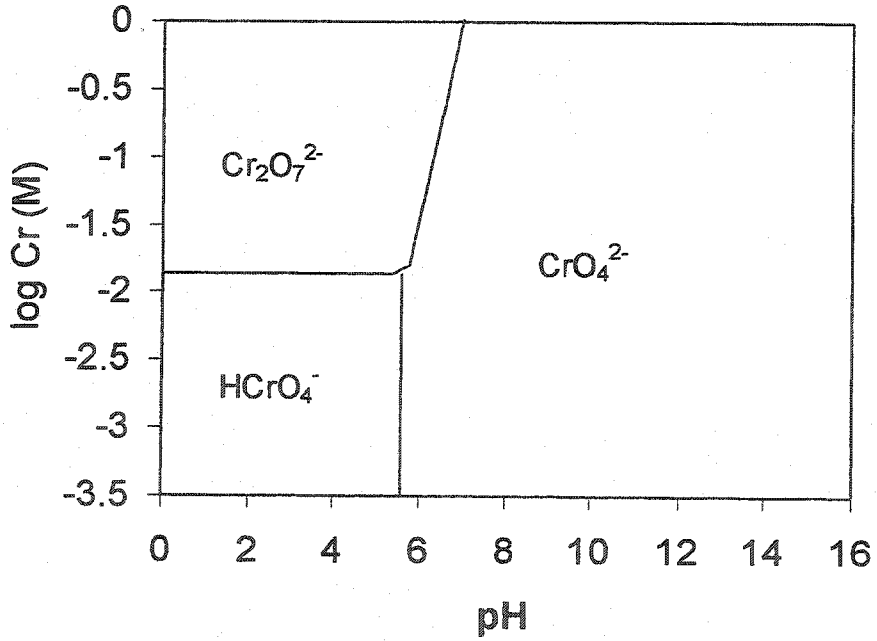

Figure 3.2. 3 Cr(VI) speciation in solution at 25°C

The solid lines represent conditions under which the predominant species in adjacent regions contain equal amounts of Cr(VI) (Baes and Mesmer, 1976c).

being a little lower than that observed for the uptake of mono-valent $Au(CN)_2^-$ anions.

Vanadium uptake isotherms determined with the solution initially containing vanadate (VO_4^{3-}) at pH of 1.5 to 4.5 are illustrated in Figure 3.2.4. The results show that the lowest V uptake was at pH 1.5, while at pH 3.5 it was slightly higher than at pH 4.5. The V isotherm at pH 2.5 starts off lower than that for pH 3.5, then it rises dramatically, showing the maximum uptake of about 0.79 mmol/g which is higher than both Au and Cr uptakes.

Vanadate (VO_4^{3-}), representing the multi-valent metal anion, appears in more complicated forms than the above metals when it is in aqueous solution (Sillen and Mortell, 1964a; Pope and Dale, 1968; Kepert, 1973; Baes and Mesmer, 1976b; Greenwood and Earnshaw, 1985e; Gupta and Krishnamurthy, 1992e; Larson, 1995). The distribution of V(V) species in aqueous solution depends on the solution pH and on the vanadium concentration as shown in Figure 3.2.5 (Greenwood and Earnshaw, 1985e). The species distribution relationship and equilibrium constants are well documented in the literature (Sillen and Mortell, 1964a; Baes and Mesmer, 1976b; Larson, 1995).

The established vanadate speciation shown in Figure 3.2.5, determines that at pH 1.5, the predominant form of vanadium is the vanadyl ion (VO_2^+) when vanadium concentration is in the range of 0 – 10 mM such as was employed in the current adsorption experiments (Greenwood and Earnshaw, 1985e). The cationic vanadyl ion VO_2^+ cannot be attracted to a positively charged amino group under this condition. Instead, it may compete with the proton for the nitrogen of the amino group. However its competition is very weak under strongly acidic conditions when the concentration of protons in the solution is high (pH 1.5).

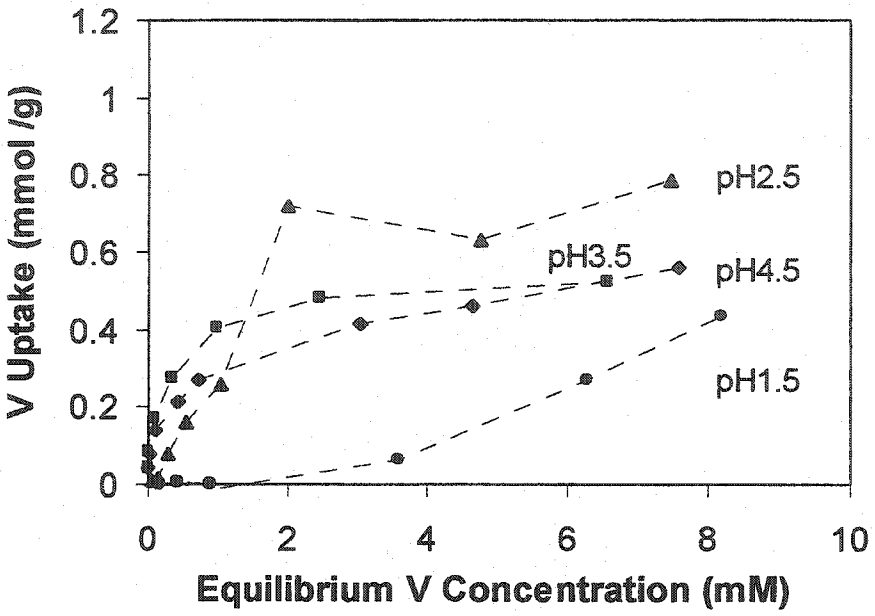

Figure 3.2. 4 Effect of pH on vanadate adsorption

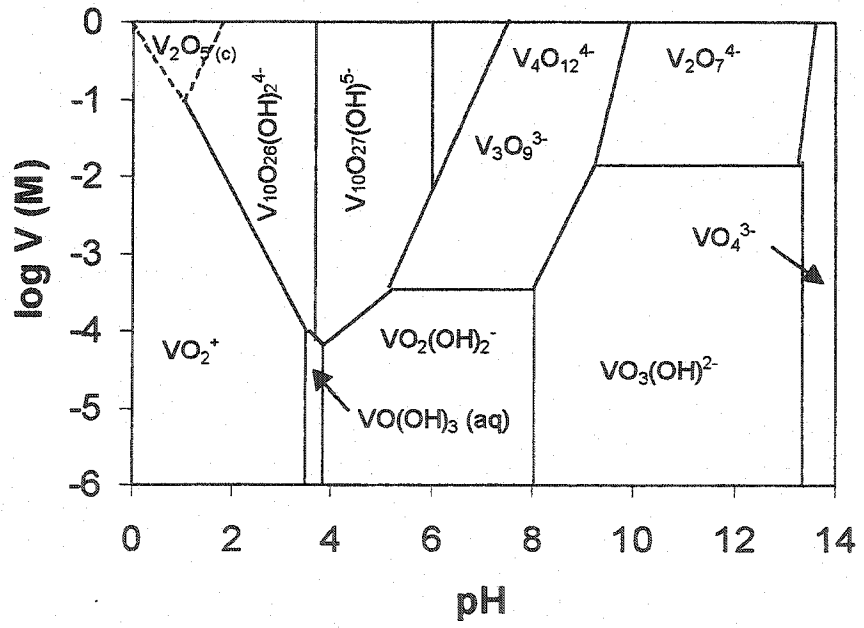

Figure 3.2. 5 V(V) speciation in solution at 25°C

The dash lines represent the solubility of V_2O_5 in terms of the V(V) concentration. The solid lines represent conditions under which the predominant species in adjacent regions contain equal amounts of V(V) (Greenwood and Earnshaw,1985e).

At pH 2.5, VO_2^+ is still predominant in the solution at low vanadium concentrations (less than ~ 1.7 mmol V/L). The weak competition of VO_2^+ with the proton for the site may account for the lower V uptake observed in the low V concentration range. However, when the vanadium concentration is continuously increased, anionic vanadate $V_{10}O_{26}(OH)_2^{4-}$ and vanadium pentoxide (V_2O_5) form (Figure 3.2.5). Vanadium pentoxide is slightly soluble in water, making pale yellow solutions that sometimes include colloidal material (Baes and Mesmer, 1976b). The precipitation of V_2O_5 occurs between pH 1 and 3 at vanadium concentration over about 50 mM (Gupta and Krishnamurthy, 1992e), which is far beyond the V concentration range in this work (0-10mM). The colloid can develop erratic localized charges all over its surface from interactions with other ions in the solution (Silberberg, 1996). Correspondingly, it is possible that three major factors account for the high uptake of vanadium at pH 2.5 and elevated vanadium concentrations in the solution. First, the colloids can develop charges on their surfaces that might attract such complexes to the binding site in the same manner as the anions. Secondly, the colloidal particles are much larger than ions, and it is possible that the diameter of such particles could be larger than some crab-shell material pores that the particle would encounter while traveling through the polymer matrix of the shells. The shells can then act as a filter as well as a sorbent, removing colloidal particles from the solution by trapping them inside its porous structure. Thirdly, one mole of anionic vanadate $V_{10}O_{26}(OH)_2^{4-}$ bound corresponds to 10 moles of vanadium. When a vanadium colloidal particle or vanadate $V_{10}O_{26}(OH)_2^{4-}$ anion is sorbed, many orders of magnitude of higher amounts of vanadium are removed from solution.

At pH 3.5, the neutral $VO(OH)_3$ predominates in the solution with low V concentration (less than ~ 0.05 mM). The anionic form of $V_{10}O_{26}(OH)_2^{4-}$ prevails at V concentrations higher than 0.05 mM (Figure 3.2.5). Vanadium uptake under these conditions could be attributed to by either anionic vanadate adsorption or neutral H_3VO_4 precipitation. However, the V uptake was low compared with that observed at pH 2.5.

At pH 4.5, the predominant forms of vanadate are anionic $VO_2(OH)_2^-$ at low V concentrations (less than ~ 0.1 mM) and $V_{10}O_{27}(OH)^{5-}$ at V concentrations higher than

0.1 mM (Figure 3.2.5). Vanadium binding under these conditions mainly involves anion binding on the positively charged amino group on AWUS. As most of chitin amide and carboxyl groups on AWUS are deprotonated at pH 4.5, being respectively neutral or negatively charged, anionic vanadate binding was insignificant.

In summary, vanadate binding could be attributed to anionic with some cationic vanadate binding, colloid sorption, and neutral molecule precipitation depending on the solution conditions. Vanadium uptake appeared to be maximum at pH 2.5, whereby the colloid V_2O_5 binding may be involved under those conditions.

The above results revealed that the main effect of pH on anionic metal species binding consists of an increase in the number of positively charged sites available with decreasing pH and an increase in the amount of metal species with high affinity for the sites.

3.2.2 Effect of Ionic Strength on Anionic Metal Species Uptakes

The effect of ionic strength (I) on the biosorption of anionic metal species was studied by adjusting the solution I using 0.01 M – 0.1 M NaCl. Each adsorption sample was prepared by mixing 40 mg of AWUS with 20 mL of metal solution at the preferred pH (Au: 3.4, Cr: 2.0 and V: 2.5), respectively. The results are presented in Figure 3.2.6-8 showing that the uptakes of all the metals studied are reduced with increasing NaCl concentration. Figure 3.2.6 illustrates the ionic strength effect on Au biosorption. As the concentration of added NaCl increased to 0.01M, maximum Au uptake in the studied concentration range was reduced to 0.14 mmol/g which was 82% of the control, and dropped to 24% at 0.1M NaCl.

The ionic strength effect on Cr uptake is seen in Figure 3.2.7. the maximum Cr uptake was reduced to 0.43 mmol/g at 0.01 M NaCl, (77% of the control), and to 39% at 0.1M NaCl. Compared with the above metal biosorption behavior, V uptake at pH 2.5 was not suppressed so seriously in the presence of NaCl, as shown in Figure 3.2.8. At

0.01M NaCl, V uptake values crossed with the control and at 0.1M NaCl, the maximum V uptake was reduced to 84% of the control. This observation may be related to the colloid V_2O_5 binding instead of anion adsorption.

Ions such as metal cations and anion species present in aqueous solution (either in free or complex forms) often display a tendency toward preferential adsorption on ionisable function groups (Tien, 1994). Changing ionic strength (i.e. the background electrolyte concentration) influences adsorption in at least two ways:

(a) by affecting the interfacial potential and therefore the activity of electrolyte ions;

(b) by affecting the competition of the electrolyte ions and adsorbing anions for available sorption sites.

Ions could be bonded on the charged surface either by forming inner-sphere complexes (covalently-bond) or outer-sphere complexes (electrostatic attraction). A strong influence of ionic strength is typical for outer-sphere complexes (Stumm and Morgan, 1996d). The significant suppression at increased ionic strength of the metal uptakes, particularly gold-cyanide and chromate, indicates that biosorption of these anionic metal species involves electrostatic attraction.

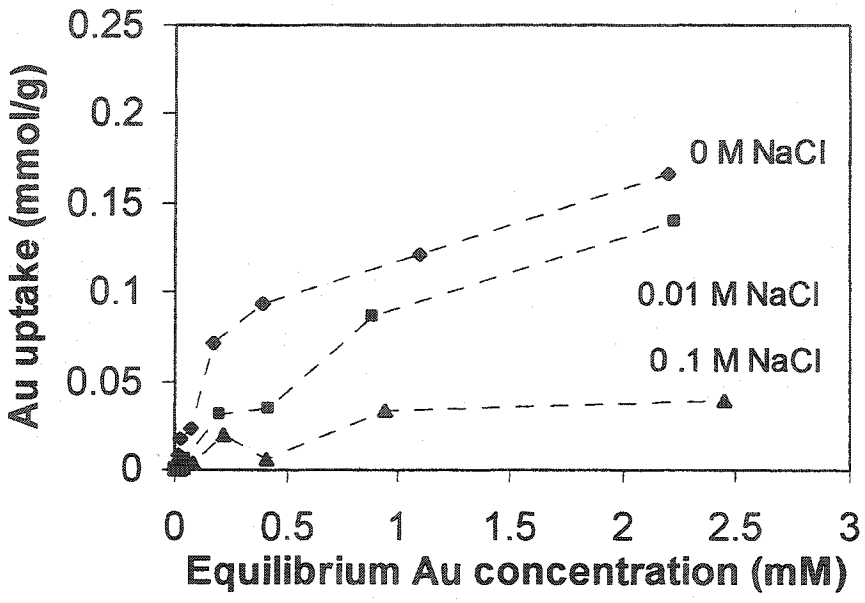

Figure 3.2. 6 Effect of NaCl concentration on gold-cyanide biosorption at pH 3.4

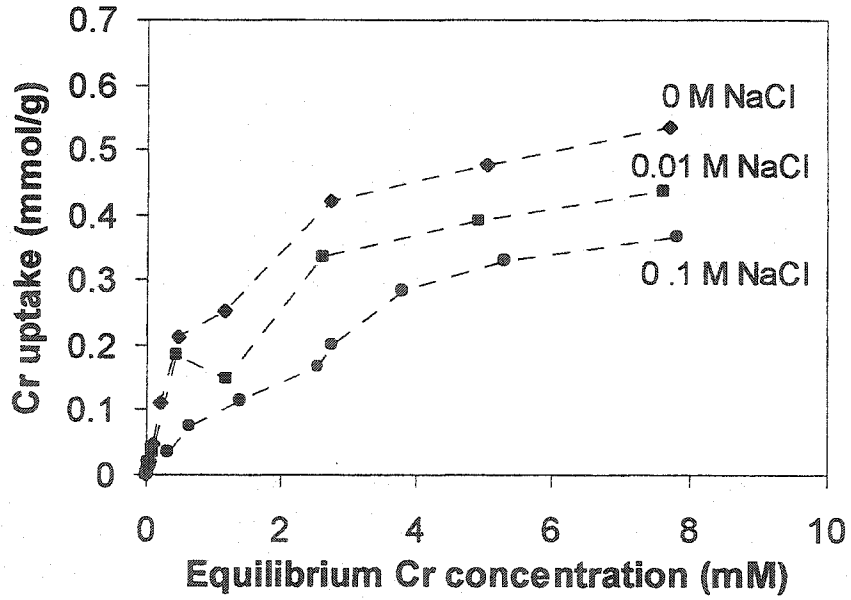

Figure 3.2. 7 Effect of NaCl concentration on chromate biosorption at pH 2.0

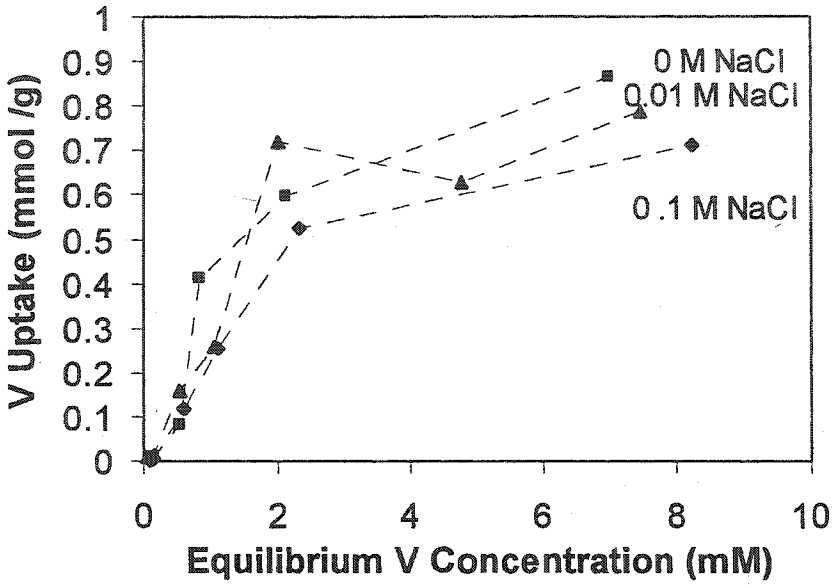

Figure 3.2. 8 Effect of NaCl concentration on vanadate biosorption at pH 2.5

3.2.3 Desorption and Reusability of AWUS

Metal desorption from metal-loaded AWUS by NaOH solution was examined. Chromate, as the strongest oxidant compared with the other selected anionic metal species in the current system, was selected to examine the desorption and reusability of AWUS. AWUS material was first loaded with Cr from the chromate solution at the preferred pH 2.0 and 9.6 mM Cr. Around 40 mg Cr–loaded AWUS materials, bearing 0.54 mmol Cr/g, were mixed with 5 mL or 10 mL of the NaOH eluant solution for 24 hours, whereby the ratio of solid (mg) to liquid (mL) (S/L) is about 8 and 4, respectively. The percentage of Cr recovery, represented by the ratio of the amount of Cr released during desorption to the equilibrium sorption uptake, was calculated for desorption experiments. All of the loaded Cr was eluted from the AWUS into the 10 mL eluant solution at pH 10.6. When Cr was eluted into only 5 mL of eluant solution, a new sorption equilibrium was established and about 4% of deposited Cr remained in the

sorbent. At pH 10.6, chromate exists as CrO_4^{2-} in the aqueous solution (Sillen and Mortell, 1964c; Greenwood and Earnshaw, 1985b; Greenwood and Earnshaw, 1985e; Gupta and Krishnamurthy, 1992e) and Cr elution does not only result from the drastically reduced number of positively charged weak-base groups but also from the competition of OH^-, HCO_3^- or CO_3^{2-} in the solution. Even though the elution experiments in this work are preliminary, the successful elution of bound Cr by the simple increase of solution pH once again confirms the electrostatic attraction involvement in the binding of anionic metal ions or complexes.

The AWUS reusability was demonstrated in several adsorption-desorption cycles. After initially sorbing Cr on the AWUS (at the optimum pH 2.0 and Cr uptake 0.54 mmol Cr/g), and then desorbing it in 5 mL NaOH eluant solution (pH 10.6, 24 hours, S/L =8), the desorbed AWUS material was separated from the eluant and rinsed with demonized water until neutral pH. Then the regenerated AWUS was used in the same adsorption procedure as before. The results (Figure 3.2.9) show that AWUS exhibited the undiminished Cr uptake after three adsorption – desorption cycles. The slightly increased Cr uptakes in the second or third cycles may have resulted from loosening of the chitin-protein structure in shells during the strongly basic elution regime (Roberts, 1992h). The TOC analysis of AWUS-containing solutions at pH 2-10.6 showed that the total TOC released from the shells was 0.25 – 0.87% of the original dry AWUS shells. The AWUS weight loss after the first adsorption-desorption cycle was 9%. The AWUS weight remained constant during the subsequent cycles. AWUS appears much more stable than some biosorbents such as brown-algae biomass. In that case the TOC release and the dry biomass weight loss could be up to 8% and 50%, respectively (Figueira, 1999). If AWUS material could be stable in contacting with a strong redox reagent such as chromate, it is expected to be even more so in conjunction with other solution systems containing less aggressive anionic metal species. The above results indicate that AWUS material makes an effective and stable biosorbent for anionic metal species featuring also a good degree of reusability.

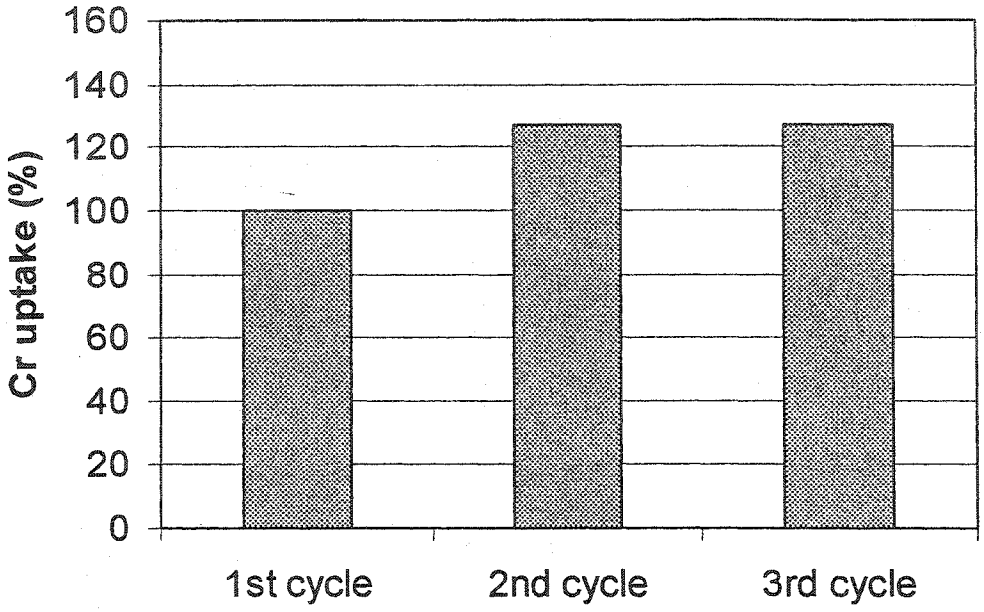

Figure 3.2. 9 Chromate biosorption by AWUS after regeneration

Adsorption: 40±1 mg AWUS, 20±0.2 mL solution with 9.6±0.1 mM Cr, pH 2.0±0.1, Cr uptake : 0.54 mmol/g in the first cycle
Desorption: around 40mg Cr-Loaded AWUS, 5±0.1 mL solution, pH 10.6±0.1, elution efficiency 96±2%

3.2.4 Section Summary

AWUS sorbed well anionic gold-cyanide ($Au(CN)_2^-$), chromate (CrO_4^{2-}), and vanadate (VO_4^{3-}) at low pH. The gold-cyanide equilibrium biosorption uptake by AWUS reached 0.17 mmolAu/g (pH 3.4).

Chromate biosorption reached its maximum at pH 2.0 with the uptake of 0.54 mmol Cr/g biomass. AWUS exhibited higher Cr uptake as compared with the Au uptake.

Vanadate biosorption is maximum at pH 2.5, whereby the V uptake observed was as high as 0.79 mmol V/g.

An increased ionic strength greatly suppressed the primary anionic gold-cyanide and chromate uptake, and mildly so for vanadate uptake.

The bound metals could easily be eluted from the biosorbent by a simple alkali wash. Repeating 3 adsorption-desorption cycles without biosorption performance deterioration indicated the reusability of the AWUS biosorbent.

3.3 The Mechanism of Anionic Metal Species Biosorption

Elucidation of the metal sequestering mechanism would assist in possible manipulation of the sorbent material to optimize its performance. It could also lead to exploring the possibility of eventually using simple analogous materials, either synthetic or natural, for metal sequestering. While the biosorption mechanism has not yet been completely clarified, the metal binding in biosorption has been attributed to a number of different sequestration mechanisms such as adsorption, ion exchange and micro-precipitation (Volesky, 1990b). Adsorption or ion exchange can be the result of three kinds of binding forces. One is a chemical force, another is a physical force, and the third is a combination of both. Different biomaterials in combination with different metals may involve different specific sequestering mechanisms.

It was determined that metal speciation in the solution and the functional groups on the biosorbents are both relevant to the metal binding mechanism. Infrared spectroscopy has been proven to provide a powerful tool for studying biological molecules and its application in obtaining structural and bonding information on complex and large molecules has been fruitful (Nakamoto, 1997).

Previous results showed that AWUS material has a promising potential for anionic metal species binding. However, the mechanism involved needs to be further clarified.

The objective of this section is to investigate the binding mechanism of AWUS and selected anionic metal complexes such as chromate (CrO_4^{2-}), vanadate (VO_4^{3-}) and gold-cyanide ($Au(CN)_2^-$).

3.3.1 Anionic Metal Speciation and Sorption Functional Groups

3.3.1.1 Chromate Biosorption

Chromate is the strongest oxidant among the selected anionic metal complexes of (CrO_4^{2-}), vanadate (VO_4^{3-}), and gold-cyanide ($Au(CN)_2^-$). The speciation of chromate in the biosorption system with AWUS could reflect the reducibility of the AWUS material.

3.3.1.1.1 The Effect of AWUS on Cr Speciation in Solution

The AWUS-containing chromate sample was prepared by mixing 40 mg dried AWUS with 20 mL chromate solution of 9.12 mM Cr at pH 2.1 (room temperature). In this system, except for the presence of AWUS, chromate theoretically exists as $HCrO_4^-$ and $Cr_2O_7^{2-}$ (Greenwood and Earnshaw, 1985c). However, in an actual solution, especially with AWUS in the solution, chromate speciation may be different. Therefore, it was necessary to investigate the chromate speciation experimentally. The total Cr concentration was determined by the ICP-ASE, and the Cr(VI) concentration by the UV Spectrophotometer. The other form of Cr will then be determined by the concentration difference between the total Cr and the Cr(VI).

Table 3.3.1.1 summarizes the concentration of different Cr ionic species in the equilibrium biosorption system as well as in the control solution (without biosorbent). The results showed that, in the control solution, up to 84.3% of the total Cr concentration was there as Cr(VI), indicating that Cr (VI) could be reduced to other forms even in the deionized water at pH 2.1. This represents a departure from the ideal thermodynamic calculations. However, the percentage of the reduced part is minor (15.7%). As known,

Table 3.3.1. 1 Determination of chromate speciation in a biosorption system (pH 2.1)

	$[Cr_{,total}]$* (mM)	[Cr(VI)]* (mM)	[Cr(VI)/$[Cr_{,\ total}]$ (%)	q^{Cr} (mmol/g)**
Control solution	9.12±0.11	7.69±0.10	84.3±0.02	/
Adsorption sample	7.93±0.13	6.70±0.11	84.5±0.03	0.59±0.06

* Equilibrium concentration.

** The uptake of chromium in all forms (mmol/g).

Cr (VI) is the highest oxidation state of Cr. While there are other possible states of Cr such as Cr (V), Cr (IV), and Cr (II), the most stable oxidation state is Cr (III) (Greenwood and Earnshaw, 1985d). Under acidic conditions, chromate is apparently reducible most possibly to Cr(III). In the biosorption system, the percentage of Cr (VI) in the solution was also 84.5%, the same as in the control solution. This was different from what was observed during chromate adsorption by *Sargassum* biomass where the concentration ratio of Cr(VI) to Cr_{total} in the solution decreased greatly with the addition of the biomass to the chromate solution (Kratochvil, 1997). It could be concluded that AWUS is not significantly active in reducing chromate. However, the form of Cr bound on the crab shells has to be determined through an instrumental assay based on the FTIR analysis.

3.3.1.1.2 FTIR Analysis

FTIR analysis was conducted to investigate the metal form(s) sequestered on AWUS and the main functional groups for metal biosorption. The metal-loaded biosorbent samples were prepared by mixing 40 mg AWUS particles (0.5-0.85 mm in diameter) with 20 mL of 9.5 mM Cr (chromate) at pH 2.0. The Cr uptake was 0.79 mmol/g.

The results of FTIR analyses of solid chromium trioxide, blank AWUS and Cr-loaded AWUS are shown in Table 3.3.1.2 and Figure 3.3.1a-b.

The spectrum of chromium trioxide (Cr(VI)) (Table 3.3.1.2) showed a characteristic peak at 954 cm^{-1} ascribed to chromate (ν_3) vibration (Gadsden, 1975a). This peak appeared on the spectrum of Cr-loaded AWUS indicating that chromate was bound on the shells. As the characteristic peaks of dichromate are also located between 800 and 950 cm^{-1}(Gadsden, 1975a), it is not possible to distinguish the form of chromate from that of dichromate bound on the shells. However, this result indicated that there was Cr(VI) bound on the shells.

Furthermore, the spectrum of blank AWUS displayed peaks at 1450 and 1739 cm^{-1} (Table 3.3.1.2) which can be ascribed to the vibration of amide II (Morrison, 1987; Schrader, 1995) and ν(C=O) of the carboxyl group (Nakamoto, 1997), respectively. The peak of amide II was invisible on the spectrum of Cr-loaded AWUS, indicating the amide group involvement in Cr adsorption. The major organic substances in AWUS material are chitin and protein. The determined N-acetylation degree of extracted chitin was 78%, indicating around 78% of N in the chitin of AWUS was in the amide form. In addition, amide is also a crucial characteristic group of proteins. The amide II peak of either chitin or protein is located around 1450 – 1580 cm^{-1} (Morrison, 1987; Roberts, 1992r; Schrader, 1995). Therefore, the change of amide II peak could be the contribution of either chitin amide or protein amide. As the Cr adsorption was performed at pH 2 at which the amide groups could theoretically be fully protonated (Roberts, 1992a) and available for anionic

chromate binding, the peak of amide II shifted and was invisible, probably overlapped by the bigger peaks next to it.

Lastly, the peak of ν(C=O) of the carboxyl group on AWUS disappeared on the spectrum of Cr-loaded AWUS. Carboxyl group is a weak-acid group that could not directly contribute to anionic chromate binding. However, the previous chromate speciation analysis indicated that there was around 15% of Cr(III) existing in the solution. Kratochvil confirmed that Cr(III) could be bonded to the carboxyl group at pH 2 (Kratochvil, 1997). Cr(III) in the present system could also be bonded onto the AWUS resulting in the shift of the ν(C=O) peak, possibly overlapped by the bigger peak next to it.

In summary, there is a strong indication that AWUS cannot significantly reduce chromate even though chromate is a strong oxidant. Cr(VI) compounds either as chromate or dichromate were found bound on the shells. Amide groups were involved in binding of anionic chromate. The carboxyl group on the protein may be responsible for the small amount of Cr(III) binding.

Table 3.3.1. 2 Cr adsorption by AWUS: Summary of FTIR spectral data (cm^{-1})

Bond vibration	Chromate (ν_3)	amideII	ν(C=O)
CrO_3	954	/	/
Blank AWUS	/	1450	1739
Cr-loaded AWUS	952	/	/

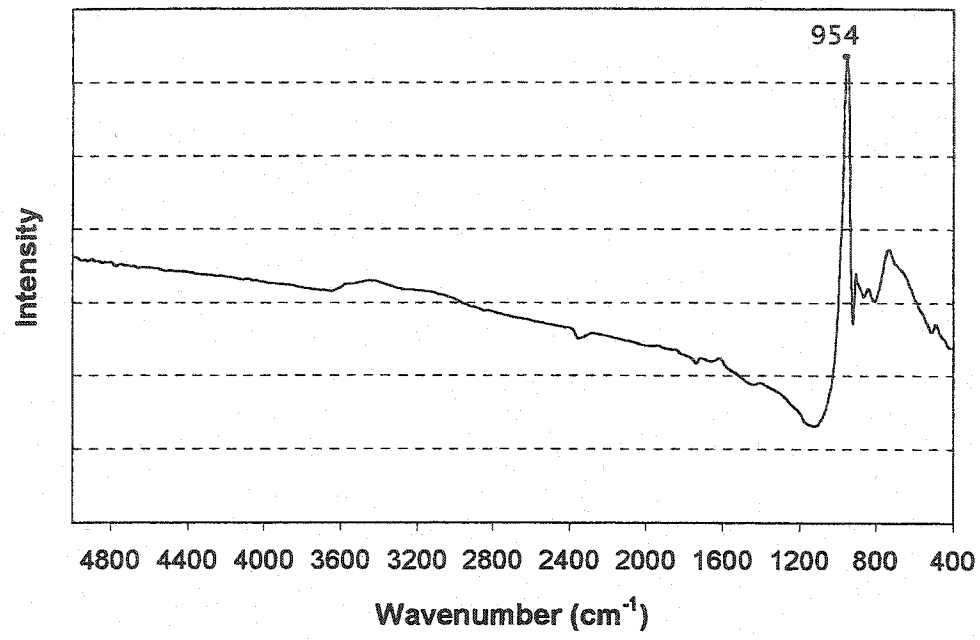

Figure 3.3.1 a FTIR spectrum of chromium trioxide (CrO_3)

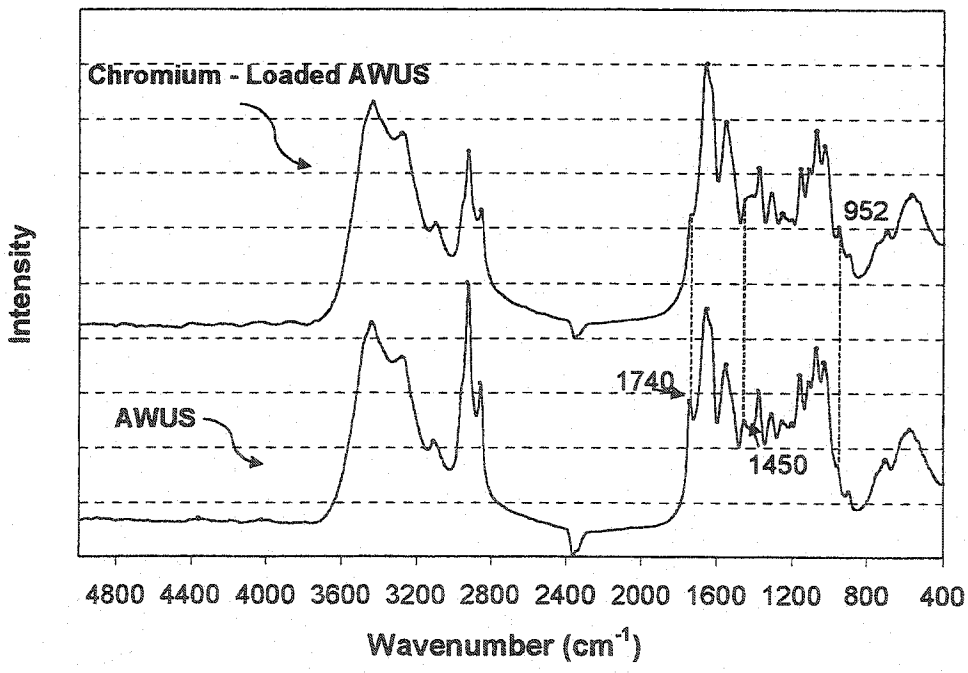

Figure 3.3.1 b FTIR spectra of blank and chromium-loaded AWUS

3.3.1.2 Vanadate Biosorption

Previous results revealed that AWUS could not effectively reduce chromate. Compared to chromate, vanadate has lower oxidizability (Greenwood and Earnshaw, 1985d). V (V) could be reduced to V (IV), V (III) and V, however, in the presence of air, V(V) is the most stable oxidized state of vanadium in aqueous solution (Gupta and Krishnamurthy, 1992e). Logically speaking, a significant reduction of vanadate is not expected in the present similar biosorption system. The form of vanadium bound on AWUS was also examined by the FTIR analysis. The V-loaded shells were prepared by mixing 40 mg AWUS particles (0.5 – 0.85 mm in diameter) with 20 mL vanadium solution initially containing 7.18 mM V (vanadate) at pH 2.5. The equilibrium uptake of V was 1.5 mmol/g.

The FTIR spectra of sodium orthovanadate, blank AWUS and V-loaded AWUS are shown in Table 3.3.1.3 and Figure 3.3.2a-b.

The spectrum of sodium orthovanadate displayed a peak at 837 cm^{-1}. This peak is characteristic for the vanadate (ν_3) vibration (Gadsden, 1975b), which appeared on the spectrum of V-loaded AWUS at 833 cm^{-1}. In addition, there was another new peak at 758 cm^{-1} that appeared on the spectrum of V-loaded shells. It could also be ascribed to the vanadate vibration usually located at around 700 – 900 cm^{-1} (Gadsden, 1975b). All these new peaks observed for the V-loaded shells confirmed that vanadate (V(V)) was bound.

Furthermore, the peak at 1550 cm^{-1} (amide II vibration) observed for the spectrum of blank AW shells shifted to 1538 cm^{-1} for V-loaded AWUS, once again confirming that amide groups on the shells involved V binding. The weak shift of less than 15 cm^{-1} was attributed to electrostatic attraction (Mooiman and Miller, 1986).

As the present biosorption system was at pH 2.5 whereby vanadate could exist as cationic VO_2^+, anionic forms of vanadate and neutral colloidal vanadium pentoxide (V_2O_5) in the aqueous solution (Sillen and Mortell, 1964a; Pope and Dale, 1968; Kepert,

1973; Baes and Mesmer, 1976b; Greenwood and Earnshaw, 1985e; Gupta and Krishnamurthy, 1992e; Larson, 1995), different adsorption mechanisms can contribute to the overall V uptake. Consequently, it cannot be concluded that vanadium adsorption involves only anionic vanadate binding.

However, the above results did confirm that vanadate (V) was bound on the shells and that the amide groups on the shells were involved in the binding through electrostatic attraction.

Table 3.3.1. 3 V adsorption by AWUS: Summary of FTIR spectral data (cm^{-1})

Bond vibration	vanadate	amide II
Solid $NaVO_4$	837	/
Blank AWUS	/	1550
V-loaded AWUS	833, 758	1538

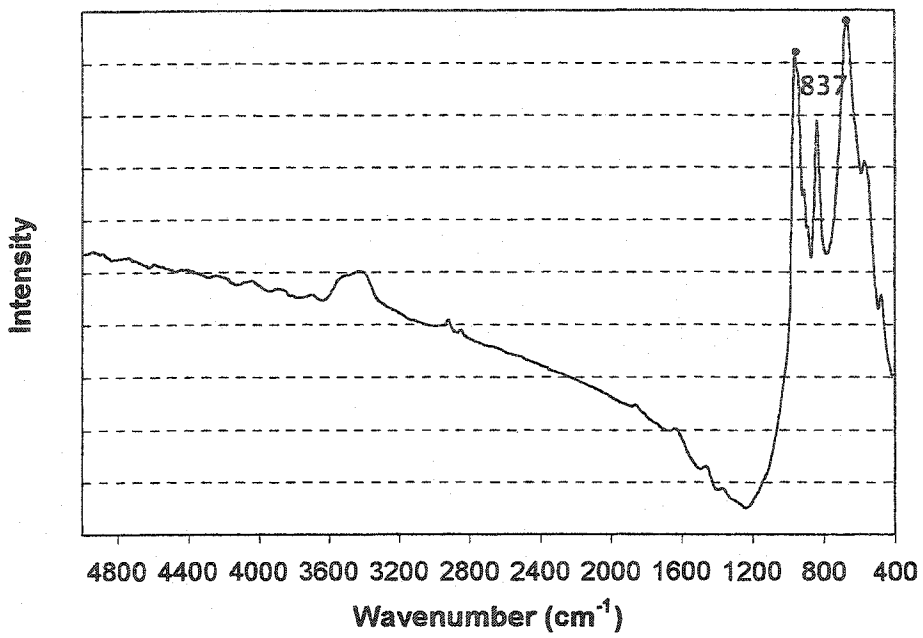

Figure 3.3.2 a FTIR spectrum of sodium orthovanadate (Na_3VO_4)

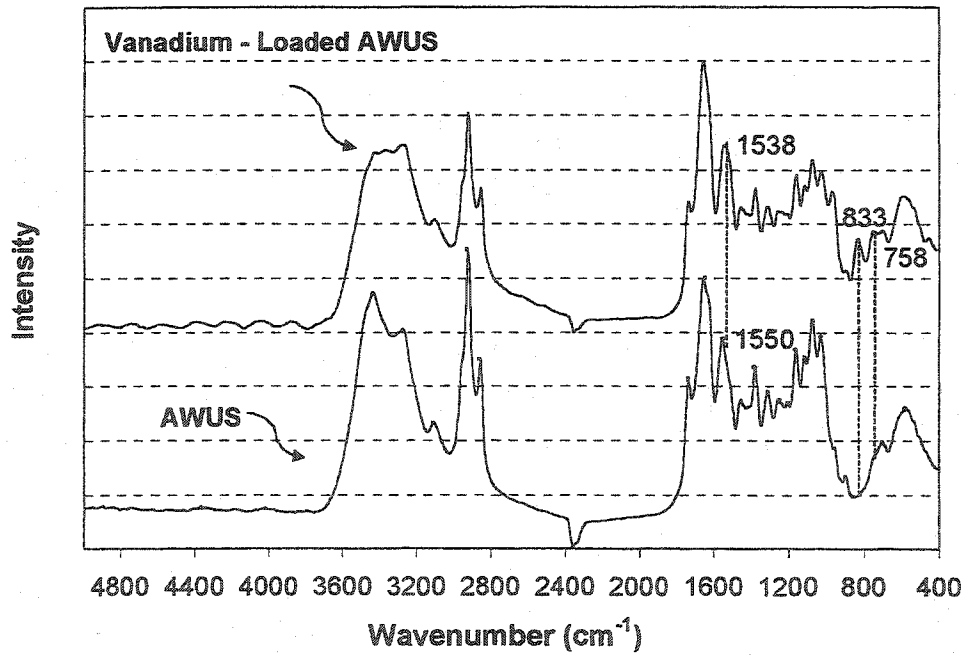

Figure 3.3.2 b FTIR spectra of blank and vanadium-loaded AWUS

3.3.1.3 Gold-cyanide Biosorption

Of the metal complexes studied, the gold-cyanide complex ($Au(CN)_2^-$) is the most stable one, with the dissociation constant of Au from the cyanide complex being $10^{-38.9}$ (Marsden and House, 1993e). $Au(CN)_2^-$ adsorption by *Sargassum* biomass confirmed that gold-cyanide is such a stable complex that it could not be reduced by *Sargassum* which was capable of significant chromate reduction (Niu and Volesky, 1999). As AWUS could not appreciably reduce chromate at all, it was not desirable to reduce Au from gold-cyanide. In order to confirm the form of $Au(CN)_2^-$ on the AWUS, the FTIR analysis was performed. The Au-loaded sample was prepared by mixing 20 mL 3.44 mM Au ($Au(CN)_2^-$) with 40 mg AWUS particles (0.5 – 0.85 mm in diameter) at pH 3.2. The Au uptake (loading) was 0.2 mmol/gAWUS.

The FTIR spectrum (Figure 3.3.3a-b) of Au-loaded AWUS confirmed that $Au(CN)_2^-$ (characteristic peak at 2150 cm^{-1}) was bound on the AWUS (Nakamoto, 1986). If Au was reduced from $Au(CN)_2^-$, there would have to be free CN^- released which could also compete for the sites. However, there was no peak observed for free CN^- on the shells, usually located at 2080 cm^{-1}(Nakamoto, 1986).

In summary, no significant redox action occurred during biosorption of the selected anionic metal species. The metal complex binding was mainly on the amide groups of AWUS. The binding force can be considered weak indicating thus electrostatic attraction.

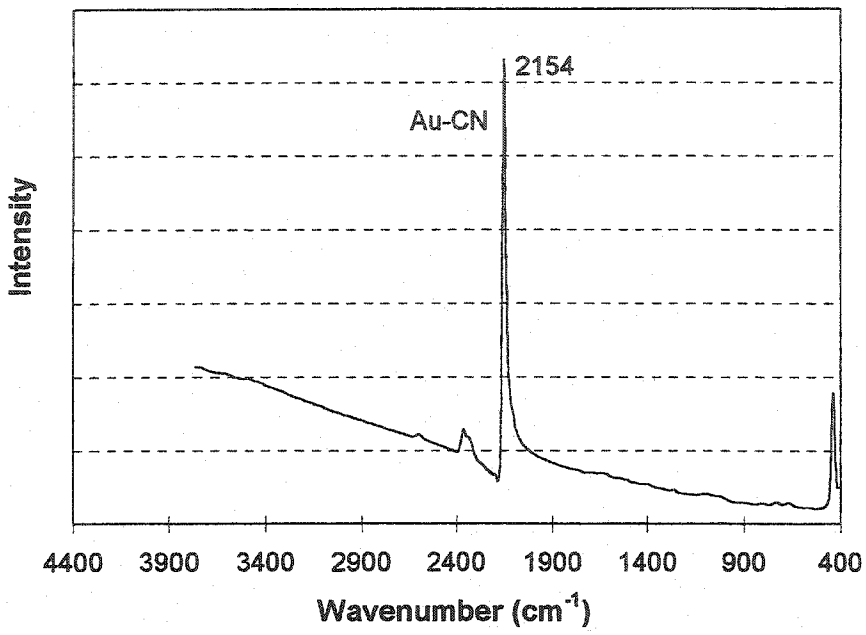

Figure 3.3.3 a FTIR spectrum of $NaAu(CN)_2$

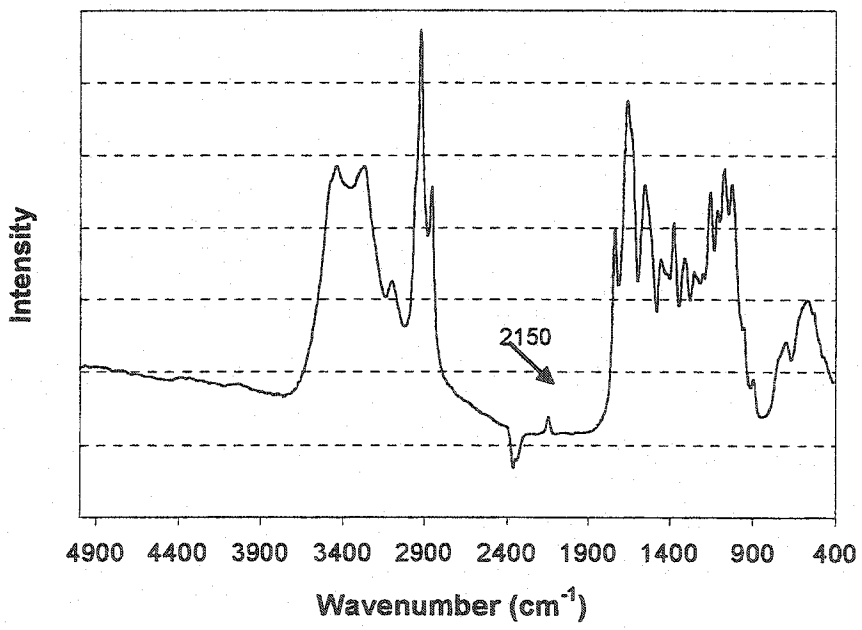

Figure 3.3.3 b FTIR spectrum of Au-loaded AWUS

3.3.2 Determination of Electrostatic Attraction

The predominant binding force of electrostatic attraction for anionic metal species biosorption by AWUS is being postulated based on the following results:

The weak shifts of the functional amide peak observed in the above FTIR analysis indicated that the anionic metal species biosorption involves electrostatic attraction.

The strong increase of the selected metal uptakes on solution pH within the range from 4.0 to 2.0 (Section 3.2) is another indication. Similar pH effect phenomena were found for anionic dye adsorption by chitin from pH 6.5-2.5 (Giles and Hassan, 1958; Giles et al., 1958) and for chromate uptake by chitosan from pH 8.0-4.0 (Roberts, 1992f) which were attributed to electrostatic attraction of anionic species to the positively charged groups of amide or amine.

Ion adsorption by electrostatic attraction is significantly affected by the enhanced ionic strength in the solution (Davis and Leckie, 1980). Previous results concerning the ionic strength effects (Section 3.2) showed the strong dependence of metal uptakes on this solution parameter, confirming that the anionic metal species adsorption by AWUS as discussed above is through electrostatic attraction.

The desorption results in the present study (Section 3.2) are showing that the loaded metals could be eluted by simply increasing the solution pH with NaOH. Once again, this confirmed that the anionic metal species adsorption was through electrostatic attraction. If chemisorption were occurring, simple pH adjustment could not accomplish the elution of the bonded metals, such as was observed for cationic metal adsorption by *Sargassum,* where Cd and Cu were covalently bonded on the biomass (Aldor et al., 1995; Figueira et al., 1999).

Vanadate binding might involve other binding forces besides electrostatic attraction as colloidal V_2O_5 present in the solution.

3.3.3 Combination of Mechanisms

The analyses in the above sections provided information on the forms of loaded metals and AWUS functional groups as well as on the binding force. However, they could not determine the approach of the metal binding, i.e. adsorption, ion exchange or others. In the context of this work, the term "adsorption" refers to the binding of a solute to free sites that had not been previously occupied by other ions. If the sites are initially occupied by other ions and if these ions are released upon the binding of the new ion, then the term "ion exchange" is used to describe the phenomenon (Schiewer, 1996b). Possibly the best proof of the exchange mechanism is the change in pH of the sorption system when the sorbent is transferred from water to a salt (NaCl) solution (Nachod, 1949a). The addition of salt (NaCl) should have little effect when the uptake mechanism is adsorption:

$$BNH + HCl = BNH_2^+ Cl^- \qquad (3.3.1)$$

In the exchange reaction,

$$BNH_3^+ OH^- + Cl^- = BNH_2^+ Cl^- + OH^- \qquad (3.3.2)$$

however, the addition of NaCl will drive the equilibrium to the right and raise the pH value.

Strong-base resin was confirmed to be involved in ion exchange that contained appreciable amounts of the ionized hydroxide, $RNH_3^+ OH^-$ (Nachod, 1949b) in a neutral and alkaline condition. However, with weak-base resins, no such significant exchange of chloride for hydroxyl was observed (Nachod, 1949b).

In the present work, AWUS sorbent was prepared by first washing the raw *Ucides cordatus* shells with 1N HCl, then rinsing with deionized water until pH stabilized at pH ~ 4.0, and finally drying at 50-55°C. In order to determine the biosorption mechanism, the experiments were performed as follows:

First, 40mg AWUS was equilibrated with 20 mL deionized water. The final solution pH was 3.9.

Second, the AWUS material was transferred from the deionized water to 20 mL 0.1M NaCl solution, the equilibrium solution pH was observed to rise to pH 4.7.

If this pH change is caused by the exchange of Cl^- and OH^- on the protonated amino groups, the released OH^- was calculated to be 0.05mmol/g AWUS.

Third, the amount of the protonated amino groups on fresh AWUS initially occupied by Cl^- during the preparation of AWUS was determined by mixing 0.04 g fresh AWUS with NaOH solution at pH 11. The total released Cl^- (analyzed by IC) was 0.06 mmol/g AWUS.

Summarizing the above results, the total amount of protonated amino sites initially on AWUS should be no higher than the sum of the released OH^- and Cl^-, i.e. 0.1mmol/g. If OH^- and Cl^- were only replaced by $Au(CN)_2^-$ and Cr (VI) ($HCrO_4^-$ or $Cr_2O_7^{2-}$ under the present biosorption conditions), the ratios of pre-occupied sites to the highest Au (0.17 mmol/g) and Cr (0.54 mmol/g) uptakes obtained in this work (Section 3.2) are 55% and 32%, respectively. These data indicated that there was 55% of Au binding and of 32% Cr binding through ion-exchange. The remainder of the respective uptakes of these metals was through adsorption. In addition, theoretically, only part of the functional amide groups in AWUS are fully protonated when stabilized in demonized water at pH ~ 4.0 during the preparation of AWUS as the conjugate acid dissociation constant (p*Ka*) of chitin amide is less than 3.5 (Roberts, 1992q). While all the amine groups on AWUS could be fully protonated initially as the conjugate acid dissociation constants (p*Ka*) of chitin and protein amine are 6.5-10 (Buffle, 1988a; Roberts, 1992a), the available capacity of amine is questionable because the metal uptakes obtained at pH 4.5 were very low (for an example, the Au uptakes in Section 3.2). In addition, FTIR analysis did not show the involvement of amine groups in the biosorption. Therefore in the gold-cyanide and chromate biosorption system, the binding mechanism is a combination of ion-exchange and adsorption.

In the case of vanadate binding, the obtained vanadium uptake was by far more than the previously calculated pre-occupied sites. As cationic VO_2^+, anionic forms of vanadate and neutral colloidal vanadium pentoxide (V_2O_5) are formed in the aqueous solution within the pH range of 1.5-4.5 and less than 10 mM V employed in the present biosorption experiments (Sillen and Mortell, 1964a; Pope and Dale, 1968; Kepert, 1973; Greenwood and Earnshaw, 1985e; Gupta and Krishnamurthy, 1992e; Larson, 1995), vanadium binding may involve other mechanism in addition to ion exchange and adsorption. It is a recognized fact that a combination of several mechanisms, each functioning independently, can contribute to the overall metal uptake in the biosorption system (Volesky, 1990b).

3.3.4 Section Summary

Biosorption of anionic metal species such as gold-cyanide, chromate and anionic vanadate species by AWUS mainly involved anions binding on the positively charged amide groups of the AWUS. The binding force may relate to electrostatic attraction.

No significant reduction of the selected metals was observed in the biosorption systems with AWUS. All selected metals were observed bound on AWUS at their respective original valent states, i.e. Au(I), Cr(VI) and V(V).

Anionic metal species biosorption takes place through a combination of ion-exchange and adsorption. In the case of vanadate, the binding mechanism might involve other mechanism in addition to the above ones.

3.4 Biosorption Modeling: Anionic Single Metal Systems

Results reported in the preceding sections demonstrated the potential of AWUS for effective binding of anionic metal species. In order to quantitatively describe and eventually predict the anionic metal species uptakes, a model will be proposed in this section.

Since the AWUS sorbent is partially penetrable without significantly swelling, theoretically, neither Surface Complexation Model for impenetrable surface nor Donnan Model for significantly swelling sorbents are applicable. To model the anion adsorption by a weak-base, one of the alternative approaches is to assume anion binding to be the acid base neutralization (Yoshida et al., 1994; Yoshida and Kishimoto, 1995). Yoshida used this approach to derive the HCl adsorption isotherm of modified chitosan, which was considered as being of Langmuirian nature, i.e.

$$\text{Chitosan-NH}_i + \text{HCl} = \text{Chitosan-NH}_{i+1}^{+}\ \text{Cl}^- \qquad (3.4.0.1)$$

$$K_{HCl} = \frac{[\text{Chitosan} - \text{NH}_{i+1}^{+}\text{Cl}^-]}{[\text{Chitosan} - \text{NH}_i][\text{HCl}]} \qquad (3.4.0.2)$$

$$q^{HCl} = \frac{Q_{HCl} K_{HCl}[\text{HCl}]}{1 + K_{HCl}[\text{HCl}]} \qquad (3.4.0.3)$$

where q^{HCl} is the HCl uptake, Q_{HCl} denotes the total binding capacity for HCl, K_{HCl} represents the HCl adsorption constant and [HCl] is the equilibrium HCl concentration.

While the above model could agree with the experimental data, the application of the model is limited as Q_{HCl} and K_{HCl} are highly dependent on solution pH and ionic

strength. It thus should be more proper to represent [HCl] by the activity product of $\{H^+\}\{Cl^-\}$, where { } represents the activity (Frey, 1997).

In this section, based on Yoshida's model, a modified model for describing the anionic metal species biosorption equilibrium data as a function of metal concentration, pH and ionic strength as well as the interference of Cl^- will be developed.

3.4.1 Model Description

3.4.1.1 Model Assumptions

The current model has been established for biosorption of anionic metal species. It is based on the following assumptions:

1) All anionic metal species binding is relating to only one fictitious weak-base group (BNH) on AWUS, which is also the only surface charge-determining group.

2) Na^+, brought into the solution by metal reagent, or ionic strength adjustment, is inert with regard to AWUS.

3) Anion is bound on the positively charged protonated weak-base group by electrostatic attraction.

4) Attribute all non-ideality to the liquid phase.

5) Cl^- brought into the solution by pH or ionic strength adjustments could compete with anionic metal species for the weak-base functional group.

6) The interference of OH^-, HCO_3^- and CO_3^{2-} on anionic metal species binding is neglected.

Assumption (1) of one fictitious weak-base site is based on the following results obtained from the previous Section 3.3: a) amide is the main functional group for anionic

metal species binding. b) even though other weak-base group such as amine might also contribute to anionic metal species binding, the available capacity of amine is questionable as discussed in the previous Section 3.3. Therefore, for simplicity, it was assumed that there was only one fictitious weak-base group (BNH) as the main weak-base N-containing group. Furthermore, this fictitious weak-base group is also assumed to determine the charge on AWUS.

Assumptions (2) and (3) were made based on the fact that alkaline light metals are indifferent to chitin, especially at low pH (Muzzarelli, 1973a). In addition, Na biosorption results in this work show the negligible Na uptake (only 0.01 mmolNa/g AWUS), corresponding to 0.1M Na in the solution. This indicates that Na^+ binding could be neglected at NaCl concentrations not exceeding 0.1 M. In the present work, all anionic metal species solutions were prepared using the corresponding sodium salts except for chromate solutions prepared with CrO_3. Therefore, it can be safely assumed that, apart from H^+, no other cations would contribute to the surface positive charge. Anionic metal species are thus bound on the positively charged protonated groups by electrostatic attraction.

Assumption (4) was made based on the fact that metal adsorption takes place from solutions with ionic strength not exceeding 0.1M. Therefore, while the model considers the non-ideality in the liquid phase by incorporating solution species activity coefficients, the activity coefficients of species in the sorbent phase (AWUS) are lumped into the reaction equilibrium constants.

Assumption (5) was made based on the relevance of Cl^- binding on inorganic oxide at Cl^- concentrations higher than 0.01M (Davis et al., 1978).

The last assumption (6) was made based on the fact that anionic metal species adsorption is performed at pH 2.5-4.5, where the OH^- concentration is low enough to be negligible. CO_2 could be dissolved in the solution exposed to the air. As the logarithm of the first order proton dissociation constant of carbonic acid is 6.37 (Lidin et al., 1995), carbonic acid remained neutral under the experimental conditions used in the present

work and could not compete significantly for the positively charged protonated sites on AWUS.

According to the above assumptions, a one-site model for biosorption of anionic metal species has been developed as follows.

3.4.1.2 Anion Binding

Anionic Metal Species Binding

Anionic metal species binding is following the acid-base neutralization:

$$BNH + zH^+ + H_xM_pL_q^{Z-} = BNH_2^+ H_xM_pL_q^{Z-} H^+_{z-1} \quad (3.4.1)$$

From the mass action law:

$${}^{ad}K_M^{int} = \frac{\{BNH_2^+H_xM_pL_q^{Z-}H^+_{z-1}\}}{\{BNH\}\{H^+\}^z\{H_xM_pL_q^{Z-}\}} \quad (3.4.2)$$

where BNH and $BNH_2^+ H_xM_pL_q^{Z-} H^+_{z-1}$ represent the free fictitious weak-base group on AWUS and adsorbed anionic metal species, respectively. $H_xM_pL_q^{Z-}$ denotes the anionic metal species in the solution, p, q and x represent the number of metal, ligand (such as cyanide or oxygen) and protons per anionic metal species, respectively. Z symbolizes the charge of the anionic metal species, ${}^{ad}K_M^{int}$ is the intrinsic equilibrium constant of $H_xM_pL_q^{Z-}$ biosorption. Finally, { } represents the species activity.

Attributing all non-ideality to the liquid phase, the activity of each species on the AWUS could be replaced by the corresponding concentration term, equation (3.4.2) becomes:

$${}^{ad}K_M = \frac{[BNH_2^+H_xM_pL_q^{Z-}H^+_{z-1}]}{[BNH]\{H^+\}^z[H_xM_pL_q^{Z-}]\gamma_{H_xM_pL_q^{Z-}}} \quad (3.4.3)$$

[ ] represents the species concentration, $\gamma_{H_xM_pL_q^{z-}}$ is the activity coefficient of $H_xM_pL_q^{Z-}$ in the solution and ${}^{ad}K_M$ denotes the equilibrium constant of $H_xM_pL_q^{Z-}$ biosorption lumping activity coefficients of species on the solid phase. The form of proton activity $\{H^+\}$ remains as could be obtained directly by pH measurement.

Water dissociation equilibrium gives:

$$H_2O = H^+ + OH^- \tag{3.4.4}$$

Its equilibrium constant is:

$$Kw = \{H^+\}\{OH^-\} \tag{3.4.5}$$

At 25°C, $Kw = 10^{-14}$ $(mol/L)^2$.

Cl^- Binding

Similarly to anionic metal species binding, Cl^- binding is as follows:

$$BNH + H^+ + Cl^- = BNH_2^+ Cl^- \tag{3.4.6}$$

$${}^{ad}K_{Cl} = \frac{[BNH_2^+Cl^-]}{[BNH]\{H^+\}[Cl^-]\gamma_{Cl^-}} \tag{3.4.7}$$

Where ${}^{ad}K_{Cl}$ is the Cl^- equilibrium binding constant, γ_{Cl^-} represents the activity coefficient of Cl^- in the solution and $BNH_2^+ Cl^-$ denotes the adsorbed Cl^-.

3.4.1.3 Mass Balance

The mass balance for the functional site is:

$$[B_T] = [BNH] + \sum_i ([BNH_2^+H_xM_pL_q^{Z-}H_{Z-1}^+])_i + [BNH_2^+ Cl^-] \tag{3.4.8}$$

For the anion metal species:

$$[M]_0 = \sum_i p*([H_xM_pL_q^{Z-}])_i + \sum_i p*([BNH_2^+H_xM_pL_q^{Z-}H_{Z-1}^+])_i * w/v \quad (3.4.9)$$

Na^+ conservation gives:

$$[Na^+]_0 = [Na^+] \quad (3.4.10)$$

Cl^- balance is:

$$[Cl^-]_0 = [Cl^-] + [BNH_2^+ Cl^-] \quad (3.4.11)$$

where $[B_T]$ is the total capacity of the functional group for anion binding, $[M]_0$ denotes the initial metal concentration in the solution. $\sum_i([H_xM_pL_q^{Z-}])_i$ and $\sum_i p*([BNH_2^+H_xM_pL_q^{Z-}H_{Z-1}^+])_i$ are the sums of the equilibrium metal concentration in the solution and of adsorbed metals, respectively. i represents i^{th} spiecies. Finally, $[Na^+]_0$ and $[Na^+]$ represent the initial and equilibrium sodium concentration in the solution.

Then metal uptake q^M could be obtained from equations. (3.4.3), (3.4.7) and (3.4.8):

$$q^M = \sum_i p*([BNH_2^+H_xM_pL_q^{Z-}H_{Z-1}^+])_i$$

$$= \sum_i \frac{p*[B_T]*{}^{ad}K_M*\{H^+\}^z*[H_xM_pL_q^{Z-}]\gamma_{H_xM_pO_q^{z-}}}{1+K_{Cl}\{H^+\}[Cl^-]\gamma_{Cl^-}+\sum_i({}^{ad}K_M*\{H^+\}^z*[H_xM_pL_q^{Z-}]\gamma_{H_xM_pO_q^{z-}})} \quad (3.4.12)$$

3.4.1.4 Anionic Metal Speciation

The anionic metal species $[H_xM_pL_q^{Z-}]$ in the above equation (3.4.12) will be determined by the solution speciation of the metal of interest. The speciation of selected metal complexes reported here is based on that in the aqueous solution with pH 2-4.5

and the metal concentration range of 0 – 10 mM. These conditions were employed for the present metal adsorption experiments.

In the case of Au, $Au(CN)_2^-$ could remain in such a form under the above conditions (Sillen and Mortell, 1964c; Marsden and House, 1993b).

However, in the case of chromate, the following equations represent the equilibria governing the species distribution in aqueous solution at 25°C (Sillen and Mortell, 1964b; Greenwood and Earnshaw, 1985c; Cabatingan et al., 2001).

$$H_2CrO_4 = HCrO_4^- + H^+ \tag{3.4.13}$$

$$Kcr,1 = \frac{[HCrO_4^-][H^+]}{[H_2CrO_4]}\gamma_{HCrO_4^-}\gamma_{H^+} = 10^{0.26} \quad \text{(mol/L)} \tag{3.4.14}$$

$$HCrO_4^- = CrO_4^{2-} + H^+ \tag{3.4.15}$$

$$Kcr,2 = \frac{[CrO_4^{2-}][H^+]}{[HCrO_4^-]}\frac{\gamma_{CrO_4^{2-}}\gamma_{H^+}}{\gamma_{HCrO_4^-}} = 10^{-5.9} \quad \text{(mol/L)} \tag{3.4.16}$$

$$2HCrO_4^- = Cr_2O_7^{2-} + H_2O \tag{3.4.17}$$

$$Kcr,3 = \frac{[Cr_2O_7^{2-}]}{[HCrO_4^-]^2}\frac{\gamma_{Cr_2O_7^{2-}}}{\gamma^2_{HCrO_4^-}} = 10^{2.2} \quad \text{(mol/L)}^{-1} \tag{3.4.18}$$

$$HCr_2O_7^- = Cr_2O_7^{2-} + H^+ \tag{3.4.19}$$

$$Kcr,4 = \frac{[Cr_2O_7^{2-}][H^+]}{[HCr_2O_7^-]}\frac{\gamma_{Cr_2O_7^{2-}}\gamma_{H^+}}{\gamma_{HCr_2O_7^-}} = 10^{0.85} \quad \text{(mol/L)} \tag{3.4.20}$$

where *Kcr,i* is the corresponding protolysis constant.

Since the first order proton dissociation constant of $H_2Cr_2O_7$ is too large, the equilibrium of this protolysis reaction is not considered (Greenwood and Earnshaw, 1985c). At pH 2.0-4.5 and the Cr concentration range 0-10 mM, only reaction (3.4.17) is considered, i.e. $HCrO_4^-$ and $Cr_2O_7^{2-}$ anions are predominantly present and their concentrations appear depending on the Cr concentration and the solution pH (Sillen and

Mortell, 1964b; Greenwood and Earnshaw, 1985c; Cabatingan et al., 2001). If the small amount of non Cr(VI) species observed in Section 3.3 is neglected, then the total equilibrium chromium concentration in the solution, Cr_T, could be expressed as:

$$[Cr_T] = [HCrO_4^-] + 2*[Cr_2O_7^{2-}] \quad \text{(mM)} \tag{3.4.21}$$

$HCrO_4^-$ and $Cr_2O_7^{2-}$ could be calculated from equations (3.4.18) and (3.4.21) and expressed respectively as:

$$[HCrO_4^-] = \frac{\sqrt{8[Cr_T]K_{Cr,3}\frac{\gamma^2_{HCrO_4^-}}{\gamma_{Cr_2O_7^{2-}}} + 1} - 1}{4K_{Cr,3}\frac{\gamma^2_{HCrO_4^-}}{\gamma_{Cr_2O_7^{2-}}}} \tag{3.4.22}$$

$$[Cr_2O_7^{2-}] = \frac{(\sqrt{8[Cr_T]K_{Cr,3}\frac{\gamma^2_{HCrO_4^-}}{\gamma_{Cr_2O_7^{2-}}} + 1} - 1)^2}{16K_{Cr,3}\frac{\gamma^2_{HCrO_4^-}}{\gamma_{Cr_2O_7^{2-}}}} \tag{3.4.23}$$

Then Cr biosorption is considered involving binding of these two anionic species.

In the case of vanadate, the complexity of V speciation indicates that vanadium binding may involve colloidal V_2O_5, anionic vanadate $VO_2(OH)_2^-$, $V_{10}O_{27}(OH)^{5-}$, $V_{10}O_{26}(OH)_2^{4-}$ and cationic VO_2^+ binding as well as neutral $VO(OH)_3$ precipitation. Therefore, the proposed anionic metal species adsorption model is not applicable to the vanadate biosorption system.

3.4.1.5 Electroneutrality Condition

The electroneutrality condition is given by the following equation:

$$[Na^+] + [H^+] = [Cl^-] + [OH^-] + Z^* \sum_i ([H_xM_pL_q^{Z-}])_i \quad (3.4.24)$$

Then $[Cl^-]$ in equation (3.4.12) could be correlated to other solution species by the above electroneutrality equation.

3.4.1.6 Calculations of Activity Coefficients in the Aqueous Phase

For the aqueous phase, an extended form of Debye-Huckel equation was proposed by Guggenheim (Guggenheim, 1935) to calculate the mean electrolyte activity coefficient as follows:

$$Log\ \gamma_{\pm} = -A|z_+z_-|\frac{\sqrt{I}}{1+Ba\sqrt{I}} + bI \quad (3.4.25)$$

Where Z_+ and Z_- are respectively the cation and anion valence of the electrolyte, the parameter a is defined as the "distance of closest approach" of the ions around. Both b and a are constants adjustable to suit the experimental curve. The constants A and B involve the absolute temperature and the dielectric constant of the solvent (Robinson and Stokes, 1959). For water at 25^0C,

$$A = 0.507 \quad (3.4.26)$$

$$B = 0.33 \quad (3.4.27)$$

I is the ionic strength in the solution, defined as:

$$I = \frac{1}{2}\sum_{y=1}^{N}[i] * Z_i^2 \quad (3.4.28)$$

[i] and Z_i are the concentration and the charge of ion i in the solution, respectively.

Equation (3.4.25) has been widely used for the analytical representation of activity coefficients, where it is usually capable of fitting the data within the experimental accuracy up to 1 M (Robinson and Stokes, 1959).

Davis (Davis, 1938) further modified the above equation by putting $b=m|z_+z_-|$, and setting m = -0.1 and a = 3.04 for all species at 25^{0}C, then equation (3.4.24) became:

$$\log \gamma_{\pm} = -0.507*|z_+z_-|(\frac{\sqrt{I}}{1+\sqrt{I}} - 0.3*I) \quad (3.4.29)$$

Davis' equation is useful as a guide to the behavior of the electrolyte activity coefficient when no experimental measurements are available. It could effectively predict the activity coefficient in solution with ionic strength up to 0.5 M.

In defining the single-ion activity coefficient, Z_+Z_- in the above equations should be replaced by Z_i^2 (squared charge of ion i) (Stumm and Morgan, 1996a). It should be noted that single ion activity coefficients are constructs and not measurable individually. However, the use of single activity coefficients greatly simplifies calculations. Then Davis' equation for calculating single ion activity coefficient γ_i in the liquid phase is:

$$\log \gamma_i = -0.507*Z_i^2(\frac{\sqrt{I}}{1+\sqrt{I}} - 0.3*I) \quad (3.4.30)$$

In the present work, Davis' equation will be used for ion activity coefficient calculations.

3.4.1.7 Model Parameter Estimation

If the parameters such as the total binding capacity B_T, metal binding constant ${}^{ad}K_M$ and chloride binding constant ${}^{ad}K_{Cl}$ are known, once the initial conditions are fixed, the developed one-site model together with equations (3.4.5), (3.4.9-12), (3.4.24), (3.4.28), (3.4.30) and with metal speciation equations if necessary, could be used to predict the anionic metal species biosorption.

In the current modeling, there would be not speciation reaction for gold-cyanide. Chromate speciation is considered by equations (3.4.22-23). The speciation equilibrium constant of chromate $K_{Cr,3}$ in equations (3.4.22-23) could be taken as $10^{2.2}$ $(mol/L)^{-1}$, the value reported by Greenwood (Greenwood and Earnshaw, 1985c). Model parameters such as B_T, ${}^{ad}K_M$ and ${}^{ad}K_{Cl}$ were evaluated, based on their ability to adequately simulate experimental data (Hayes et al., 1991), by minimizing the sum of the squared uptake residuals between the experimental data and model predicted values. The objective function is as follows:

$$\text{Err} = \sum \left(\frac{q_{exp} - q_{cal}}{q_{exp}}\right)^2 \qquad (3.4.31)$$

3.4.2 Modeling Results

3.4.2.1 Modeling the pH Effect on Biosorption

Equations (3.4.5), (3.4.9-12), (3.4.24), (3.4.28) and (3.4.30) were used together with speciation equations if necessary, to fit the experimental data at pH 2.4-4.5 and NaCl concentration 0.01M-0.1M. The regressed average values of parameters for Au biosorption are listed in Table 3.4.1. They are independent of solution pH and ionic strength. The modeling results of Au isotherms of AWUS at pH 2.4 – 4.5 are shown in Figure 3.4.1. The solid lines represent the one-site model fitting. It is seen that the anionic metal species adsorption model represents the trend of pH effect on the Au isotherms reasonably well, whereby Au uptake is the best at pH 3.4 among tested, and suppressed at pH 2.4, however, higher than that at pH 4.5. The correlation coefficient was 0.98. Model calculations correlate with the data at pH 2.4 and 3.4 reasonably well, indicating the rationality of incorporating the interference of Cl^- in the model. The regressed capacity of AWUS for Au binding is 0.18 mmol/g, which is 20 times higher

than those of bacterial *Bacillus* and fungal *Penicillium*. The affinity of $Au(CN)_2^-$ is higher than that of Cl^- in agreement with the fact that smaller ions have lower affinities for the sorbent active sites because of higher water hydration. The comparison of the binding constants appearing in the current work with those reported in the literature cannot be readily made because either modeling approaches or adsorption systems differ.

Table 3.4. 1 Model parameters for Au biosorption system*

Parameters \ Models	One-site	Two-sites
B_T (mmol/g)	0.18	0.15
$\log {}^{ad}K_{Au(CN)_2^-}$	6.99	6.75
$\log {}^{ad}K_{Cl^-}$	5.94	5.96
$B_{T\,2}$** (mmol/g)	/	0.03
$\log {}^{ad}K_{Au(CN)_2^-,\,2}$	/	9.9
$\log {}^{ad}K_{Cl^-,\,2}$	/	9.11
Corr. coef.	0.98	0.98
Std. Err. (%)	1.21	1.08

* $\log {}^{ad}K_M$ represents log of ${}^{ad}K_M$ in $(mol/L)^{-2}$;

** subscript 2 denotes parameters for the second sites.

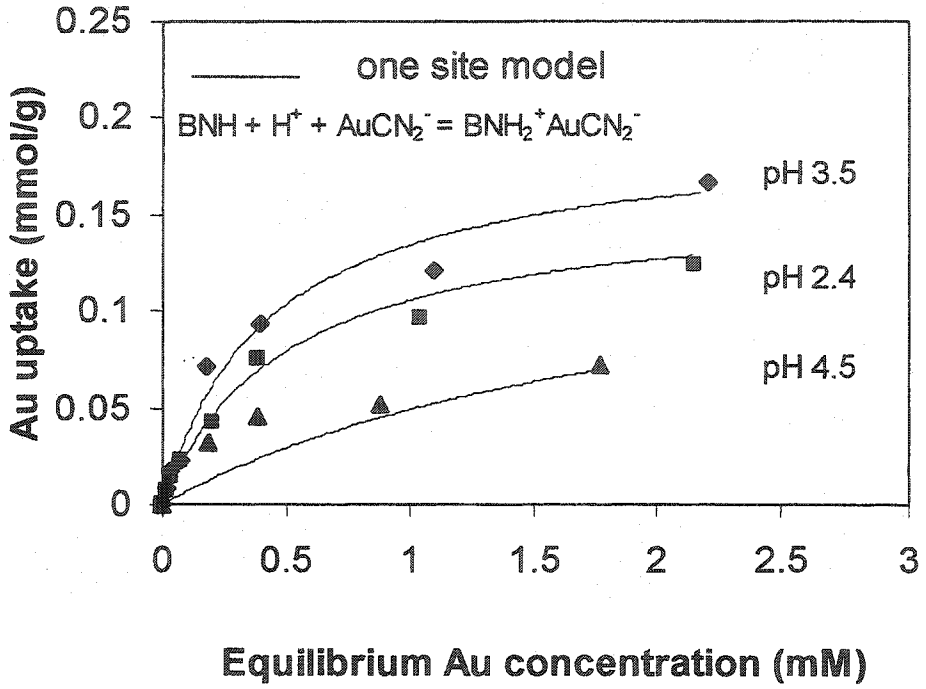

Figure 3.4. 1 Modeling the pH effect on Au biosorption isotherms

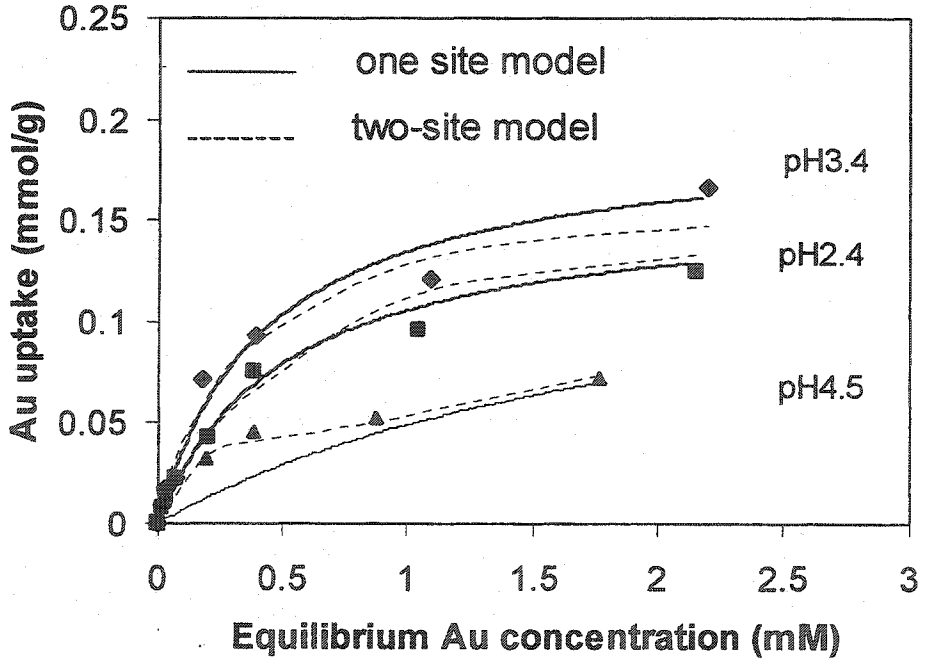

Figure 3.4. 2 Comparison of one - and two-site models

At pH 4.5, the model agrees well with experimental data at the high concentration range, while it deviates at the lower one. The deviation may be mainly caused by the assumption of one type of weak-base functional groups. This could be confirmed by adding one more weak-base site to the established model. Accordingly, the number of model parameters is doubled and the regressed values are also listed in Table 3.4.1. The result is shown in Figure 3.4.2 where the dashed line represents the model with two weak-base sites. It can be seen that the two-site model very well improves the data fitting in the low concentration range at pH 4.5. However, it gives similar fitting results to one-site model at pH 2.4 and 3.4 but with the number of parameters doubled. The regressed capacity of the second site is 0.03 mmol/g, which is much lower than that of the first site (Table 3.4.1). These results indicate that the one-site anionic metal species biosorption model is simple but adequate in reflecting the experimental gold-cyanide biosorption data at pH values from 2.4 to 3.4. Therefore one-site model will be applied to the following chromate biosorption system.

Modeling the Cr isotherms of AWUS at pH 2.0 - 3.6 (Figure 3.4.3) confirms that the one-site model could fit the data very well. The regressed parameters for Cr biosorption are listed in Table 3.4.2. The model considering $HCrO_4^-$ and $Cr_2O_7^{2-}$ binding accurately illustrates chromate uptake increasing with solution pH decreasing from pH 3.6 to 2.0. The correlation coefficient is 0.98. The regressed capacity for chromate binding is 0.30mmol/g, higher than that for Au. These differing capacities could result from the following reasons:

a) it is possible that, under actual conditions, some of the binding sites for chromate are unavailable to gold-cyanide;

b) part of Cr could be bound through cation Cr (III) binding, even in a small amount as illustrated in section 3.3, which was attributed to the anion binding approach in the current model;

c) the modeling error could also contribute to the regressed binding capacity difference.

The regressed binding constants, indicating the affinity of the studied anions, followed the decreasing sequence: $Cr_2O_7^{2-} > HCrO_4^- > Au(CN)_2^- > Cl^-$, confirming thus that the higher the charge and the bigger the size of the complex, the higher the affinity of the anion for the site (Helfferich, 1995).

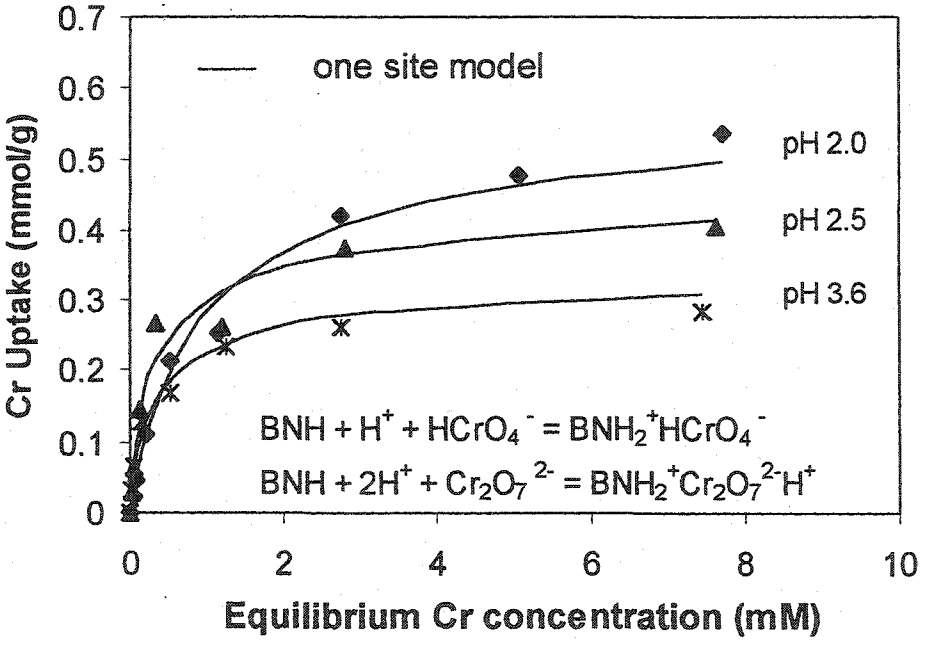

Figure 3.4. 3 Modeling the pH effect on chromate biosorption isotherms

Table 3.4. 2 Model parameters for chromate biosorption system*

Models	B_T (mmol/g)	$\log {}^{ad}K_{HCrO_4^-}$	$\log {}^{ad}K_{Cr_2O_7^{2-}}$	$\log {}^{ad}K_{Cl^-}$	Corr. coef.	Std. err. (%)
One-site	0.31	7.29	9.80	5.89	0.98	4.4

* $\log {}^{ad}K_M$ represents log of ${}^{ad}K_M$ in $(mol/L)^{-(Z+1)}$

In addition, the regressed value of $\log {}^{ad}K_{Cl^-}$ (5.89) in the Cr system showed only a slight deviation of 0.8% from that determined for the Au system (5.94), indicating the stability of the parameters of the one-site model.

The modeling results establish that the proposed one-site anionic metal species biosorption model can describe the anionic metal species biosorption as a function of pH within the pH range of 2.4-3.4 for Au and 2.0-3.6 for Cr. The proposed model can be applied for both mono- and multi-anionic metal species biosorption systems.

3.4.2.2 Modeling the Ionic Strength Effect on Biosorption

The modeling results of ionic strength effect on Au uptake are shown in Figure 3.4.4. The solid line represents the one-site model curve. It is seen that the model fits the data of Au uptakes at pH 3.4 within the NaCl concentration range of 0 M to 0.1 M reasonably well. It can accurately predict the trend of the Au uptake as it became significantly suppressed by the elevated ionic strength. The results indicate that the model considering the non-ideality in the liquid phase, coupled with the interference of Cl^-, is adequate for describing the ionic strength effect on anionic metal species

adsorption. It has also been demonstrated that in the case of mono-valent anionic $Au(CN)_2^-$ biosorption, the one-site model simplified by neglecting the non-ideality in the liquid phase, i.e. the activity coefficient of anionic metal species being set to 1, could still well predict Au uptakes at ionic strength up to 0.1M. This is shown in Figure 3.4.5. The dashed lines represent the one-site model prediction with the activity coefficient of solution species equaling 1. They almost overlap with the one-site model fitting curves (solid lines) whereby the activity coefficients are considered. This observation illustrates that the proposed model could be simplified by neglecting the non-ideality of solution species when applied to pure mono-valent anionic binding at I up to 0.1M.

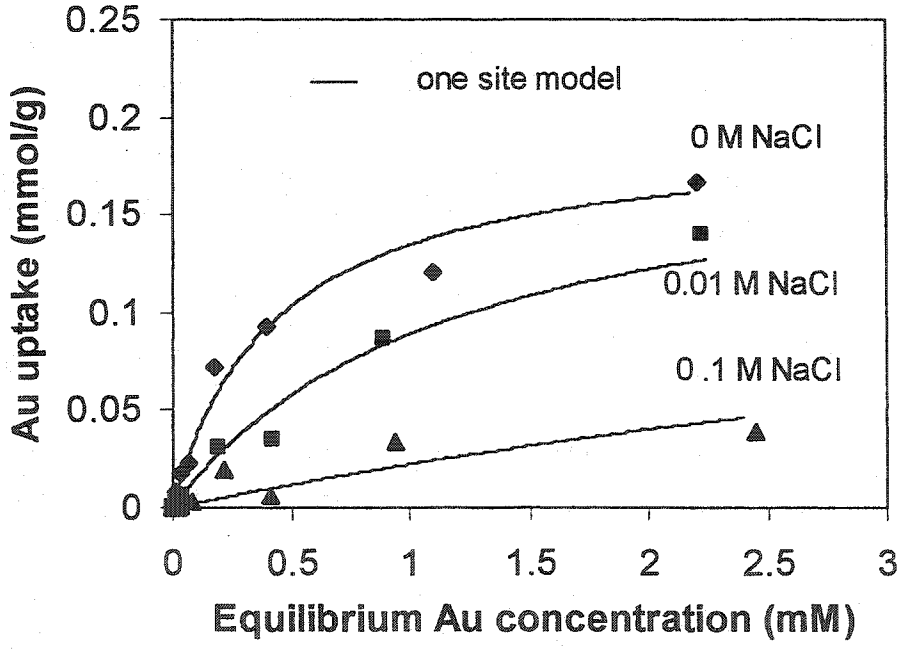

Figure 3.4. 4 Modeling the effect of ionic strength on Au biosorption at pH 3.4

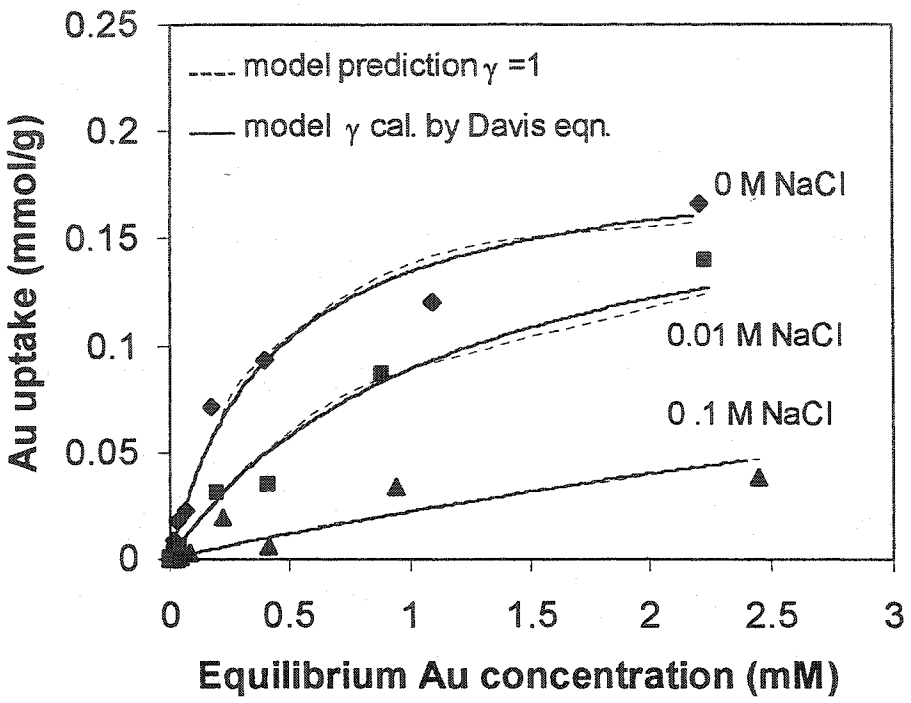

Figure 3.4. 5 Comparison of models for Au biosorption at pH 3.4

However, when multi-valent anionic metal species are involved, the non-ideality of liquid phase is relevant which could be illustrated by the case of Cr biosorption. The modeling results for Cr uptakes at 0 – 0.1 M NaCl are presented in Figure 3.4.6. The solid lines, representing the one-site model fitting curves, demonstrate that the current model could also very well describe the dependence of the metal biosorption system with divalent anionic metal species on solution ionic strength. However, when setting the activity coefficient of solution species to 1 in the model, the prediction of such a model for Cr uptakes (the dashed line) is shown in Figure 3.4.7. It is seen that the model prediction deviates from the experimental data significantly at elevated NaCl concentrations. Figure 3.4.8 shows the activity coefficients of Cr(VI) species such as $HCrO_4^-$ and $Cr_2O_7^{2-}$ in the solution as a function of Cr and NaCl concentration at pH 2.0. It is seen that the activity coefficients of divalent ion $Cr_2O_7^{2-}$ decreased to 0.66 at 0.01M

NaCl and to 0.36 at 0.1M NaCl. The results confirm the rationality of the proposed model that considers the non-ideality in the liquid phase for multi-valent species biosorption. The proposed one-site model appears adequate and flexible when applied to both mono-valent and multi-valent anionic metal species biosorption systems. Even though the obtained equilibrium constants in the current work are apparent in nature as the surface non-ideality is not accounted for, this modeling approach greatly simplifies the model calculations and the model quite adequately describes the experimental data at pH 2.0-3.6 with ionic strength up to 0.1 M. These are the most common conditions for relevant biosorption applications.

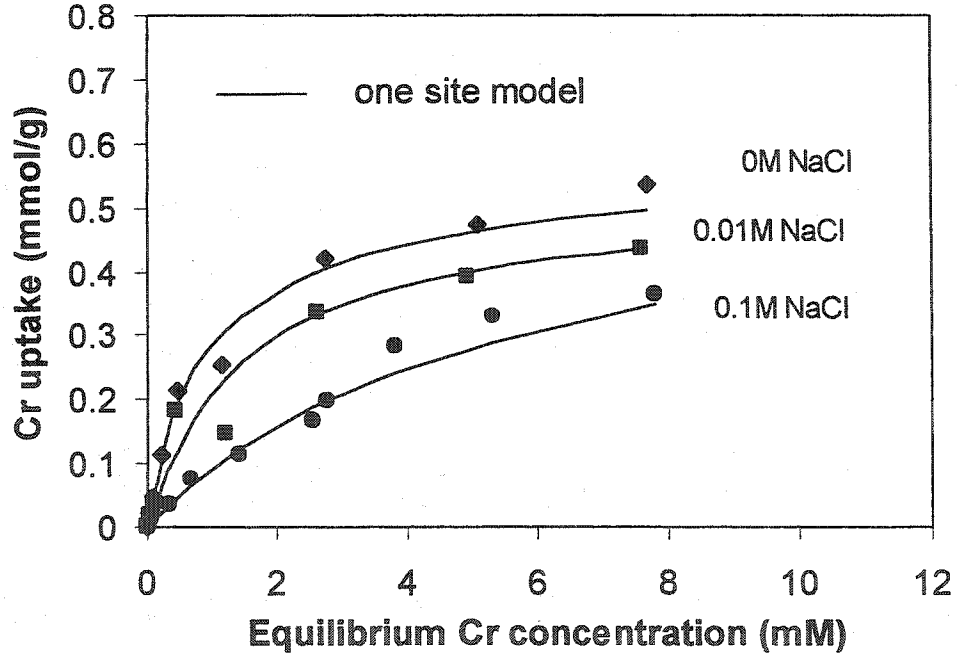

Figure 3.4. 6 Modeling the effect of ionic strength on Cr biosorption at pH 2.0

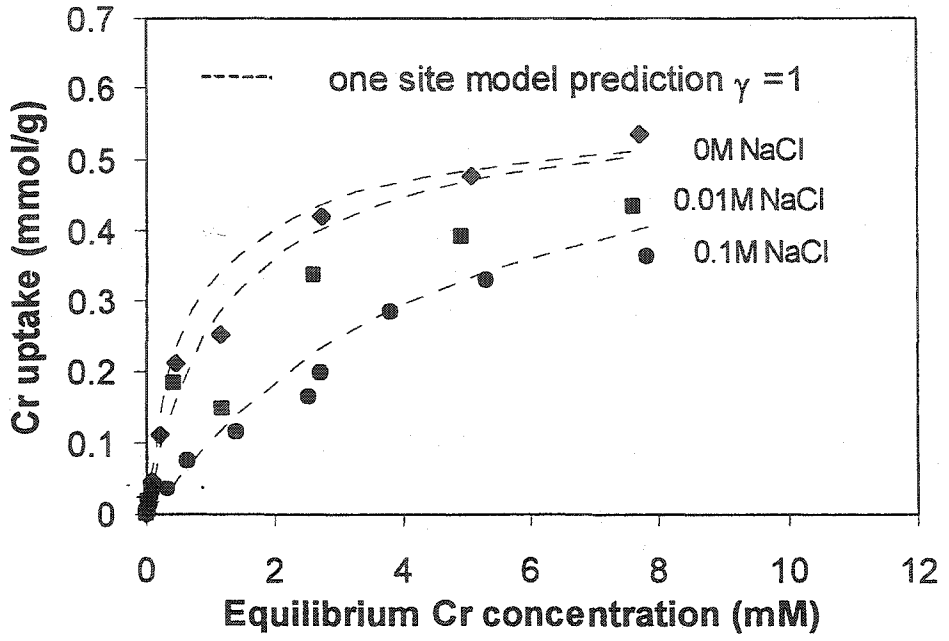

Figure 3.4. 7 Model Prediction of Cr uptake at pH 2.0 by neglecting the non-ideality in the liquid

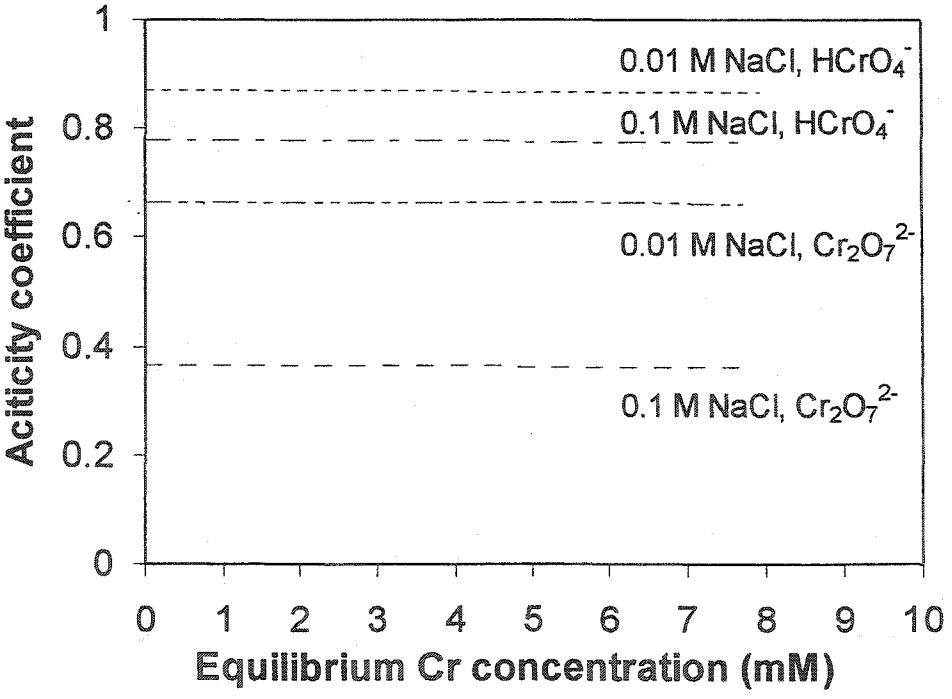

Figure 3.4. 8 Activity coefficients of Cr (VI) species in the solution

3.4.3 Section Summary

A mathematical model was developed in order to describe and quantify the performance of the biosorption process. The one-site anionic metal species adsorption equilibrium model considering the non-ideality in the liquid phase and the interference of Cl^- effectively described the anionic metal species adsorption by AWCS as a function of solution pH (in the range of pH 2.4-3.4 for Au and 2.0-3.4 for Cr), ionic strength (up to 0.1M), and the concentration of metals and chloride. The regressed model parameters are independent of the solution pH or ionic strength. The proposed model can be applied to both mono- and multi-anionic metal species biosorption systems.

When applied to pure mono-valent anionic metal species binding at IS up to 0.1 M, the proposed model could be simplified by neglecting the non-ideality of solution species. However, when multi-valent anionic metal species are involved, the non-ideality of liquid phase is relevant. The proposed one-site model reasonably describes the suppressed anionic metal species uptakes when the solution ionic strength is elevated.

The regressed binding constants indicate that the affinity of the studied anions for AWUS follows the decreasing sequence: $Cr_2O_7^{2-} > HCrO_4^- > Au(CN)_2^- > Cl^-$, confirming that the higher the charge and the bigger the size of the anion, the higher the affinity of the anion for the site.

3.5 Biosorption Modeling: Anionic Multi – Metal System

The previous sections presented characteristics of anionic metal species adsorption by AWUS in mono-metal systems. Practical attempts to apply biosorption in purification of industrial metal solution will rarely encounter a system containing only one type of metal ions. Therefore, it is desirable to be able to investigate the binding of one type of anionic metal species in the presence of other metal species. Vanadate, known for its occurrence in the vanadium extractive metallurgical industry (Rostoker, 1975; Greenwood and Earnshaw, 1985a), is often accompanied by chromate. The interference between these two metals during the biosorption process is of interest.

Biosorption of cationic metals in binary systems was quantitatively described by a multi-component Langmuir-type equation (Chong and Volesky, 1995). Yun (Yun et al., 2001) also established that the single-metal vanadate sorption behavior of AWUS was well approximated by an extended Langmuir-type isotherm. However, a multi-metal equilibrium adsorption model is also needed to predict the interaction between different metal species in the biosorption system.

The objective of this section is to determine the interference of vanadate and chromate on one another's uptakes. A multi-metal biosorption equilibrium model is applied to describe the binary experimental data.

3.5.1 Model Description

As discussed in the previous sections, vanadate is prone to hydrolyze and to produce V_2O_5 and cationic VO_2^+ in addition to several types of anionic vanadium species under the conditions for biosorption. The initial conceptual anionic metal species biosorption binary system of vanadate and chromate actually becomes the one involving colloid and cation sorption in addition to anionic species binding. Therefore the established anionic metal species biosorption model approach in the previous section is not applicable. Since it has been demonstrated that either vanadium (V) or chromium (VI) mono-metal biosorption could be reasonably well described by the Langmuir isotherm (Yun et al., 2001), an extended multi-component Langmuir Model (Butler and Ockrent, 1930) can conveniently be proposed to describe the vanadate and chromate biosorption system. For this purpose it is assumed that the binary solution contains only one of each ionic species of vanadium and of chromium, each having its one fictitious binding site. The corresponding total binding capacities of AWUS can also be assumed to be known. The fictitious binding site for each metal could actually be attributed to different sites on AWUS, part of which might also be available to both metals. At specific pH and ionic strength, the adsorption model can be proposed:

For vanadium uptake,

$$B^{(V)} + V = B^{(V)}\text{-}V \tag{3.5.1}$$

Then vanadium binding constant K_V is defined as:

$$K_V = \frac{[B^{(V)} - V]}{[B^{(V)}][V]} \tag{3.5.2}$$

Where $[B^{(V)}]$ represents the vanadium binding site (mmol/g), [V] is the total equilibrium vanadium concentration in the solution (mM), and $[B^{(V)}\text{-}V]$ denotes the adsorbed V (mmol/g).

The interference of chromium on vanadium binding is described as:

$$B^{(V)} + Cr = B^{(V)}\text{-}Cr \tag{3.5.3}$$

Then the constant K_{Cr}^{V}, representing the affinity of chromium for the vanadium binding site, is:

$$K_{Cr}^{V} = \frac{[B^{(V)} - Cr]}{[B^{(V)}][Cr]} \tag{3.5.4}$$

The mass balance of vanadium binding site is:

$$[B_T{}^{(V)}] = [B^{(V)}] + [B^{(V)}\text{-}V] + [B^{(V)}\text{-}Cr] \tag{3.5.5}$$

where $[B_T{}^{(V)}]$ is the total vanadium binding capacity (mmol/g). [Cr] denotes the equilibrium concentration of chromium in the solution (mM) and $[B^{(V)}\text{-}Cr]$ represents the adsorbed Cr on vanadium binding sites.

Therefore vanadium uptake q^{V} could be calculated by combining equations (3.5.2) and (3.5.4-5):

$$q^{V} = \frac{[B_T{}^{(V)}]K_V[V]}{1 + K_V\ [V] + K_{Cr}^{V}[Cr]} \tag{3.5.6}$$

Similarly, the chromium uptake in a binary system can be described as:

$$B^{(Cr)} + Cr = B^{(Cr)}\text{-}Cr \tag{3.5.7}$$

Then chromium binding constant K_{Cr}, is:

$$K_{Cr} = \frac{[B^{(Cr)} - Cr]}{[B^{(Cr)}][Cr]} \tag{3.5.8}$$

The interference of vanadium with chromium binding can be described as:

$$B^{(Cr)} + V = B^{(Cr)}\text{-}V \tag{3.5.9}$$

And the constant K_{V}^{Cr} representing the affinity of vanadium for chromium binding sites is:

$$K_V^{Cr} = \frac{[B^{(Cr)} - V]}{[B^{(Cr)}][V]} \tag{3.5.10}$$

Then the mass balance for chromium binding sites will be:

$$[B_T{}^{(Cr)}] = [B^{(Cr)}] + [B^{(Cr)}\text{-}Cr] + [B^{(Cr)}\text{-}V] \tag{3.5.11}$$

Chromium uptake q^{Cr} is thus obtained:

$$q^{Cr} = \frac{[B_T{}^{(Cr)}]K_{Cr}[Cr]}{1 + K_{Cr}[Cr] + K_V^{Cr}[V]} \tag{3.5.12}$$

where $[B^{(Cr)}]$ represents the concentration of chromium binding sites (mmol/g), $[B^{(Cr)}\text{-}Cr]$ and $[B^{(Cr)}\text{-}V]$ respectively denote the adsorbed Cr and V on chromium binding sites (mmol/g). $[B_T{}^{(Cr)}]$ is the total chromium binding capacity (mmol/g).

When the interfering metal concentration is zero, the above equations (3.5.6) and (3.5.12) assume the conventional one-component Langmuir form.

$$q^V = \frac{[B_T{}^{(V)}]K_V[V]}{1 + K_V[V]} \tag{3.5.13}$$

$$q^{Cr} = \frac{[B_T{}^{(Cr)}]K_{Cr}[Cr]}{1 + K_{Cr}[Cr]} \tag{3.5.14}$$

This extended multi-component Langmuir model is different from the multi-component Langmuir model used to describe biosorption of cations in binary systems by seaweed biomass (Chong, 1995; Figueira et al., 1997), whereby it was assumed that both metals had the same binding site and binding capacity. The present extended multi-component Langmuir model considering different binding sites and capacities for each metal is more rational when applied in binary biosorption system containing metal species with different types of charges. However, it should be noted that this multi-component model is empirical in nature and therefore could not reflect the actual binding mechanism that was determined through studying the corresponding metal anion speciation and AWUS functional groups responsible for metal binding (Section 3.3).

Parameter estimation: The values of the total vanadium binding capacity [$B_T^{(V)}$] and the vanadium binding constant K_V were estimated from the metal isotherm in the mono-vanadium system with equation 3.5.13. K_{Cr}^{V} representing the affinity of chromium for vanadium binding sites was determined by fitting extended multi-component Langmuir equation (3.5.6) to the experimental vanadium biosorption data in the V-Cr system. Similarly, the total chromium binding capacity [$B_T^{(Cr)}$] and the chromium binding constant K_{Cr} were obtained from the metal isotherm in the mono-chromium system with equation 3.5.14. K_{V}^{Cr} representing the affinity of vanadium for chromium binding sites was obtained from the value of K_V, or expressed through fitting equation (3.5.12) to chromium biosorption data in the V-Cr system for comparison.

The optimal combination of parameter sets will be obtained by minimizing the objective function error:

$$\text{err} = \sum \left(\frac{q_{\text{exp}} - q_{cal}}{q_{\text{exp}}}\right)^2 \qquad (3.5.15)$$

3.5.2 Results and Discussion

The biosorption of vanadate and chromate in a binary system was performed at pH 2.5 with 0.1 M NaCl present. The correct and most illustrative way of representing the biosorption equilibrium of a two-metal system is to construct a three-dimensional sorption isotherm plot whereby the metal uptake is plotted as a function of equilibrium concentrations of the two metals. In order to make an appropriate quantitative assessment of mutual metal interferences, experimental 3-D sorption isotherm plots need to be mathematically represented. The sorption model used for smoothing of the sorption isotherm surface makes it possible to eventually derive two-dimensional sorption isotherm curves from the complex 3-D image by cutting through it with a series of parallel "iso-concentration" planes for selected metal concentrations of one or the other

metal, respectively (Chong and Volesky, 1995). The two resulting sets of sorption isotherm curves depict either the effect of the second metal on the biosorption of the first one or vice versa in an easily understandable manner. These curves reflect then correctly the actual equilibrium biosorption conditions as appropriate (Carvalho et al., 1995). For this purpose the extended multi-component Langmuir model will be used to fit the experimental data.

3.5.2.1 Interference of Chromate in Vanadate Uptakes

In order to quantitatively describe the interference of chromate in the uptake of vanadate, the parameters in the multi-component Langmuir equation (3.5.6) have to be determined. The values of the total vanadium binding capacity [$B_T^{(V)}$] and the vanadium binding constant K_V in equation (3.5.6) were obtained through fitting mono-component Langmuir equation 3.5.13 to the experimental mono-vanadium biosorption data at pH 2.5 (with 0.1M NaCl). The regressed parameters with standard errors are listed in Table 3.5.1. Figure 3.5.1 confirms that Langmuir equation can reasonably well reflect V uptakes in the mono-vanadium biosorption system. K_{Cr}^{V} representing the affinity of chromium for vanadium binding sites was regressed from the vanadium biosorption data in the V-Cr binary system. The quality of the fit was reasonably good as evaluated also in Table 3.5.1. The correlative coefficient determined for binary system was 0.979 and the standard error of the estimate was 5.07%.

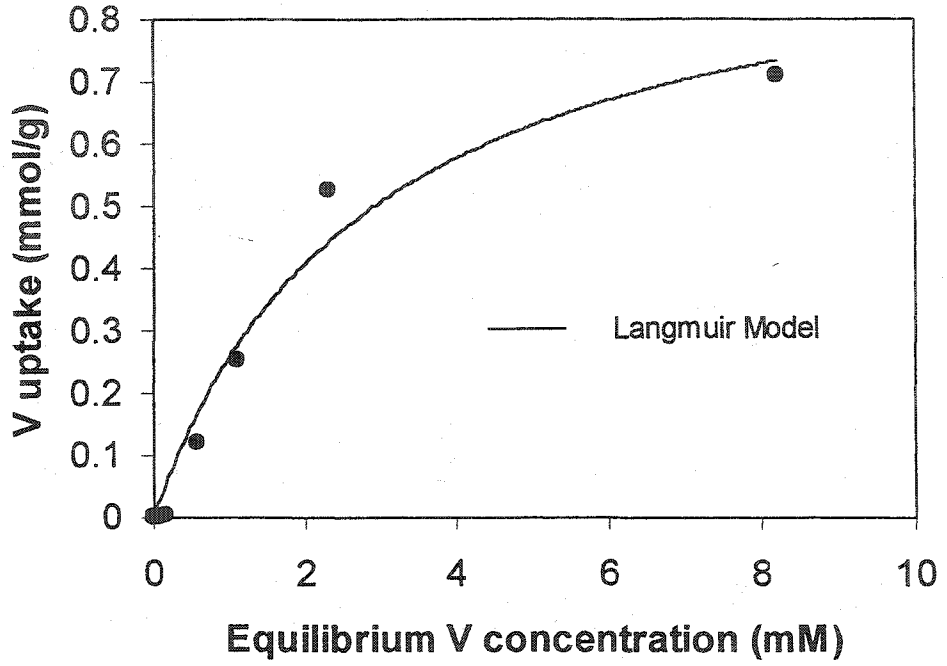

Figure 3.5. 1 Vanadium biosorption isotherm of AWUS: without chromium in the solution (pH 2.5 and 0.1 M NaCl)

Table 3.5. 1 Langmuir modeling results for V biosorption (pH 2.5 and 0.1 M NaCl)

System	$[B_T{}^V]$ (mmol/g)	K_V (L/mmol)	K_{Cr}^V (L/mmol)	Corr.coef.	Std. Err. (%)
Mono-V	0.98±0.09	0.35±0.09	/	0.986	5.14
Binary	0.98*	0.35*	$< 10^{-9}$	0.979	5.07

* obtained from mono-vanadium biosorption data.

The regressed constant K_{Cr}^{V} is so small that it can be negligible compared with K_V, indicating that chromate could not compete for vanadate binding sites and that AWUS could bind vanadium in the presence of chromium in the solution with the same effectiveness as without it.

This could be further clearly seen in the corresponding 3-D plot and in its derivative 2-D cuts (Figure 3.5.2a-c). In Figure 3.5.2a the two equilibrium Cr and V concentrations are plotted against vanadate uptakes. The 3-D surface was created by fitting the extended multi-component Langmuir model (equation 3.5.6) to the experimental vanadium biosorption data from the binary system. By cutting this surface with a series of iso-equilibrium Cr concentrations, a series of 2-D V biosorption isotherm plots was generated as shown in Figure 3.5.2b. The results showed that vanadium uptake was not affected by different equilibrium Cr concentrations (0 – 5.3 mM). This indicates that, under the present experimental conditions, AWUS has a much higher selectivity for vanadate.

Figure 3.5.2c summarizes the effect of Cr on V uptake in different selected concentration regions. At the V concentration from 0 – 8.2 mM, vanadium uptakes were not affected by increasing the equilibrium Cr concentrations from 0 to 5.3 mM. At pH 2.5, the predominant forms of vanadate are colloid V_2O_5, anionic $V_{10}O_{26}(OH)_2^{4-}$ and cationic VO_2^+ (Greenwood and Earnshaw, 1985c), while the main forms of chromate in solution (at pH 2.0 – 3.5) are anionic $HCrO_4^-$ and $Cr_2O_7^{2-}$ (Greenwood and Earnshaw, 1985c). Obviously, under these conditions, the binding approaches for vanadium could be quite different from those binding chromium. In addition, colloidal V_2O_5 could also be physically removed from the solution while being retained by AWUS within the polymer matrix of the shell material. As a result, the uptake of anionic chromate does not reach the levels of vanadate binding. These results demonstrate that AWUS could extract vanadate more selectively in the presence of chromate. This feature could be interesting for the extractive vanadate hydrometallurgical industry.

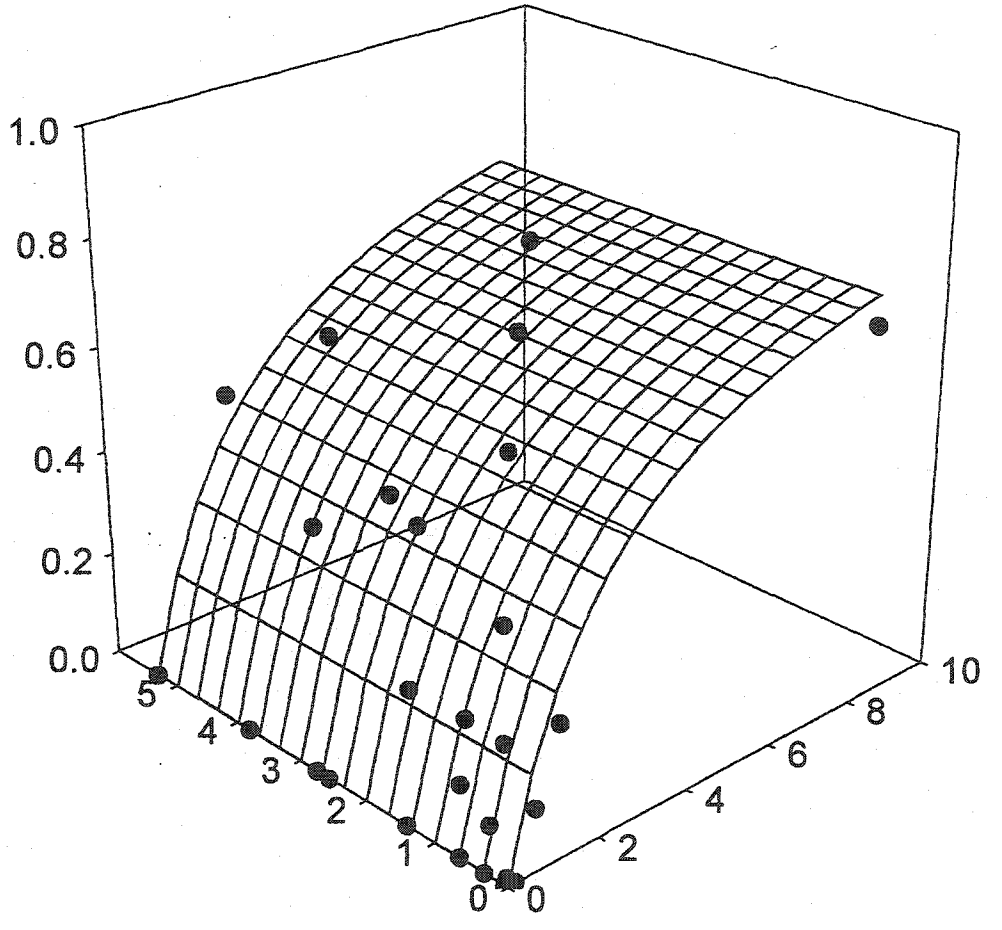

Figure 3.5.2 a A three-dimensional sorption surface for the V-Cr AWUS biosorption system: V uptake at pH 2.5 and 0.1 M NaCl

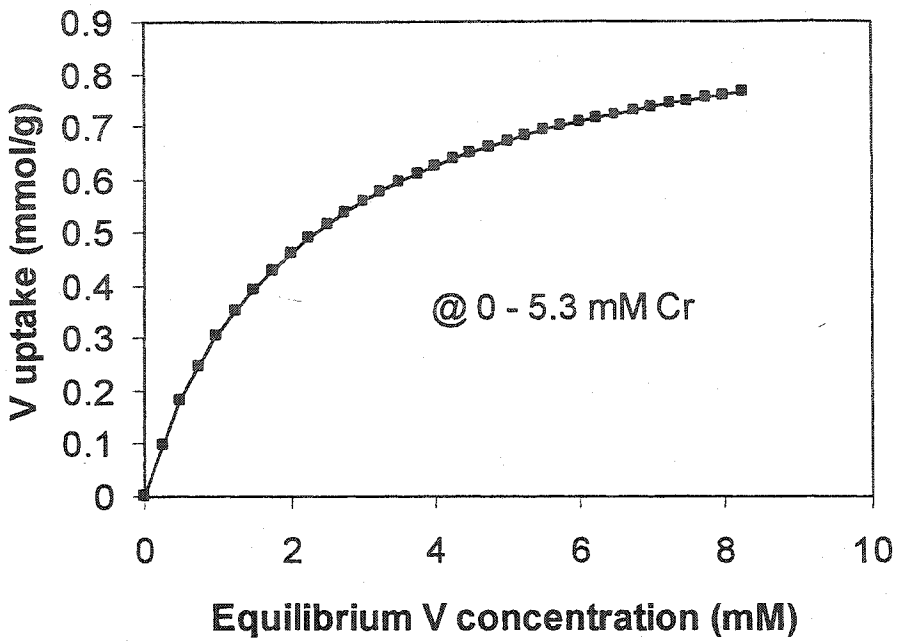

Figure 3.5.2 b The effect of Cr on equilibrium V uptake: obtained from Figure 3.5.2a surface cutting

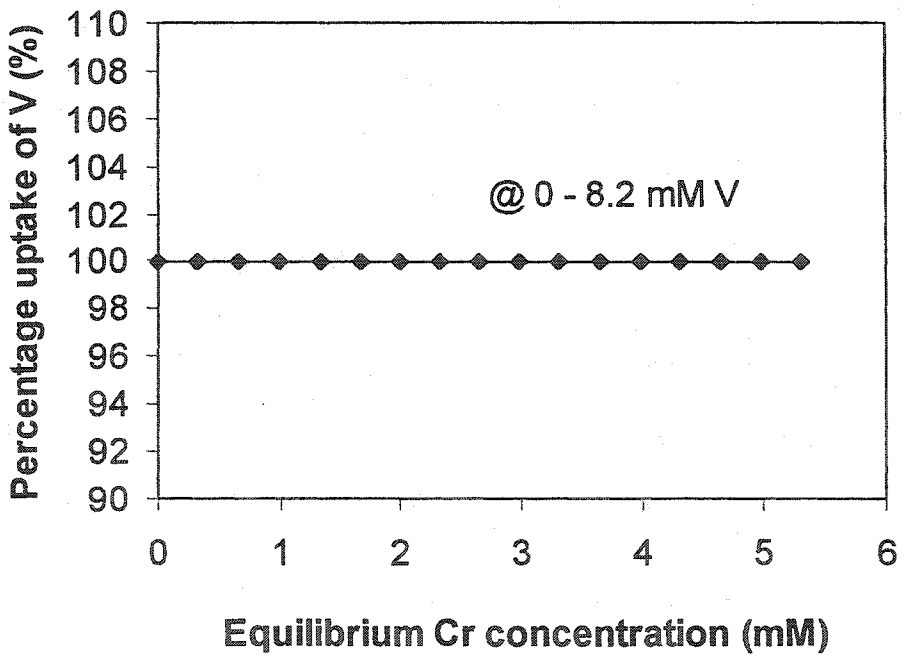

Figure 3.5.2 c Summary of the effect of Cr on the equilibrium V uptake: obtained from Figure 3.5.2 a surface cutting

3.5.2.2 Interference of Vanadate in Chromate Uptakes

Similarly as in the previous section, to quantitatively describe the interference of vanadate in the uptake of chromate, the parameters in the extended multi-component Langmuir equation (3.5.12) were determined. The values of the total chromium binding capacity [$B_T^{(Cr)}$] and the chromium binding constant K_{Cr} (Table 3.5.2) were obtained through fitting mono-component Langmuir equation (3.5.14) to the experimental mono-chromium biosorption data at pH 2.5 (with 0.1M NaCl). Figure 3.5.3 confirms that Langmuir equation agrees very well with Cr uptakes in the mono-chromium biosorption system. K_V^{Cr} representing the affinity of vanadium for the chromium binding sites was determined by the value of K_V from the mono-vanadium system, and also regressed from the vanadium biosorption data in the binary system with equation (3.5.12) for comparison. The quality of both the prediction and the fit in the binary system was good as evaluated in Table 3.5.2. The value of the regressed K_V^{Cr} is very close to that of K_V from mono-vanadium system. The present multi-component Langmuir model (equation 3.5.12) with the parameters from the corresponding mono-metal biosorption system could very well predict the Cr uptakes in the V-Cr binary system. The correlative coefficient was 0.996 and the standard error of the estimate was 0.67% (Table 3.5.2). The value of K_{Cr} is smaller than K_V, indicating that the presence of vanadate could interfere in the chromium binding.

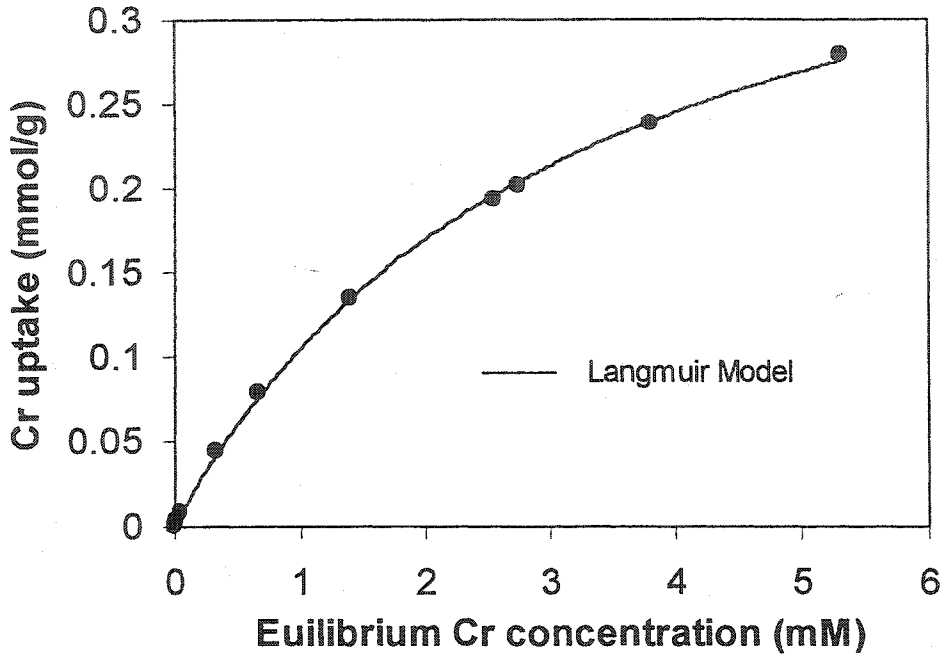

Figure 3..5. 3 Chromium biosorption isotherm of AWUS: without vanadium in the Solution (pH 2.5 and 0.1 M NaCl)

Table 3.5. 2 Langmuir modeling results for Cr biosorption (pH 2.5 and 0.1 M NaCl)

System	$[B_T{}^{Cr}]$ (mmol/g)	K_{Cr} (L/mmol)	K_V^{Cr} (L./mmol)	Corr.coef.	Std. Err. (%)
Mono-Cr	0.44±0.01	0.31±0.01	/	0.999	0.23
Binary fitting	0.44*	0.31*	0.41±0.02	0.998	0.54
Binary prediction	0.44*	0.31*	0.35**	0.996	0.67

* obtained from mono-chromium biosorption system

** obtained from the value of K_V regressed in mono-vanadium biosorption system.

The interference of vanadate in chromate binding was further quantitatively shown in Figures 3.5.4a-c. In Figure 3.5.4a the chromium uptake was plotted against the two equilibrium concentrations of Cr and V. The 3-D surface was created by the extended multi-component Langmuir model (equation 3.5.12) with parameters from the corresponding mono-metal biosorption system. By cutting this surface with a series of selected equilibrium V concentrations, the 2-D plots of Cr biosorption isotherms were generated as shown in Figure 3.5.4b. The results showed that the chromium uptake was strongly and progressively reduced with the equilibrium V concentration increasing from 0 to 8.2 mM. This is quite different from the opposite situation discussed in the previous section. Figure 3.5.4c summarizes the effect of V on the Cr uptake in different selected concentration regions. In the range of low equilibrium Cr concentrations (1.3 mM and 3.3 mM), the Cr uptake is more severely affected by the presence of V. The effect of V is less pronounced at higher Cr concentrations. For example, the uptake of Cr at the Cr concentration of 5.3 mM was 43% of its full value at 8.2 mM V in this system. At the same V presence, however, only 30% of the Cr full uptake remained when the Cr concentration was low (1.3 mM). The possible reasons that vanadate could suppress the binding of anionic chromium species such as $HCrO_4^-$ and $Cr_2O_7^{2-}$ under the present experimental conditions can be postulated as follows:

1) A colloidal particle can develop erratic localized charges all over its surface from interactions with other ions in the solution (Silberberg, 1996). Correspondingly, colloidal V_2O_5 can develop surface charges that might attract such particles to the binding site on AWUS in the same manner as for anions.

2) Colloidal particles trapped inside the porous shell structure could prevent penetration of chromium species into AWUS and they cannot access the binding site.

3) Colloidal particle retained chromate in the solution.

4) Anionic $V_{10}O_{26}(OH)_2^{4-}$ could compete with anionic Cr(VI) species for the sites.

5) Cationic VO_2^+ may compete with protons for the nitrogen of the weak-base amino groups for anion binding, preventing thus their attraction to positively charged amino groups under these circumstances.

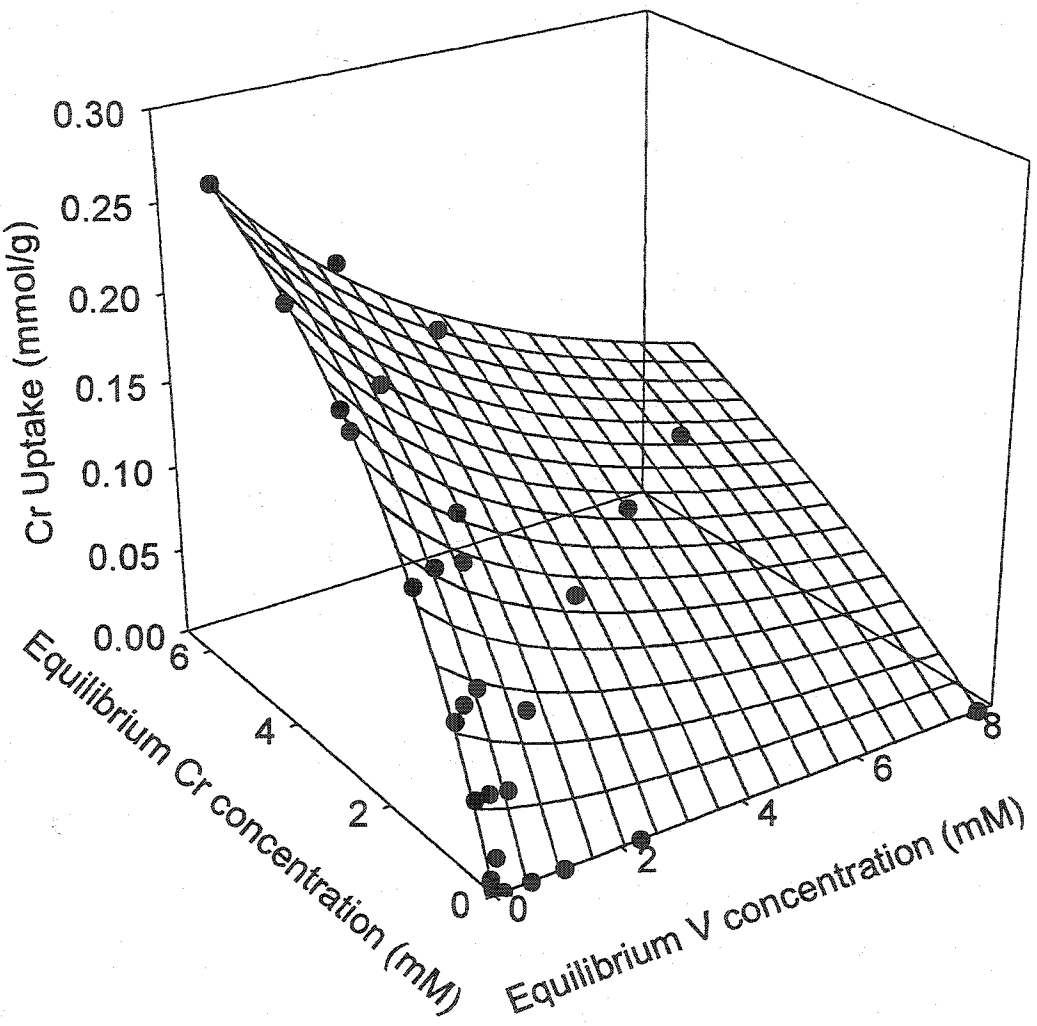

Figure 3.5.4 a A three-dimensional sorption surface for the V-Cr AWUS biosorption system: Cr uptake at pH 2.5 and 0.1 M NaCl

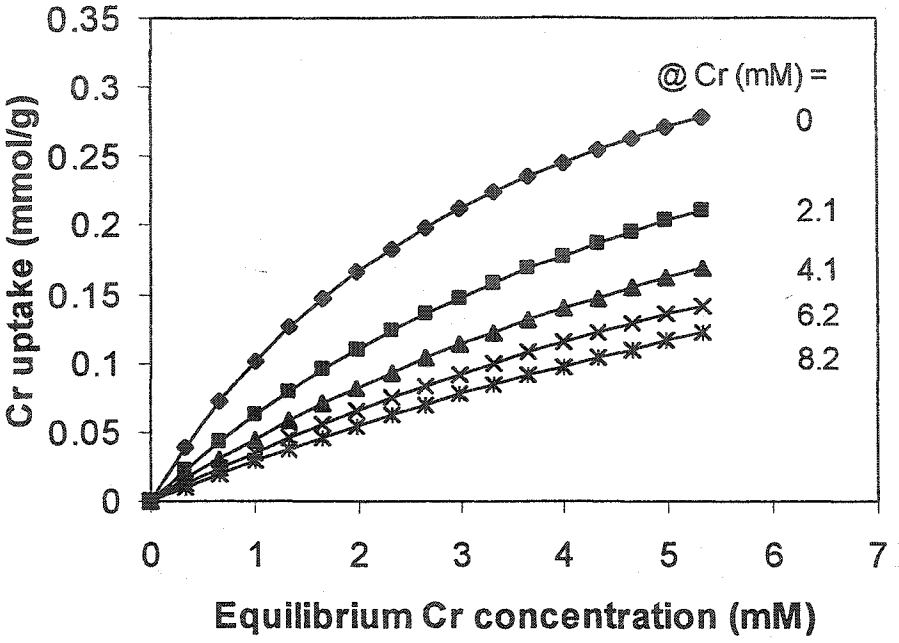

Figure 3.5.4 b The effect of V on equilibrium Cr uptake: obtained from Figure 3.5.4a surface cutting

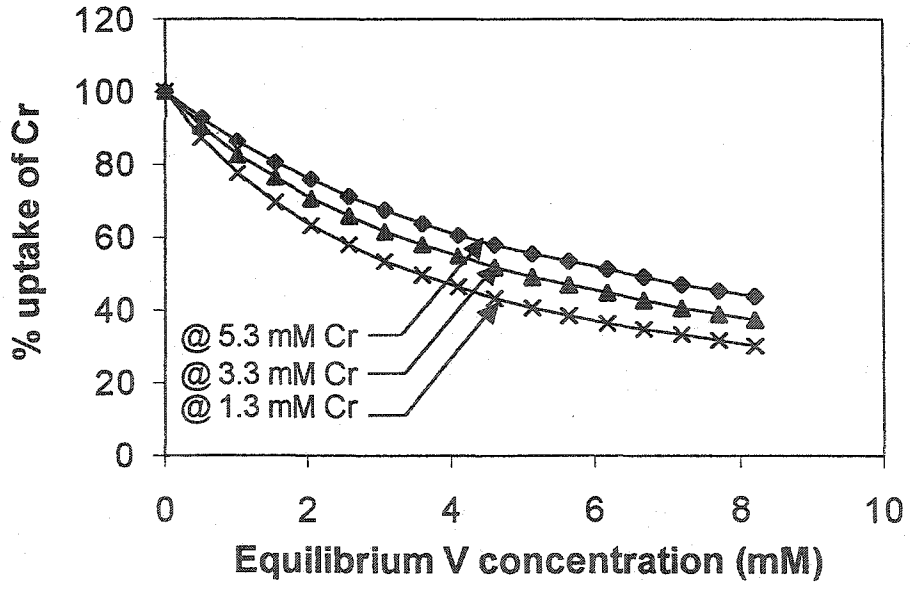

Figure 3.5.4 c Summary of the effect of V presence on the equilibrium Cr uptake: obtained from Figure 3.5.4a surface cutting

3.5.3 Section Summary

A binary biosorption system of metal complexes such as vanadate and chromate was studied by performing the adsorption experiments at pH 2.5 and 0.1 M NaCl. The results showed a higher vanadate affinity for AWUS than observed for chromate. The presence of chromate does not affect the vanadate uptake. However, chromium uptake was severely reduced at the presence of vanadate. The results indicated that vanadate could be selectively separated from the vanadate-chromate mixture.

An extended multi-component Langmuir model reasonably well described the metal interference behavior in the vanadate and chromate system.

3.6 Improvement of Anionic Metal Complex Biosorption

3.6.1 Anionic Metal Complex Adsorption at Elevated pH by Pretreated *Ucides* Shells

In the previous sections, it was determined that biomaterial containing base groups, usually amide or amine group, could serve as an effective biosorbent for anions. As the natural base groups are weak, they can only effectively bind anions at acidic pH. In some cases, such as gold mining process, the pH of industrial gold-cyanide leach solutions, however, is usually high, around pH 10. The leach solutions contain free CN^- and/or metal-cyanide complexes (Marsden and House, 1993a). Lowering the pH of the cyanide leach solution has an associated risk of releasing toxic HCN from solution. When the pH is lower than 9.3, HCN is formed in the gold leaching solution and it tends to evaporate causing high toxicity (Marsden and House, 1993a). This drawback prompted further work on finding a workable alkaline pH for effective biosorption of the gold-cyanide complex.

It is known that activated carbon has been considered as H-carbon when heated at temperatures slightly exceeding 800°C in the absence of oxygen, resulting in a greater affinity for anionic species (Mattson and Mark, 1971). In order to make the adsorption of $Au(CN)_2^-$ possible at pH 10, a high-temperature treatment of crab shells was undertaken. In the present study, Raw *Ucides* Shells (RUS) as well as AWUS were heated at 900°C in a closed furnace for 3 minutes.

The objective of this section was to investigate the characteristics of anionic $Au(CN)_2^-$ adsorption at elevated pH by *Ucides cordatus* shells treated by heating.

3.6.1.1 Au Uptake by Burnt *Ucides* Shells

Raw *Ucides* Shells (RUS) as well as Acid-Washed *Ucides* Shells (AWUS) with the particle size range of 1-3.35mm were burnt in a closed furnace at 900°C for 3 minutes.

Biosorption behavior of burnt *Ucides* shells for Au uptake at pH 5 and 10 is shown in Fig. 3.6.1.1. While AWUS removed only 10% of $Au(CN)_2^-$ from the solution at pH 5, burnt AWUS were capable of removing 100% of $Au(CN)_2^-$. Even at pH 10, burnt AWUS removed 83% of Au from solution. RUS burnt could only remove 10% $Au(CN)_2^-$. Both RUS and AWUS with no high-temperature pre-treatment showed no $Au(CN)_2^-$ uptake under the same conditions. At pH 10, the weak-base groups such as amide or amine originally present in RUS and AWUS do not acquire a positive charge. As a result these materials could not bind the anionic gold-cyanide.

RUS contained 59% of their weight in inorganic compounds such as $CaCO_3$. The critical temperature for $CaCO_3$ dissociation is 898°C (Weast and Astle, 1979). CaO probably remained in burnt RUS after heating at 900°C. When burnt RUS were mixed with $Au(CN)_2^-$ solution, CaO was likely to have dissolved in solution instead of contributing to $Au(CN)_2^-$ binding. However, AWUS containing merely 0.2% of inorganic substances did not have such a problem. Thus burnt AWUS had a high potential for the uptake of $Au(CN)_2^-$ anions at elevated solution pH and its further characterization was carried out by instrumental analysis.

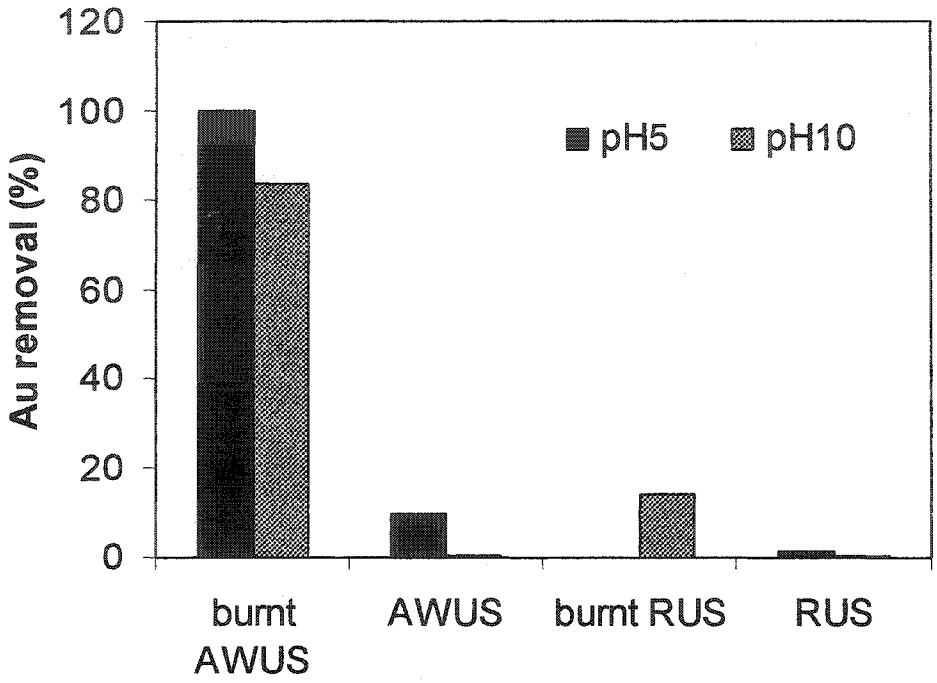

Figure 3.6.1. 1 Au adsorption by *Ucides* shells treated by different methods
initial Au 0.025mM, 20±0.2 mL solution, 40±1 mg sorbent

3.6.1.2 Instrumental Analysis

In order to investigate the effect of heating on the structures of blank AWUS and blank burnt AWUS, and their main components, a scanning electron-micrograph (SEM) and x-ray energy dispersive spectrometer analysis (EDAX) were carried out. While SEM of AWUS (Fig.3.6.1.2a) showed tight and dense structures, pores could be seen in the burnt AWUS material (Fig.3.6.1.2b). EDAX analyses showed a lower ratio of O/C for burnt AWUS (Fig. 3.6.1.3a) than that for AWUS (Fig. 3.6.1.3b) indicating that some oxygen was removed from AWUS during the high-temperature treatment. Apparently, heating removed some oxygen-containing groups and created pores, increasing the available surface area and the amount of accessible functional groups on AWUS for $Au(CN)_2^-$ binding.

In order to further investigate the characteristics of burnt AWUS and Au binding on it, the FTIR spectra comparison was made for virgin, burnt AWUS and Au-loaded burnt AWUS (Fig. 3.6.1.4a-b). The Au-loaded burnt AWUS sample was prepared by mixing 40 mg burnt AWUS with 20 mL gold-cyanide solution containing 0.025 mmol Au/L at pH10. The Au uptake was 10 μmol/g. The FTIR spectrum of burnt AWUS is greatly different from that of AWUS, however, similar to that of activated carbon. The peaks of amide or amine located at 1500-1650 cm^{-1} on the FTIR spectrum of AWUS (Roberts, 1992b) disappeared on the spectrum of the burnt AWUS indicating that AWUS amino groups were destroyed by the heating. Similarly, another peak at 1731 cm^{-1} for the C=O stretching (Nakamoto, 1986) was also missing on the spectrum of burnt AWUS implying that the C=O band was broken, thus supporting the EDAX observation of a lowered O/C ratio for burnt AWUS. Moreover, there are peaks appearing in the region of 1205-1195 cm^{-1} on the spectrum of burnt AWUS. Those peaks could be identified as belonging to the phenol type oxygen-hydrogen bonds (Cheremisinoff and Ellerbush, 1978). Marsden also considered those functional groups on activated carbon formed at higher temperatures to be phenolic (Marsden and House, 1993a). When organics are heated at temperatures higher than 800°C, some strong-base or weak-base groups of high fully protonated constant value could form which are capable of binding anionic complexes from aqueous solutions with an alkaline pH (Mattson and Mark, 1971). The current results indicated that weak-base phenol groups were formed during the high-temperature treatment of AWUS material.

The FTIR spectral data for burnt AWUS and Au-loaded burnt AWUS also show a peak appearing on the spectrum of Au-loaded burnt-shells at 2375 cm^{-1} which can be ascribed to $Au(CN)_2^-$ (Nakamoto, 1986) confirming that the Au uptake by burnt AWUS involved binding of the whole anionic $Au(CN)_2^-$ complex. However, no significant peak shifts were observed on the spectrum of Au-loaded AWUS indicating that the loaded Au did not affect the characteristics of the peaks of interest, or Au binding might be through weak physical forces.

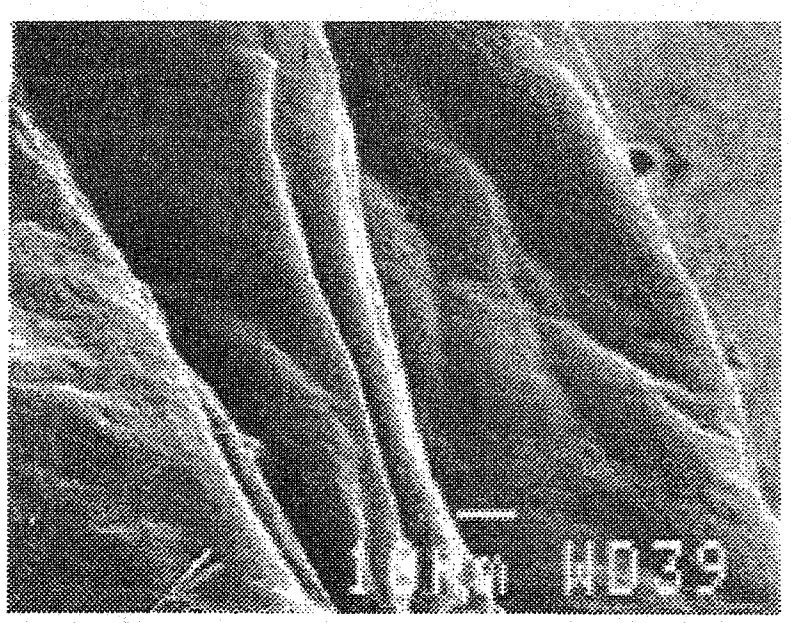

Figure 3.6.1.2 a SEM of AWUS

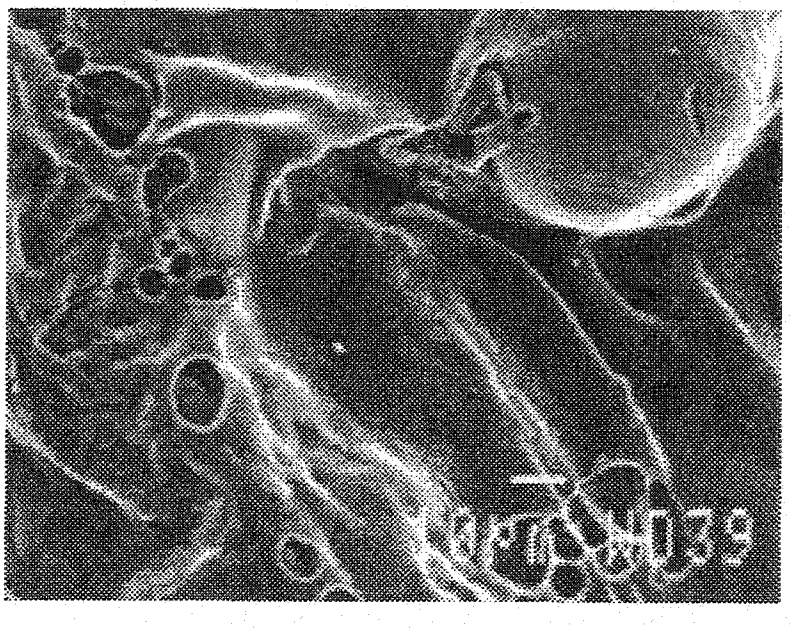

Figure 3.6.1.2 b SEM of burnt AWUS

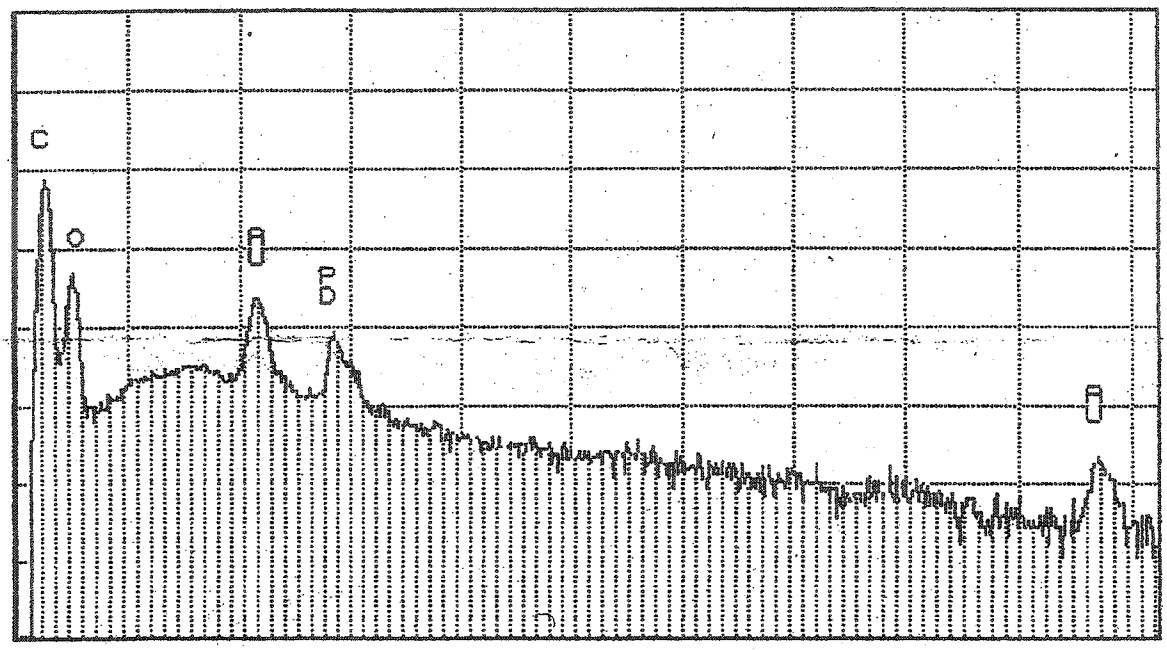

Figure 3.6.1.3 a EDAX of AWUS

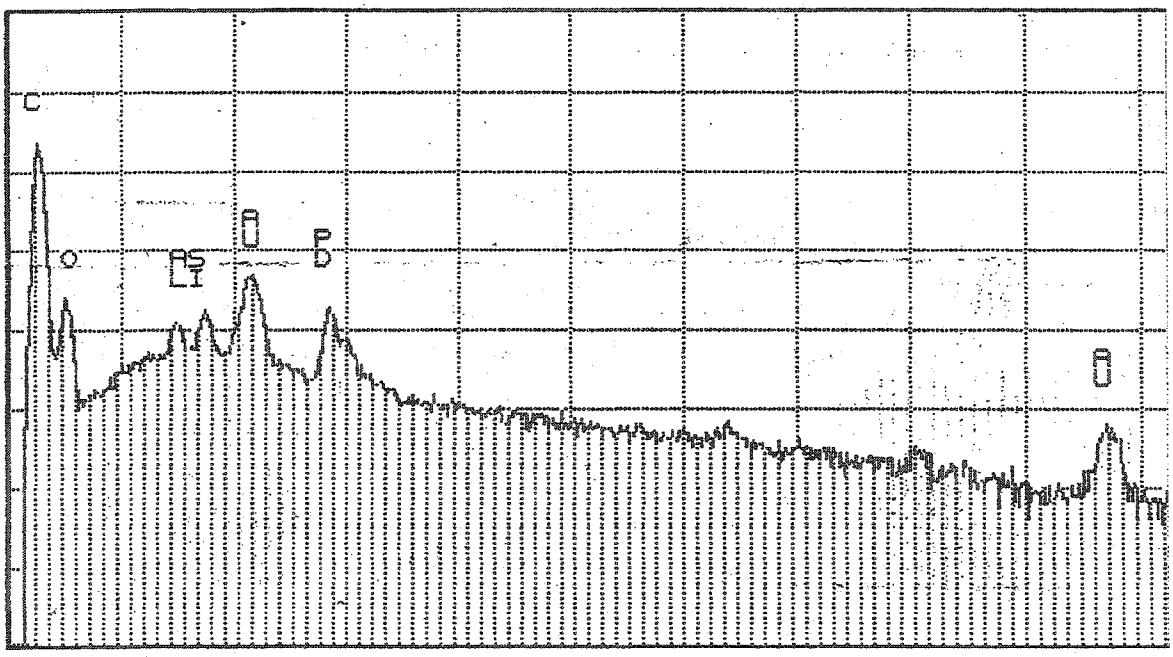

Figure 3.6.1.3 b EDAX of burnt AWUS

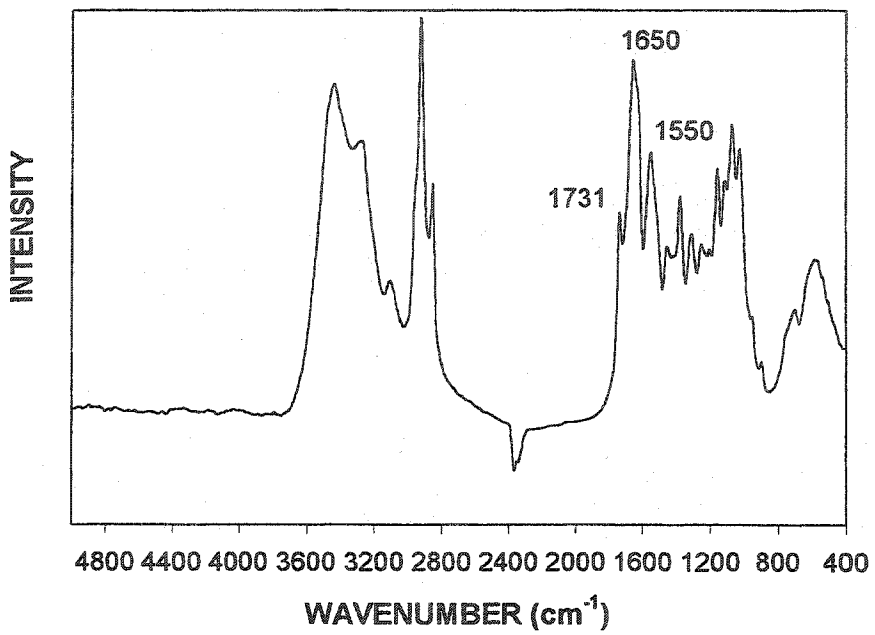

Figure 3.6.1.4 a FTIR spectrum of AWUS

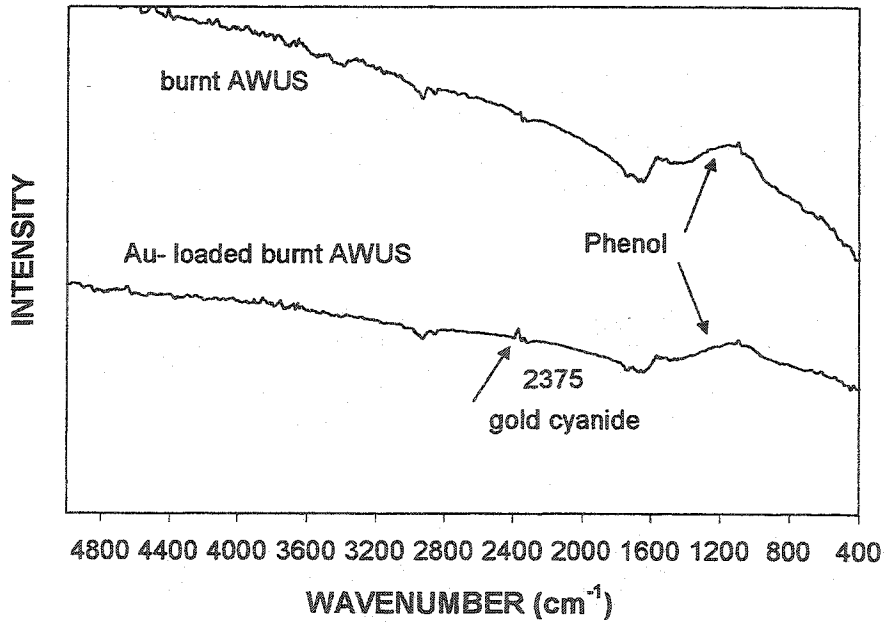

Figure 3.6.1.4 b FTIR spectra of burnt AWUS and Au-loaded burnt AWUS

3.6.1.3 Section Summary

The working pH for $Au(CN)_2^-$ uptake by AWUS was raised to pH 10 after heat-treatment of the biosorbent in the absence of oxygen. While there was no $Au(CN)_2^-$ uptake by AWUS at pH 10, the $Au(CN)_2^-$ removal by this heat-treated biosorbent reached 83% at pH 10.

Instrumental analysis showed that heating removed some oxygen-containing groups and created pores on AWUS, increasing the available surface area and the amount of accessible functional groups on AWUS for $Au(CN)_2^-$ binding.

Some functional groups such as phenolic group formed on the burnt AWUS. $Au(CN)_2^-$ complex was bound on burnt AWUS probably through a weak physical binding force.

Burnt RUS containing inorganic compounds such as CaO could not effectively bind $Au(CN)_2^-$ at elevated pH 10.

3.6.2 Enhanced Anionic Metal Complex Adsorption by Waste Biomass

Previous experimental results demonstrated that *Bacillus subtilis, Penicillium chrysogenum* and *Sargassum fluitans* biomass could extract gold-cyanide anions (Section 3.1), however, the uptakes were unsatisfactory.

Proteins are known to be capable of complexing with metal ions. Cysteine, which figures prominently in discussions of metal ion binding to proteins, has three possible coordination sites, namely sulfhydryl, amino and carboxylate groups (Shindo and Brown, 1965). Hussain attributed the protection of isolated human lymphocytes from silver toxicity to cysteine through the formation of Ag-thiol complexes (Hussain and Volet, 1995). The complexation of Cu-cysteine was ascribed to the complexing of Cu to thiol as well as amino groups (Li and Manning, 1955). These results showed that cysteine had a tendency to combine well with metals. However, the behavior of an L-cysteine anion biosorption system has never been examined.

The objective of this section was to reveal the effect of L-cysteine on characteristics of Au biosorption from cyanide solutions by three types of common and ubiquitous biomass representing different types of organisms, specifically, dead *Bacillus subtilis*, *Penicillium chrysogenum* and *Sargassum fluitans*.

3.6.2.1 Effect of L-Cysteine on Au Uptake

In order to enhance the $Au(CN)_2^-$ complex uptake by *Bacillus*, *Penicillium* and *Sargassum* biomass, L-cysteine was added to the adsorption system. Experimental results revealed that, at pH 2, L-cysteine did enhance Au biosorption by *Bacillus*, *Penicillium* and *Sargassum* biomass particles with diameters ranging in size from 0.5 to 0.85 mm. This is illustrated in Figure 3.6.2.1 where the ratio of gold uptake in the presence of cysteine to that without cysteine is plotted versus the final cysteine concentration. In the final cysteine concentration range (0 - 0.5 mM), the gold uptake by all of the three biomass types increased, following the sequence: *Bacillus*, *Penicillium* and *Sargassum* biomass. The final cysteine concentration around 0.5 mM enhanced Au uptakes by *Bacillus*, *Penicillium* and *Sargassum* biomass up to 250%, 200% and 148% of those without cysteine in the system, respectively (originally, 0.008mmol Au/g *B.* biomass, 0.007 mmol Au/g *P.* Biomass and 0.003 mmol Au/g *S.* biomass in Section 3.1 in this thesis). In the presence of cysteine, the Au uptake by *Bacillus*, *Penicillium* or *Sargassum* biomass was also found to be strongly affected by solution pH. The equilibrium uptakes of Au at pH 2 were greater than those at pH > 2 (Figure 3.6.2.2), and similar to the behavior observed for biosorption of anionic $Au(CN)_2^-$ by *Bacillus*, *Pencillium* and *Sargassum* biomass without cysteine addition.

L-cysteine biosorption isotherms at pH 2 for *Bacillus*, *Penicillium* and *Sargassum* biomass in Figure 3.6.2.3 show encouraging uptakes by *Bacillus* and *Penicillium* biomass, while *Sargassum* biomass sorbed very little. Under the experimental conditions, the sequence for the cysteine uptake by the three biomass types is *Bacillus* > *Penicillium* > *Sargassum*, which agreed with the sequence of increased Au uptake in the presence of cysteine.

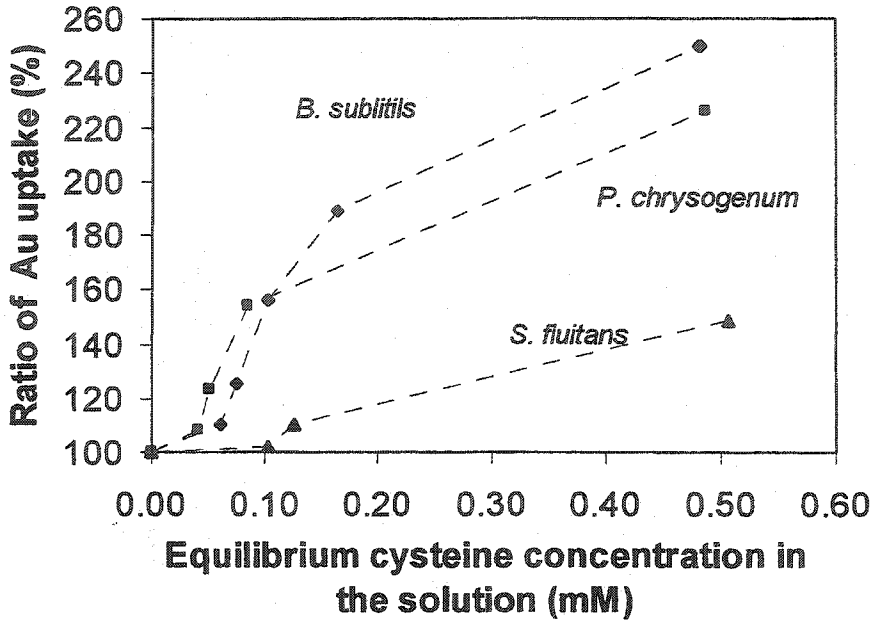

Figure 3.6.2. 1 Effect of cysteine on gold uptake (pH 2.0)

Au uptake without cysteine is 0.008 mmol/g *B.* biomass, 0.007 mmol/g *P.* biomass and 0.003 mmol/g *S.* biomass.

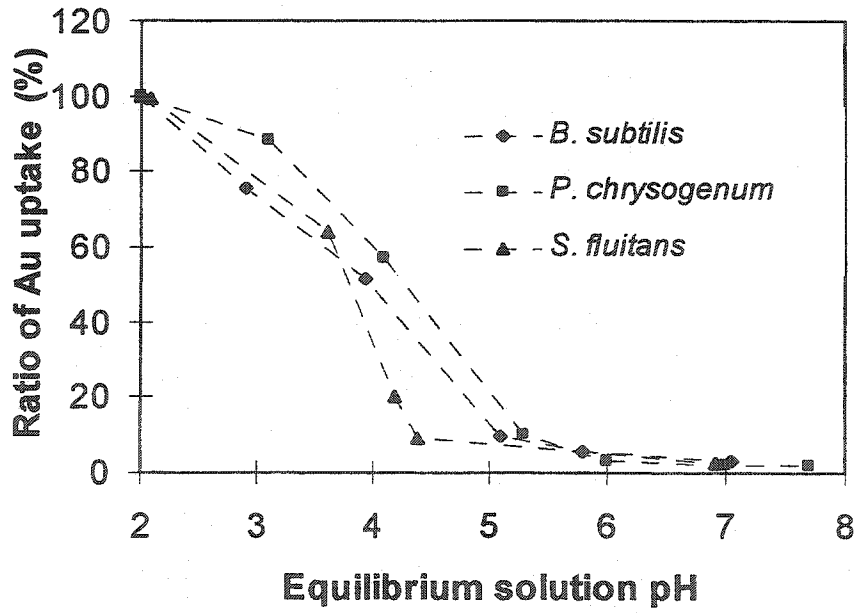

Figure 3.6.2. 2 Effect of pH on Au uptake with L-cysteine

Au uptake at pH 2 is 0.02 mmol/g *B.* biomass, 0.014 mmol/g *P.* biomass and 0.004 mmol/g *S.* biomass, ini. Cysteine cnc.: 0.60 mM.

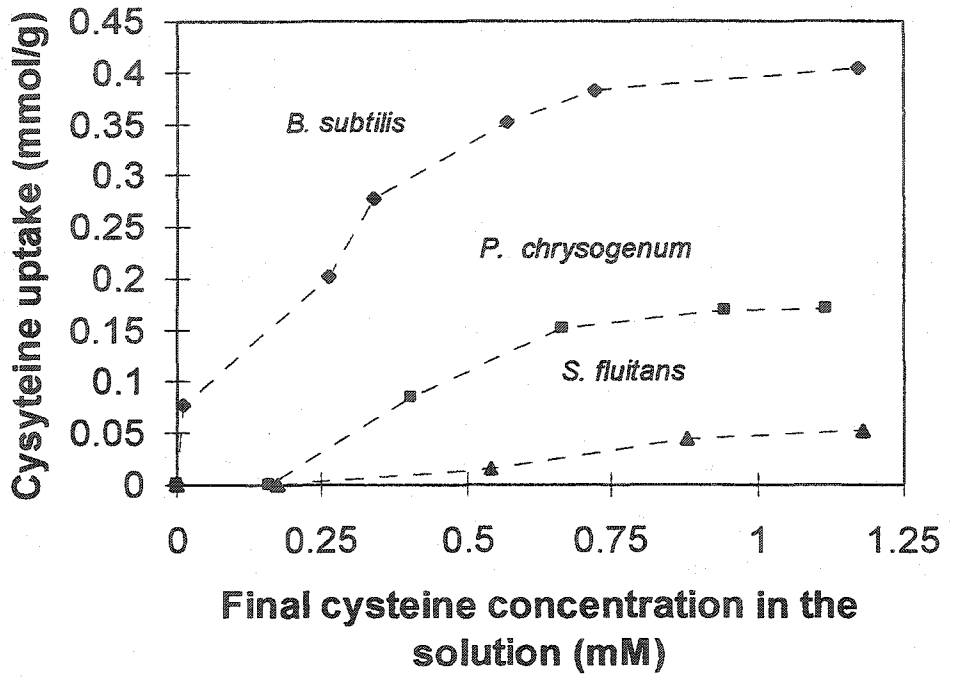

Figure 3.6.2. 3 Cysteine biosorption isotherms (pH 2.0)

Enhanced Au biosorption in the presence of cysteine probably relates to the "bridging" function provided by the cysteine molecule between the gold-cyanide complex and biomass. Cysteine has three possible coordination sites, namely amino, sulfhydryl and carboxyl groups (Shindo and Brown, 1965). The logarithm of the proton dissociation constants of those fully protonated groups are, respectively, 10.36, 8.12 and 1.90 (Perrin, 1979). At pH 2.0, the cysteine carboxyl group is partially deprotonated and charged negatively which enables it to combine with positively charged groups on biomass, while sulfhydryl group is neutral. At the same time, the cysteine amino group is protonated and charged positively which allows for its combination with anionic $Au(CN)_2^-$. The peptidoglucans in *Bacillus* cell walls (Beveridge and Murray, 1976) and chitin in *Penicillium* cell walls (Troy and Koffler, 1969) contain weak-base groups like amide and amine. As the conjugate acid dissociation constants of amino groups are 3.5 - 10 (Buffle, 1988a; Roberts, 1992a), almost all amino groups on these two biomass types could be positively charged by protons at pH 2.0. This makes them amenable to

combining with the carboxyl moiety on cysteine under the above acidic conditions. Eventually, anionic $Au(CN)_2^-$ bound on the positively charged cysteine amino groups became indirectly sorbed on biomass through cysteine as a bridge: (BFH_2^+–$^-$OOC–R–NH_3^+ – $Au(CN)_2^-$), where BFH_2^+ stands for the biomass functional group bearing a positive charge. The biomass, having higher affinity for cysteine than for gold-cyanide, brought in extra weak-base groups for binding $Au(CN)_2^-$ on biomass resulting in enhanced Au uptake.

Sargassum biomass contains alginates, up to 45% of its dry weight (Fourest et al., 1996). The active groups in alginates are carboxyl groups. Since the carboxyl groups of the biomass with the protonation constant 4.5 (Schiewer and Volesky, 1997a) should still be protonated and therefore charged neutral at pH 2, they are less likely to contribute to either cation or anion binding. The low cysteine binding by *Sargassum* may be rather due to a smaller amount of phenolic groups known to be also present in brown seaweeds (Ragan and Craigie, 1978). This work confirmed that the presence of cysteine did increase the gold-cyanide complex uptake by biomass and, in turn, the increased Au uptake was related to the cysteine-only uptake by biomass.

3.6.2.2 Ionic Strength Effect

Increasing ionic strength of the solution containing anionic sorbate species basically results in reducing its uptake as demonstrated in studying the biosorption of Au in the previous sections. Figure 3.6.2.4 shows the results of Au uptake in the presence of L-cysteine as affected by the ionic strength made up by NaCl. As the concentration of NaCl increased to 150 mM (ionic strength 160 mM), the uptake of Au by *Bacillus* and *Penicillium* biomass was respectively reduced to 64% and 46% of that without NaCl (ionic strength 10 mM) in the solution. The Au uptake by *Sargassum* decreased almost to zero at 60 mM NaCl (ionic strength 70 mM). Similar to Au biosorption by AWUS,

changing ionic strength (i.e. the background electrolyte concentration) influences Au adsorption by biomass in at least two ways: first by affecting the interfacial potential and therefore the activity of electrolyte ions and adsorption; and second by affecting the competition of the electrolyte ions and adsorbing anions for available sorption sites (Tien, 1994). In the present biosorption system, the added Cl^- apparently competed with the gold-cyanide complex as a counter-ion for the positively charged binding sites on cysteine or biomass. As a result, the Au uptake was reduced.

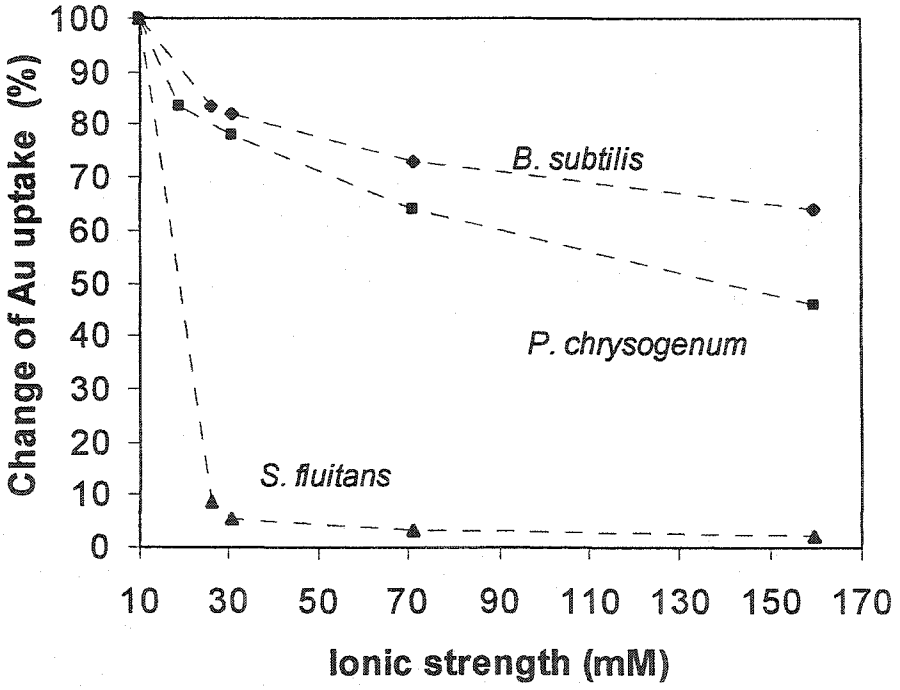

Figure 3.6.2. 4 Effect of ionic strength on the Au uptake

The change of Au uptake is based on that without NaCl addition (0.02 mmol/g *B.* biomass, 0.014 mmol/g *P.* biomass and 0.0047 mmol/g *S.* biomass).

pH 2.0, ini. cysteine 0.6 mM.

3.6.2.3 Desorption of Au-Loaded Biomass

The possibility of desorbing Au from biomass was examined by first sorbing Au onto biomass in the presence of L-cysteine at pH 2 and then desorbing Au with deionized water at pH 3, 4 or 5. The pH level was adjusted with 0.1 M NaOH. Gold-cysteine pre-loaded *Bacillus* biomass contained 20.5 μmol Au /g of dry biomass, *Penicillium* biomass contained 14.2 μmol/g, and *Sargassum* biomass 4.7 μmol/g. 0.02 g Au–cysteine-loaded biomass was mixed with 5 mL of the eluant solution for 4 hours. The percentage of Au recovery, represented by the ratio of the amount of Au released per gram of the biosorbent during desorption to the equilibrium sorption uptake, was calculated for desorption experiments.

Experimental results indicated that Au could be effectively eluted from Au-loaded biomass. Figure 3.6.2.5 shows that more than 92% of Au was recovered upon elution at pH 5 based on the equilibrium establishment with the solid-liquid ratio S/L (mg/mL) = 4 for all three biomass types studied, indicating that their Au binding was easily reversible. As the pH of the sorption system increased, protons dissociated from the positively charged amine groups on the biomass, thereby rendering these groups charge-neutral so that they did not attract the COO- of cysteine any longer. That led to breaking the binding "bridge" (BFH_2^+–$^-$OOC–R–NH_3^+ – $Au(CN)_2$), and the Au-complex became dissociated from the solid phase (Niu and Volesky, 2000).

However, the use of concentrated NaOH leads to massive leaching of a variety of compounds from the biomass and to the destruction of its cellular structures. Therefore, Au elution was limited to a pH of no higher than pH 6.

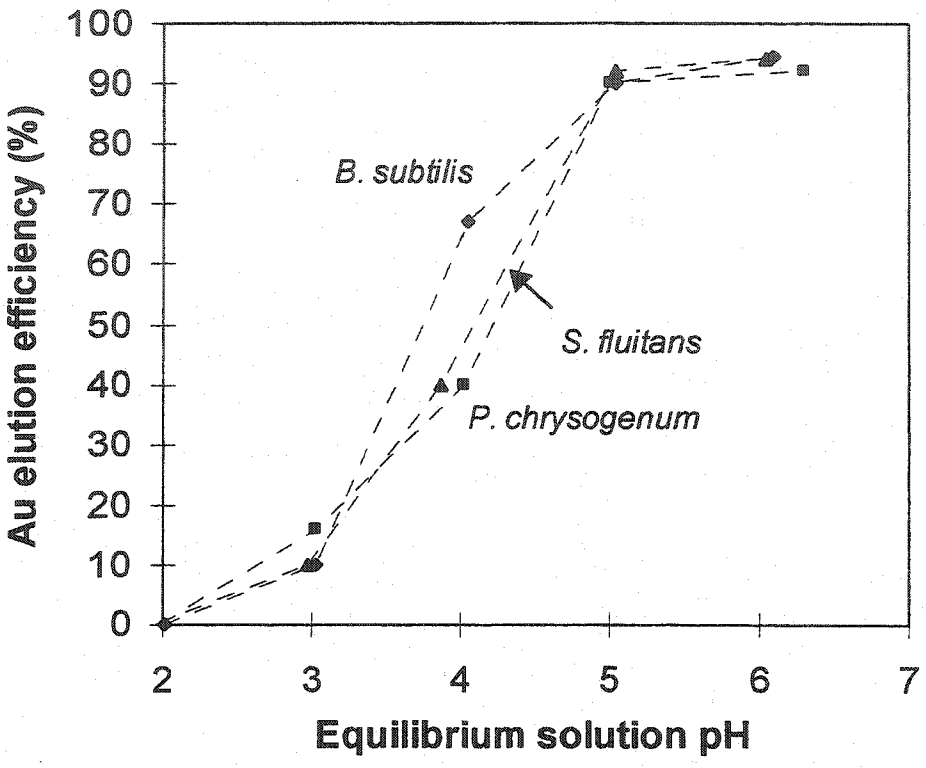

Figure 3.6.2. 5 Effect of pH on Au elution efficiency

3.6.2.4 Section Summary

The presence of "bridging" compounds such as L-cysteine can enhance anion complex biosorption at low pH (demonstrated for pH 2 with $Au(CN)_2^-$ and *Bacillus*, *Penicillium* and *Sargassum* biomass).

At pH 2, the sequence of increasing anion uptake by different biomass types agreed with that of capacity for cysteine-only adsorption by biomass: *Bacillus* > *Penicillium* > *Sargassum*

The uptake of anions may significantly decrease with increasing solution ionic strength (NaCl concentration from 0.005 M to 0.15 M).

Biosorption of most anions may be reversible: More than 92% of biosorbed gold-cyanide complex could be eluted at pH 5 under the present experimental condition.

CHAPTER 4

SUMMARY, ORIGINAL CONTRIBUTIONS, AND SUGGESTIONS FOR FUTURE RESEARCH

4.1 Summary

A promising anionic metal species binding by Acid Washed *Ucides* Shells (AWUS) particles was established upon comparison with conventional biosorbents such as *Bacillus*, *Penicillium*, and *Sargassum* biomass. The bound metals could easily be eluted from the biosorbent by a simple alkali wash. Repeating 3 adsorption-desorption cycles without performance deterioration indicated the reusability of the biosorbent.

The mechanism of biosorption of anionic metal species such as gold-cyanide, chromate and vanadate by AWUS adsorption was identified as the anionic metal species binding on the positively charged amide groups on the AWUS. The binding force may relate to electrostatic attraction. No significant reductions of the selected metals were observed in the biosorption systems with AWUS. All selected metals were observed bound on AWUS as its original valent state, i.e. Au(I), Cr(VI) and V(V). Anionic metal species biosorption is through a combination of ion-exchange and adsorption. In the case of vanadate, the binding might involve other mechanism in addition to the above one.

Anionic metal species biosorption is strongly affected by solution pH. AWUS sorbed well anionic gold-cyanide ($Au(CN)_2^-$), chromate (CrO_4^{2-}), and vanadate (VO_4^{3-}) at low pH. Gold-cyanide equilibrium biosorption uptake by AWUS is up to 0.17 mmol Au/g (pH 3.4). Chromate biosorption is preferred at pH 2.0, whereby the uptake reaches 0.54 mmol Cr/g biomass. Vanadate biosorption is favored at pH 2.5, whereby V uptake is up to 0.79 mmol V/g. The current results elucidate that the main effect of pH on anionic

metal species binding consists of an increase in the number of positively charged sites available with decreasing pH and an increase in the amount of metal species with high affinity for the sites. The corresponding established methodology could be applied to further optimize the biosorption system.

An increased ionic strength greatly suppressed the primary anionic gold-cyanide and chromate uptake, and mildly vanadate uptake as higher ionic strength (IS) reduced the activity of ions in solution and chloride ions competed for biosorbent protonated sites.

A mathematical model was developed for the performance of anionic metal species biosorption process. The one-site anionic metal species adsorption equilibrium model, considering the non-ideality in the liquid phase and the interference of Cl^-, could reasonably well quantify the anionic metal species adsorption by AWUS as a function of solution pH (in the range of pH 2.4-3.4 for Au and 2.0-3.4 for Cr, ionic strength (up to 0.1M), and the concentration of metals and chloride. The regressed model parameters are independent of the solution pH and ionic strength. The proposed model can be applied to both mono- and multi-anionic metal species biosorption system.

A binary biosorption system of anionic vanadate and chromate was studied by performing the adsorption experiments at pH 2.5 and 0.1 M NaCl. The presence of chromate does not affect vanadate uptake. However, chromium uptake was severely reduced with the presence of vanadate. The results determined that vanadate could be selectively separated from the vanadate-chromate mixture which is very useful when applied to an industrial vanadate extractive process.

An extended multi-component Langmuir biosorption model could also reasonably well predict the interference of one metal to the other metals uptake.

Anionic metal species biosorption could perform well at elevated solution pH with AWUS heat-treated in an oxygen-free atmosphere. While there was no $Au(CN)_2^-$ uptake by AWUS at pH 10, the $Au(CN)_2^-$ removal by this heat-treated biosorbent reached 83% at pH 10. Heating removed some oxygen-containing groups and created pores on AWUS, increasing the amount of accessible strong-base or weak-base functional groups

having high fully protonated constants on AWUS for anionic metal species binding at elevated pH.

A novel methodology was provided for improving the anionic metal species biosorption system. The originally poor anionic metal species uptakes by *Bacillus*, *Penicillium* and *Sargassum* biomass could be greatly enhanced by the addition of "bridging" compounds such as L-cysteine, preferred at low ionic strength and pH (demonstrated for pH 2 with $Au(CN)_2^-$ and *Bacillus*, *Penicillium* and *Sargassum* biomass). The increased metal uptakes are dependent on the capacity for cysteine adsorption by biomass, following the sequence: *Bacillus* > *Penicillium* > *Sargassum*. Cysteine-enhanced anion (gold-cyanide complex) binding most probably results from indirectly increasing the amount of weak-base functional groups such as amine on the biomass when it adsorbs cysteine. Loaded metals could be eluted at elevated pH 5.

4.2 Original Contributions

The mechanism of anionic metal species biosorption with a novel biosorbent AWUS was established, providing a methodology for biosorption optimization. Consequently, the "Results and Discussion" chapter of this thesis contains unique information which may be considered an original contribution to the field of biosorption. The key contributions may be summarized as follows:

- Establishment of anionic metal species biosorption mechanism by AWUS

  - The anionic metal species were bound on weak-base amide groups.
  - The bound anionic metal species were identified as their original valence state (Au(I), Cr(VI) and V(V)).
  - The combination of ion-exchange and adsorption mechanism was formulated for anionic metal species binding.

- Examination of crucial factors affecting the metal biosorption

  - Anionic metal species binding by AWUS is preferred at low solution pH < 3.5.
  - The depressed metal uptakes were demonstrated by increasing solution ionic strength.
  - The interference of one metal to the other was assessed in vanadate and chromate binary system.

- Establishment of the reusability of AWUS

  - The elution of loaded metals was demonstrated at elevated pH.
  - The numbers of adsorption-desorption was evaluated with chromate system.

- Development of a model for anionic metal species biosorption

  - A one-site sorption model was derived.
  - Equilibrium binding constants were determined.
  - Influence of solution pH, ionic strength, Cl^- competition and metal speciation was quantified.

- Establishment of a model for multi-metal biosorption system

  - A model with different binding capacity was derived.
  - Equilibrium binding constants were determined.
  - The interference of one metal on the other was quantified in vanadate and chromate system.

- Improvement of anionic metal species biosorption

  - The working pH for anionic metal complex ($Au(CN)_2^-$) biosorption was raised to high pH10 with heat-treated AWUS.

- The originally poor anionic metal species uptake demonstrated with $Au(CN)_2^-$ and *Bacillus*, *Penicillium* and *Sargassum* biomass was enhanced by the addition of L-cysteine.

4.3 Suggestions for Future Research

- Investigate the possibility of increasing the penetrability of sorbent AWUS.
- Extend the anioic metal species biosorption model to multi-metal system.
- Improve the metal adsorption equilibrium model by considering the non-ideality in the sorbent phase and multi-types of binding approaches in order to apply the model to more extended conditions.
- Elucidate the mechanism of the adsorption rate-controlling step.

  Variables: the AWCS particle size and mixing velocity.
- Establish the applicability of the mass transfer model to describe the adsorption in dynamic batch systems.
- Evaluate the performance of anionic metal species adsorption in a continuous-flow column packed with AWUS.
- Determine the criteria for the optimum performance of column for biosorption.

  Variables: inlet metal concentrations, pH, ionic strength, flow rate, sorbent size distribution, and packing density.
- Establish the applicability of the Mass Transfer Column Model to describe the biosorption process, providing the basis for the reactor scale-up.

REFERENCES

Aldor, I., Fourest, E. and Volesky, B. 1995. Desorption of cadmium from algal biosorbent. *Can. J. Chem. Eng.* **73**: 516-522.

AOAC 1984. *Official Methods of Analysis of the Association of Official Analytical Chemists*. The Association of Official Analytical Chemists: Washington, DC, pp. 18.025.

AOAC 1990. *Official Methods of Analysis of the Association of Official Analytical Chemists*. The Association of Official Analytical Chemists: Washington, DC, pp. 928.08.

Baes, C. F. J. and Mesmer, R. E. 1976a. *The Hydrolysis of Cations*. Wiley-Interscience, John Wiley & Sons: New York, pp. 397-419.

Baes, C. F. J. and Mesmer, R. E. 1976b. *The Hydrolysis of Cations*. Wiley-Interscience, John Wiley & Sons: New York, pp. 208-210.

Baes, C. F. J. and Mesmer, R. E. 1976c. *The Hydrolysis of Cations*. Wiley-Interscience, John Wiley & Sons: New York, pp. 220.

Bemiller, J. N. and Whistler, R. L. 1962. Alkaline degradation of amino sugar. *J. Org. Chem.* **27**: 1161-1164.

Beveridge, T. J. and Murray, R. G. E. 1976. Uptake and retention of metals by cell walls of *Bacillus subtilis*. *J. Bacteriol.* **127**: 1502.

Bosinco, S., Roussy, J., Guibal, E. and LeCloirec, P. 1996. Interaction mechanisms between hexavalent chromium and corncob. *Environ.Technol.* **17**: 55-62.

Brierley, J. A., Brierley, C. L. and Goyak, G. M. 1986. AMT-BIOCLAIM: A new wastewater treatment and metal recovery technology. *Fundamental and Applied*

Biohydrometallurgy. R. W. Lawrence, R. M. R. Branion and H. G. Ebner, Eds. Elsevier: Amsterdam, The Netherlands, pp. 291-304.

Bromley, L. A. 1973. Thermodynamic propertise of strong electrolytes in aqueous solutions. *AICHE J.* **19:** 313-320.

Buffle, J. 1988a. *Complexation Reactions in Aquatic Systems: An Analytical Approach.* Ellis Horwood Ltd.: Chichester, UK, pp. 195-303.

Buffle, J. 1988b. *Complexation Reactions in Aquatic Systems: An Analytical Approach.* Ellis Horwood Ltd.: Chichester, U.K., pp. 323.

Butler, J. A. V. and Ockrent, C. 1930. Studies in electrocapillarity. Part III. The surface tensions of solutions containing two surface-active solutes. *J. Phys. Chem.* **34:** 2841-2859.

Cabatingan, L. K., Agapay, R. C., Rakels, J. L. L., Ottens, M. and Wielen, L. A. M. V. 2001. Potential of biosorption for the recovery of chromate in industrial wastewater. *Ind. Eng. Chem. Res.* **40:** 2302-2309.

Carvalho, R. P., Chong, K.-H. and Volesky, B. 1995. Evaluation of the Cd, Cu and Zn biosorption in two-metal systems using algal biosorbent. *Biotechnol. Prog.* **11:** 39-44.

Cheremisinoff, P. N. and Ellerbush, F. 1978. *Carbon Adsorption Handbook*. Ann Arbor Science: Ann Arbor, MI, pp. 251.

Chong, H. K. 1995. *Biosorption of Cu, Cd and Zn in binary and ternary systems. Chemical Engineering*. McGill University: Montreal, Canada.

Chong, K. H. and Volesky, B. 1995. Description of two-metal biosorption equilibria by Langmuir-type models. *Biotechnol. Bioeng.* **47:** 451-460.

Crist, R. H., Oberholser, K., McGarrity, J., Crist, D. R., Johnson, J. K. and Brittsan, J. M. 1992. Interaction of metals and protons with algae. 3. Marine algae, with emphasis on lead and aluminum. *Environ. Sci. Technol.* **26:** 496-502.

Crist, R. H., Oberholser, K., Schwartz, D., Marzoff, J., Ryder, D. and Crist, D. R. 1988. Interactions of metals and protons with algae. *Environ. Sci. Technol.* **22:** 755-760.

Dambies, L., Roze, A., Roussy, J. and Guibal, E. 1999. As(V) removal from dilute solutions using MICB (molybdate-impregnated chitosan beads). *Biohydrometeallurgy and the Environment Toward the Mining of the 21st Century (Part B). International Biohydrometallurgy Symposium - Proceedings*. R. Amils and B. A., Eds. Elsevier: Amsterdam, **B:** 277-287.

Davis, C. W. J. 1938. The extent of dissociation of salts in water. Part VIII. An equation for the mean ionic activity coefficient of an electrolyte in water, and a revision of the dissociation constants of some sulphates. *J. Chem. Soc.* **(1938)-Part II:** 2093 - 2098.

Davis, J. A., James, R. O. and Leckie, J. O. 1978. Surface ionization and complexation at the oxide-water interface: 1. Computation of electrical double layer properties in simple electrolytes. *J. Coll. Interf. Sci.* **63:** 399-499.

Davis, J. A. and Leckie, J. O. 1980. Surface ionization and complexation at the oxide-water interface: 3. Adsorption of anions. *J. Colloid Interface Sci.* **74:** 32-43.

Dodge, J. D. 1973. *The Fine Structure of Algal Cells*. Academic Press: London, U.K., pp. 14-45.

Domard, A. 1987. pH and CD measurements on a fully deacetylated chitosan: application to Cu (II) - polymer interactions. *Int. J. Biol. Macromol.* **9:** 98-104.

Dzombak, D. A. and Morel, F. M. M. 1990. *Surface Complexation Modeling*. John Wiley & Sons: NY, pp. 1-35.

Eaton, A. D., Clesceri, L. S. and Greenberg, A. E. 1995a. American Public Health Association: Washington, pp. Ch.4: 19-71.

Eaton, A. D., Clesceri, L. S. and Greenberg, A. E. 1995b. *Standard Methods for the Examination of Water and Wastewater*. American Public Health Association (APHA), AWWA, WPCF: Washington, DC, pp. Ch.4:23.

Ephraim, J., Alegret, S., Mathuthu, A., Bicking, M., Malcolm, R. L. and Marinsky, J. A. 1986. A united physicochemical description of the protonation and metal ion complexation equilibria of natural organic acids (humic and fulvic acids). 2. Influence of polyelectrolyte properties and functional group heterogeneity on the protonation equilibria of fulvic acid. *Environ. Sci. Technol.* **20:** 354-366.

Ephraim, J. and Marinsky, J. A. 1986. A unified physicochemical description of the protonation and metal ion complexation equilibria of natural organic acids (humic and fulvic acids). 3. Influence of polyelectrolyte properties and functional□□ heterogeneity on the copper ion binding equilibria in an Armandale horizons Bh fulvic acid sample. *Environ. Sci. Technol.* **20:** 367-376.

EPS 1977. *Metal Finishing Liquid Effluent Guidelines, Report EPS 1-WP-77-5.* Water Pollution Control Directorate, Environmental Protection Service, Fisheries and Environment Canada, pp. 5958-5960.

EPS 1987a. *Overview of the surface finishing industry: Status of the industry and measures for pollution control.* Environment Canada: Ottawa, Canada **EPS 2/SF/1:** 4.

EPS 1987b. *Overview of the surface finishing industry: Status of the industry and measures for pollution control.* Environment Canada: Ottawa **EPS 2/SF/1:** 43.

Fen, B. J., Daughney, C. J., Yee, N. and Davis, T. A. 1997. A chemical equilibrium model for metal adsorption onto bacterial surfaces. *Geochim. Cosmochim. Acta* **61:** 3319-3328.

Ferrer, J., Paez, G., Marmol, Z., Ramones, E., Garcia, H. and Forster, C. F. 1996. Acid hydrolysis of shrimp-shell wastes and the production of single cell protein from the hydrolysate. *Biores. Tech.* **57:** 55-60.

Figueira, M. M. 1999. *Biosorption of Metals by Brown Seaweeds. Metallurgical Engineering.* Universidade Federal de Minas Gerais: Belo Horizonte, MG, Brazil, pp. 32.

Figueira, M. M., Volesky, B. and Ciminelli, V. S. T. 1997. Assessment of interference in the biosorption of a heavy metal. *Biotechnol. Bioeng.* **54:** 344-350.

Figueira, M. M., Volesky, B. and Mathieu, H. J. 1999. Instrumental analysis study of iron species biosorption by *Sargassum* biomass. *Environ. Sci. Technol.* **33:** 1840-1846.

Fourest, E. and Roux, J. C. 1994. Improvement of heavy metal biosorption by mycelial dead biomass (*Rhizopus arrhizus, Mucor miehei* and *Penicillium chrysogenum*): pH control and cationic activation. *FEMS Microbiol. Rev.* **14:** 325-332.

Fourest, E., Serre, A. and Roux, J.-C. 1996. Contribution of carboxyl groups to heavy metal binding sites in fungal wall. *Toxicol. Environ. Chem.* **54:** 1-10.

Fourest, E. and Volesky, B. 1996. Contribution of sulphonate groups and alginate to heavy metal biosorption by the dry biomass of *Sargassum fluitans*. *Environ. Sci. Technol.* **30:** 277-282.

Frey, D. D. 1997. Mechanism for glutamic acid adsorption on a weak-base ion exchanger. *Chem. Eng. Sci.* **52:** 1227-1231.

Furman, N. H. 1962. *Standard Methods of Chemical Analysis*. D. Van Nostrand Company, Inc.: NY, pp. 1414-1415.

Gadsden, J. A. 1975a. *Infrared Spectra of Minerals and Related Inorganic Compounds*. Butterworth: NY, pp. 29.

Gadsden, J. A. 1975b. *Infrared Spectra of Minerals and Related Inorganic Compounds*. Butterworth: NY, pp. 26.

Ghafourian, H. and Latifi, A. M. 2001. Adsorption and concentration of uranium by a new species of Bacillus bacterium MGL-75. *Sci. Bull. At. Energy Organ. Iran* **22:** 31-37.

Giles, C. H. and Hassan, A. S. A. 1958. Adsorption at organic surfaces. V - A study of the adsorption of dyes and other organic solutes by cellulose and chitin. *J. Soc. Dyers Colour.* **74:** 846-857.

Giles, C. H., Hassan, A. S. A. and Subramanian, R. V. R. 1958. Adsorption at organic surfaces. IV - Adsorption of sulphonated azo dyes by chitin from aqueous solution. *J. Soc. Dyers Colour.* **74:** 681-688.

Grahame, D. C. 1947. The electrical double layer and the theory of eletrocapillarity. *Chem. Review* **41:** 443.

Greenwood, N. W. and Earnshaw, A. 1985a. *Chemistry of the Elements*. Pergamon Press: NY, pp. 1139-1142.

Greenwood, N. W. and Earnshaw, A. 1985b. *Chemistry of the Elements*. Pergamon Press: NY, pp. 891.

Greenwood, N. W. and Earnshaw, A. 1985c. *Chemistry of the Elements*. Pergamon Press: NY, pp. 1175.

Greenwood, N. W. and Earnshaw, A. 1985d. *Chemistry of the Elements*. Pergamon Press: NY, pp. 1169.

Greenwood, N. W. and Earnshaw, A. 1985e. *Chemistry of the Elements*. Pergamon Press: NY, pp. 1147-1148.

Guggenheim, E. A. 1935. The specific thermodynamic propertises of aqueous solutions of strong electrolytes. *Phil. Mag. Ser.* **7:** 588-643.

Guibal, E., Milot, C. and Roussy, J. 1999. Molybdate sorption by cross-linked chitosan beads: Dynamic studies. *Wat. Environ. Res.* **71:** 10-17.

Gupta, C. K. and Krishnamurthy, N. 1992a. *Extractive Metallurgy of Vanadium*. Elsevier: NY, pp. 234.

Gupta, C. K. and Krishnamurthy, N. 1992b. *Extractive Metallurgy of Vanadium*. Elsevier: NY, pp. 231.

Gupta, C. K. and Krishnamurthy, N. 1992c. *Extractive Metallurgy of Vanadium*. Elsevier: NY, pp. 236.

Gupta, C. K. and Krishnamurthy, N. 1992d. *Extractive Metallurgy of Vanadium*. Elsevier: NY, pp. 222-229.

Gupta, C. K. and Krishnamurthy, N. 1992e. *Extractive Metallurgy of Vanadium*. Elsevier: NY, pp. 209.

Harland, C. E. 1994. *Ion Exchange: Theory and Practice*. The Royal Society of Chemistry: Cambridge, UK, pp. 40.

Haug, A. and Smidsrod, O. 1970. Selectivity of some anionic polymers for divalent metal ions. *Acta Chem. Scand.* **24:** 843-854.

Hayes, K. F. and Leckie, J. O. 1987. Modeling ionic strength effects on cation adsorption at hydrous oxide solution interfaces. *J. Colloid Interface Sci.* **115:** 564-572.

Hayes, K. F. and Leckie, J. O. 1988. Modeling ionic strength effects on anion adsorption at hydrous oxide solution interfaces. *J. Colloid Interface Sci.* **125:** 717-726.

Hayes, K. F., Redden, G., Ela, W. and Leckie, J. O. 1990. Surface complexation models: An evaluation of model parameter estimation using FITIQL and oxide mineral titration data. *J. Coll. Interf. Sci.* **142:** 448-469.

Hayes, K. F., Redden, G., Ela, W. and Leckie, J. O. 1991. Surface complexation models: An evaluation of model parameter estimation using FITEQL and oxide mineral titration data. *J. Coll. Interf. Sci.* **142:** 448-469.

Heininger, M. W. and Meloan, C. E. 1992. A selective reagent for the removal and recovery of chromate, molybdate, tungstate, and vanadate from aqueous solution. *Sep. Sci. Tech.* **27:** 663-9.

Helfferich, F. 1995. *Ion Exchange*. Dover Publications Inc.: NY, pp. 168.

Holan, Z. R., Volesky, B. and Prasetyo, I. 1993. Biosorption of cadmium by biomass of marine algae. *Biotechnol. Bioeng.* **41:** 819-825.

Hussain, S. and Volet, B. 1995. Uptake of silver by isolated human lymphocytes in presence of L-cysteine or N-acetyl-L-cysteine. *In Vitro Toxicol.* **8:** 377-388.

Jaworski, J. F. 1985. *Chromium Update*. National Research Council of Canada: Ottawa, Canada: 11-13.

Jeffers, T. H. and Corwin, R. R. 1993. Waste water remediation using immobilized biological extractants. *Biohydrometallurgical Technologies, Proceedings of the International Biohydrometallurgy Symposium*. A. E. Torma, M. L. Apel and C. L. Brierley, Eds. The Minerals, Metals and Materials Society: Warrendale, PA, **2:** 1-14.

Jeffers, T. H., Ferguson, C. R. and Bennet, P. 1991. Biosorption of metal contaminants from acidic mine water. *Mineral Bioprocessing*. R. W. Smith and M. Misra, Eds. The Minerals, Metals, and Materials Society, pp. 289-299.

Kepert, D. L. 1973. Chap.51. Isopolyanions and heteropolyanions. *Comprehensive Inorganic Chemistry* Pergamon Press: Oxford, UK, **4:** 607-72.

Kratochvil, D. 1997. *A Study of the Metal Biosorption Process Utilizing Sargassum Seaweed Biomass. Chemical Engineering*. McGill University: Montreal, pp. 186.

Kratochvil, D., Pimentel, P. and Volesky, B. 1998. Removal of trivalent and hexavalent chromium by seaweed biosorbent. *Environ. Sci. Technol.* **32:** 2693-2698.

Kuyucak, N. 1987. *Algal biosorbents for gold and cobalt*. Department of Chemical Engineering, McGill University, Montreal, Canada.

Kuyucak, N. and Volesky, B. 1989a. Accumulation of cobalt by marine alga. *Biotechnol. Bioeng.* **33:** 809-814.

Kuyucak, N. and Volesky, B. 1989b. The mechanism of cobalt biosorption. *Biotechnol. Bioeng.* **33:** 823-831.

Kuyucak, N. and Volesky, B. 1989c. The mechanism of gold biosorption. *Biorecovery* **1:** 219-235.

Langmuir, I. 1918. The adsorption of gases on plane surfaces of glass, mica and platinum. *J. Am. Chem. Soc.* **40:** 1361-1403.

Larson, J. W. 1995. Thermochemistry of vanadium(5+) in aqueous solutions. *J. Chem. Eng. Data* **40:** 1276-1280.

Lee, M. Y., Park, J. M. and Yang, J. W. 1997. Microprecipitation of lead on the surface of crab shell particles. *Process. Biochem.* **32:** 671-677.

Li, N. C. and Manning, R. A. 1955. Some metal complexes of sulfur-containing amino acids. *J. Amer. Chem. Soc.* **77:** 5225-5528.

Lidin, R. A., Adreeva, L. L. and Molochko, V. A. 1995. *Constants of Inorganic Substances: Handbook.* Begell House, Inc.: NY, pp. 319-324.

Lin, F. G. and Marinsky, J. A. 1993. A Gibbs-Donnan-based interpretation of the effect of medium counterion concentration levels on the acid dissociation properties of alginic acid and chondroitin sulfate. *React. Polymers* **19:** 27-45.

Mahan, C. A. and Holcombe, J. A. 1992. Immobilization of algae cells on silica gell and their characterization for trace metal preconcentration. *Anal. Chem.* **64:** 1933-1939.

Marinsky, J. A. 1987. A two-phase model for the interpretation of proton and metal ion interaction with charged polyelectrolyte gels and their linear analogs. *Aquatic Surface Chemistry*. W. Stumm, Ed. Wiley Interscience, John Wiley & Sons: New York, pp. 49-81.

Marinsky, J. A. and Ephraim, J. 1986. A unified physicochemical description of the protonation and metal ion complexation equilibria of natural organic acids (humic and fulvic acids). I. Analysis of the influence of polyelectrolyte properties on protonation equilibria in ionic media: Fundamental concepts. *Environ. Sci. Technol.* **20:** 349-354.

Marinsky, J. A., Gupta, S. and Schindler, P. 1982a. The interaction of Cu(II) ion with humic acid. *J. Coll. Int. Sci.* **89:** 401-411.

Marinsky, J. A., Gupta, S. and Schindler, P. 1982b. A unified physicochemical description of the equilibria encountered in humic acid gels. *J. Coll. Int. Sci.* **89:** 412-426.

Marsden, J. and House, L. 1993a. *Chemistry of Gold Extraction.* Ellis Horwood: Hartnoll, UK, pp. 100-150.

Marsden, J. and House, L. 1993b. *Chemistry of Gold Extraction.* Ellis Horwood: Hartnoll, UK, pp. 259-300.

Marsden, J. and House, L. 1993c. *Chemistry of Gold Extraction.* Ellis Horwood: Hartnoll, UK, pp. 380.

Marsden, J. and House, L. 1993d. *Chemistry of Gold Extraction.* Ellis Horwood: Hartnoll, UK, pp. 47.

Marsden, J. and House, L. 1993e. *Chemistry of Gold Extraction.* Ellis Horwood: Hartnoll, UK, pp. 193.

Marsden, J. and House, L. 1993f. *Chemistry of Gold Extraction.* Ellis Horwood: Hartnoll, UK, pp. 309.

Marsden, J. and House, L. 1993g. *Chemistry of Gold Extraction.* Ellis Horwood: Hartnoll, UK, pp. 349.

Marsden, J. and House, L. 1993h. *Chemistry of Gold Extraction.* Ellis Horwood: Hartnoll, UK, pp. 351-365.

Marsden, J. and House, L. 1993i. *Chemistry of Gold Extraction.* Ellis Horwood: Hartnoll, UK, pp. 369-374.

Mattson, J. S. and Mark, J., H. B. 1971. *Activated Carbon.* Marcel Dekker: New York, pp. 31.

Mattson, J. S. and Mark Jr., H. B. 1971. *Activated Carbon.* Marcel Dekker: NY, pp. 132-133.

Milot, C., Guibal, E., Roussy, J. and LeCloirec, P. 1997. Chitosan gel beads as a new biosorbent for molybdate removal. *Mineral Processing and Extractive Metallurgy Review*. F. M. Doyle, N. Arbiter and N. Kuyucak, Eds. Gordon and Breach Sci. Publ.: Newark, NJ, pp. 293-308.

Mooiman, M. B. and Miller, J. D. 1986. The chemistry of gold solvent extraction from cyanide solution using modified amines. *Hydrometallurgy* **16:** 245-261.

Morel, F. M. M. 1983. *Principles of Aquatic Chemistry*. John Wiley & Sons: New York, pp. 237-266.

Morrison, R. T. 1987. *Organic Chemistry*. Allyn and Bacon, Inc.: Newton, pp. 985.

Muzzarelli, R. A. A. 1973a. *Natural Chelating Polymers*. Pergamon Press: Toronto, Ont., pp. 207.

Muzzarelli, R. A. A. 1973b. *Natural Chelating Polymers*. Pergamon Press: Toronto, Ont.

Muzzarelli, R. A. A. 1977. *Chitin*. Pergamon Press: London, U.K.

Muzzarelli, R. A. A., Tanfani, F. and Emanuelli, M. 1981. The chelating ability of chitinous materials from *Streptomyces, Mucor rouxii, Phycomyces blakesleeamus*, and *Choanephora cucurbitarum*. *J. Appl. Biochem.* **3:** 322.

Myers, D. 1991. *Surfaces, Interfaces, Colloids. Principles and Applications*. VCH: Weinheim, Germany, pp. 39-67.

Nachod, F. C. 1949a. *Ion Exchange - Theory & Application*. Academic Press: NY, pp. 65.

Nachod, F. C. 1949b. *Ion Exchange - Theory & Application*. Academic Press: NY, pp. 25.

Nakamoto, K. 1986. *Infrared and Raman Spectra of Inorganic and Coordination Compounds*. J. Wiley & Sons: New York, NY, pp. 231.

Nakamoto, K. 1997. *Infrared and Raman Spectra of Inorganic and Coordination Compounds - B. Application in Coordination, Organometallic, and Bioinorganic Chemistry*. John Wiley & Sons: New York, pp. 60.

Niu, H. and Volesky, B. 1999. Characteristics of gold biosorption from cyanide solution. *J.Chem. Technol. Biotechnol.* **74:** 778-784.

Niu, H. and Volesky, B. 2000. Gold-cyanide biosorption with L-cysteine. *J. Chem. Technol. Biotechnol.* **75:** 436-442.

Niu, H., Xu, X. S., Wang, J. H. and Volesky, B. 1993. Removal of lead from aqueous solutions by *Penicillium* biomass. *Biotechnol. Bioeng.* **42:** 785-787.

Nurdogan, Y. and Meyer, C. L. 1995. Vanadium removal from petroleum refinery wastewater. *Proceedings of the 50th Industrial Waste Conference*. P. University, Ed. Ann Arbor Press, Inc.: West Lafayette, Indiana, pp. 73-83.

Ouki, S. K. and Neufeld, R. D. 1997. Use of activated carbon for the recovery of chromium from industrial wastewaters. *J. Chem. Tech. Biotech.* **70:** 3-8.

Pagenkopf, G. K. 1978. *Introduction to Natural Water Chemistry*. Marcel Dekker: NY, pp. 162.

Perrin, D. D. 1979. *Stability Constants of Metal-Ion Complexes*. Pergamon Press: Oxford, UK.

Pitzer, K. S. 1979. Theory: ion interaction approach. *Activity Coefficients in Electrolyte Solutions*. R. M. Pytkowicz, Ed. CRC Press: Boca Raton, FL, USA, **1:** 157-208.

Pope, M. T. and Dale, B. W. 1968. Isopoly-vanadates, -niobates and -tantalates. *Quart. Rev.* **22:** 527-548.

Ragan, M., A, and Craigie, J. S. 1978. Phenolic compounds in brown and red algae. *Handbook of Phycological Methods*. Hellebust J.A. and J. S. Craigie, Eds. Cambridge University Press: New York, pp. 157-179.

Remacle, J. 1990. The cell wall and metal binding. *Biosorption of Heavy Metals*. B. Volesky, Ed. CRC Press, Inc.: Boca Raton, FL, pp. 83-92.

Roberts, G. A. F. 1992a. *Chitin Chemistry*. Macmillan: London, UK, pp. 204-206.

Roberts, G. A. F. 1992b. *Chitin Chemistry*. Macmillan: London, UK, pp. 28.

Roberts, G. A. F. 1992c. *Chitin Chemistry*. Macmillan: London, UK, pp. 1.

Roberts, G. A. F. 1992d. *Chitin Chemistry*. Macmillan: London, UK, pp. 230.

Roberts, G. A. F. 1992e. *Chitin Chemistry*. Macmillan: London, UK, pp. 55-58.

Roberts, G. A. F. 1992f. *Chitin Chemistry*. Macmillan: London, UK, pp. 213.

Roberts, G. A. F. 1992g. *Chitin Chemistry*. Macmillan: London, UK, pp. 4.

Roberts, G. A. F. 1992h. *Chitin Chemistry*. Macmillan: London, UK, pp. 55.

Roberts, G. A. F. 1992i. *Chitin Chemistry*. Macmillan: London, UK, pp. 6.

Roberts, G. A. F. 1992j. *Chitin Chemistry*. Macmillan: London, UK, pp. 21.

Roberts, G. A. F. 1992k. *Chitin Chemistry*. Macmillan: London, UK, pp. 38.

Roberts, G. A. F. 1992l. *Chitin Chemistry*. Macmillan: London, UK, pp. 38-43.

Roberts, G. A. F. 1992m. *Chitin Chemistry*. Macmillan: London, UK, pp.

Roberts, G. A. F. 1992n. *Chitin Chemistry*. Macmillan: London, UK, pp. 5.

Roberts, G. A. F. 1992o. *Chitin Chemistry*. Macmillan: London, UK, pp. 34.

Roberts, G. A. F. 1992p. *Chitin Chemistry*. Macmillan: London, UK, pp. 91-101.

Roberts, G. A. F. 1992q. *Chitin Chemistry*. Macmillan: London, UK, pp. 203-206.

Roberts, G. A. F. 1992r. *Chitin Chemistry*. Macmillan: London, UK, pp. 89.

Roberts, K. S. 1993. *Protein Purification - Principles and Practice*. Springer-Verlag: NY, pp. 45.

Robinson, R. A. and Stokes, R. H. 1959. *Electrolyte Solutions, 2nd ed.* Butterworths: London, UK, pp. 223-252.

Rostoker, W. 1958. *The Metallurgy of Vanadium*. Wiley: New York, pp. 7-50.

Rostoker, W. 1975. *The Metallurgy of Vanadium*. John Wiley & Sons: NY, pp. 7.

Ruiz, M., Sastre, A. M., Zikan, M. C. and Guibal, E. 2001. Palladium sorption on glutaraldehyde-crosslinked chitosan in fixed-bed systems. *J. Appl. Polym. Sci.* **81:** 153-165.

Russell, J. B. 1980. *General Chemistry*. McGraw-Hill: NY, pp. 314-316.

Sandler, S. I. 1989. *Chemical Engineering Thermodynamics*. John Wiley & Sons: NY, pp. 359.

Schiewer, S. 1996a. *Multi-Metal Ion Exchange in Biosorption. Chemical Engineering*. McGill University: Montreal, Canada.

Schiewer, S. 1996b. *Multi-Metal Ion Exchange in Biosorption. Chemical Engineering*. McGill University: Montreal, Canada, pp. 8.

Schiewer, S. 1996c. *Multi-Metal Ion Exchange in Biosorption. Chemical Engineering*. McGill University: Montreal, Canada, pp. 6.

Schiewer, S. and Volesky, B. 1995. Modeling of the proton-metal ion exchange in biosorption. *Environ. Sci. Technol.* **29:** 3049-3058.

Schiewer, S. and Volesky, B. 1997a. Ionic strength and electrostatic effects in biosorption of divalent metal ions and protons. *Environ. Sci. Technol.* **31:** 2478-2485.

Schiewer, S. and Volesky, B. 1997b. Ionic strength and electrostatic effects in biosorption of protons. *Environ. Sci. Technol.* **31:** 1863-1871.

Schrader, B. 1995. *Infrared and Raman Spectroscopy: Methods and Applications*. VCH: Weinheim, pp. 356.

Shallcross, M., Herrmann, C. C. and McCoy, B. J. 1988. An improved model for the prediction of multicomponent ion exchange equilibria. *Chem. Eng. Sci.*. **43:** 279-288.

Sharma, D. C. and Forster, C. F. 1993. Removal of hexavalent chromium using sphagnum moss peat. *Water Res.* **27:** 1201-1208.

Shindo, H. and Brown, T. L. 1965. Infrared spectra of complexes of L-cysteine and related compounds with zinc (II), cadmium (II), mercury (II), and lead(II). *J. Amer. Chem. Soc.* **87:** 1904-1908.

Silberberg, M. 1996. *The Chemical Nature and Charge*. Mosby: St. Louis, MI, pp. 497-499.

Sillen, L. G. and Mortell, A. E. 1964a. *Stability Constants of Metal-Ion Complexes: Special Publication 17*. The Chemical Society: London, UK, pp. 84-86.

Sillen, L. G. and Mortell, A. E. 1964b. *Stability Constants of Metal-Ion Complexes: Special Publication 17*. The Chemical Society: London, UK, pp. 89-90.

Sillen, L. G. and Mortell, A. E. 1964c. *Stability Constants of Metal-Ion Complexes: Special Publication 17*. The Chemical Society: London, UK, pp. 111.

Smith, J. M. 1981. *Chemical Engineering Kinetics*. McGraw-Hill: New York, pp. 310-322.

Smith, R. P. and Woodburn, E. T. 1978. Prediction of multicomponent ion exchange equilibria for the ternary system SO_4^{2-}-NO_3^--Cl^- from data of binary systems. *AIChE J.* **24:** 577-587.

Stryer, L. 1988. *Biochemistry*. W. H. Freeman & Company: NY, pp. 15-17.

Stumm, W., Kummert, R. and Sigg, L. 1980. A ligand exchange model for the adsorption of inorganic & organic ligands at hydroxide oxide surface. *Chem. Acta* **53:** 291-312.

Stumm, W. and Morgan, J. J. 1970a. *Aquatic Chemistry*. John Wiley & Sons: New York, pp. 238-299.

Stumm, W. and Morgan, J. J. 1970b. *Aquatic Chemistry*. John Wiley & Sons: NY, pp. 447.

Stumm, W. and Morgan, J. J. 1996a. *Aquatic Chemistry*. John Wiley & Sons: NY, pp. 103.

Stumm, W. and Morgan, J. J. 1996b. *Aquatic Chemistry*. John Wiley & Sons: NY, pp. 49-51.

Stumm, W. and Morgan, J. J. 1996c. *Aquatic Chemistry*. John Wiley & Sons: NY, pp. 35-43.

Stumm, W. and Morgan, J. J. 1996d. *Aquatic Chemistry*. John Wiley & Sons: New York, pp. 540-542.

Takatsuji, W. and Yoshida, H. 1998. Study the equilibrium of organic acid adsorption on weakly basic ion exchanger. *AICHE J.* **44:** 1216-1221.

Tien, C. 1994. *Adsorption Calculations and Modeling*. Butterworth-Heinemann: Boston, pp. 29-40.

Troy, F. A. and Koffler, H. 1969. The chemistry and molecular architecture of the cell walls of *Penicillium chrysogenum*. *J. Biol. Chem.* **244:** 5563-5576.

Tsezos, M. and Deutschmann, A. A. 1990. An investigation of engineering parameters for the use of immobilised biomass particles in biosorption. *J. Chem. Tech. Biotechnol.* **48:** 29-39.

Volesky, B. 1990a. Biosorption and biosorbents. *Biosorption of Heavy Metals*. B. Volesky, Ed. CRC Press: Boca Raton, FL, pp. 3-6.

Volesky, B. 1990b. Removal and recovery of heavy metals by biosorption. *Biosorption of Heavy Metals*. B. Volesky, Ed. CRC Press: Boca Raton, FL, pp. 7-43.

Volesky, B. and Holan, Z. R. 1995. Biosorption of heavy metals. *Biotechnol. Prog.* **11:** 235-250.

Weast, R. C. and Astle, M. J. 1979. *Handbook of Chemistry and Physics, 60th ed.* CRC Press: Boca Raton, FL, pp. F-89.

Weppen, P. and Hornburg, A. 1995. Calorimetric studies on interactions of divalent cations and microorganisms or microbial envelopes. *Thermochim. Acta* **269/270:** 393-404.

Westall, J. C. 1987. Adsorption mechanisms in aquatic surface chemistry. *Aquatic Surface Chemistry*. W. Stumm, Ed. John Wiley & Sons: NY, pp. 6.

Wilson, G. M. 1964. Vapor-liquid equilibrium XI: A new expression for the excess energy of mixing. *Am. Chem. Soc. J.* **86:** 127-130.

Yang, J. 2000. *Biosorption of Uranium and Cadmium on Sargassum Seaweed Biomass. Chemical Engineering*. McGill University: Montreal, Canada, pp. 116.

Yoshida, H. and Kishimoto, N. 1995. Adsorption of glutamic acid on weakly basic ion exchange equilibrium. *Chem. Eng. Sci.* **50:** 2203-2210.

Yoshida, H., Kishimoto, N. and Kataoka, T. 1994. Adsorption of strong acid on polyaminated highly porous chitosan: Equilibrium. *Ing. Eng. Chem. Res.* **33:** 854-859.

Yun, Y. S., Niu, H. and Volesky, B. 2001. The effect of impurities on metal biosorption. *Biohydrometallurgy: Fundamentals, Technology and Sustainable Development. Part B - Biosorption and Bioremediation*. V. S. T. Ciminelli and J. O. Garcia, Eds. Elsevier Science B.V.: Amsterdam, **B:** 181-187.